4

Voltage Sags—Characterization

4.1 INTRODUCTION

Voltage sags are short duration reductions in rms voltage, caused by short circuits, overloads, and starting of large motors. The interest in voltage sags is mainly due to the problems they cause on several types of equipment: adjustable-speed drives, process-control equipment, and computers are notorious for their sensitivity. Some pieces of equipment trip when the rms voltage drops below 90% for longer than one or two cycles. In this and the two following chapters, it will become clear that such a piece of equipment will trip tens of times a year. If this is the process-control equipment of a paper mill, one can imagine that the damage due to voltage sags can be enormous. Of course a voltage sag is not as damaging to industry as a (long or short) interruption. But as there are far more voltage sags than interruptions the total damage due to sags is still larger. Short interruptions and most long interruptions originate in the local distribution network. However, voltage sags at equipment terminals can be due to short-circuit faults hundreds of kilometers away in the transmission system. A voltage sag is thus much more of a "global" problem than an interruption. Reducing the number of interruptions typically requires improvements on one feeder. Reducing the number of voltage sags requires improvements on several feeders, and often even at transmission lines far away.

An example of a voltage sag due to a short-circuit fault is shown in Fig. 4.1. We see that the voltage amplitude drops to a value of about 20% of the pre-event voltage for about two cycles. After these two cycles the voltage comes back to about the pre-sag voltage. This magnitude and duration are the main characteristics of a voltage sag. Both will be discussed in more detail in the forthcoming sections. We can also conclude from Fig. 4.1 that magnitude and duration do not completely characterize the sag. The during-sag voltage contains a rather large amount of higher frequency components. Also the voltage shows a small overshoot immediately after the sag.

Most of the current interest in voltage sags is directed to voltage sags due to short-circuit faults. These voltage sags are the ones which cause the majority of equipment trips. But also the starting of induction motors leads to voltage sags. Figure 4.2 gives an

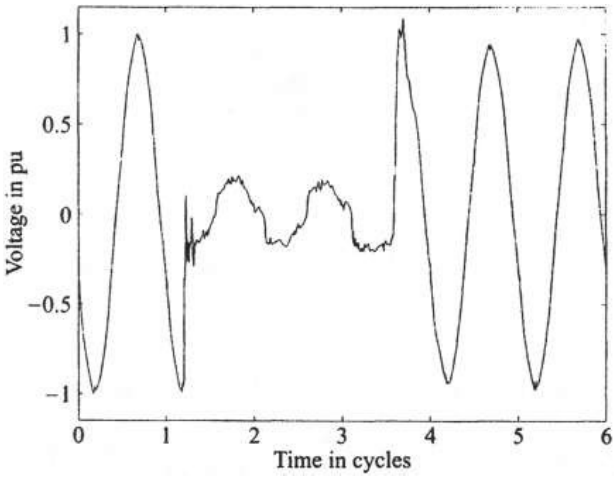

Figure 4.1 A voltage sag due to a short-circuit fault—voltage in one phase in time domain. (Data obtained from [16].)

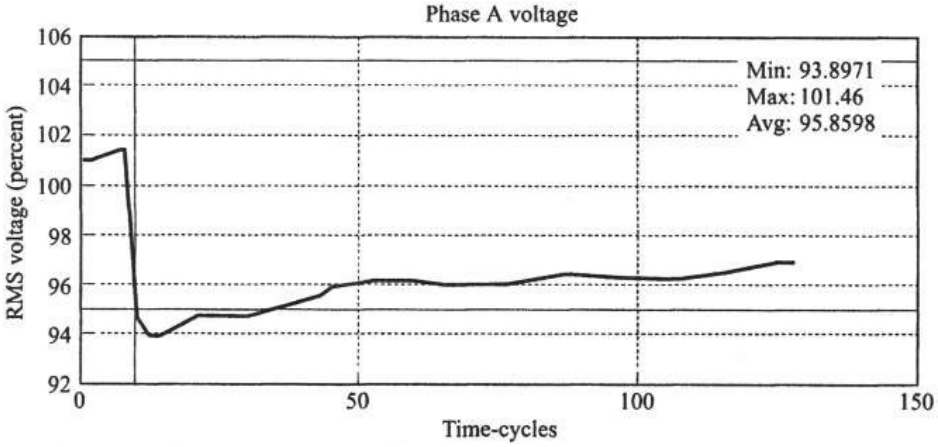

Figure 4.2 A voltage sag due to induction motor starting. (Data obtained from Electrotek Concepts [19].)

example of such a voltage sag [19]. Comparing this figure with Fig. 4.1 shows that no longer the actual voltage as a function of time is given but the rms voltage versus time. The rms voltage is typically calculated every cycle or half-cycle of the power system frequency. Voltage sags due to induction motor starting last longer than those due to short circuits. Typical durations are seconds to tens of seconds. The remainder of this chapter will concentrate on voltage sags due to short circuits. Voltage sags due to motor starting will be discussed in short in Section 4.9.

4.2 VOLTAGE SAG MAGNITUDE

4.2.1 Monitoring

The magnitude of a voltage sag can be determined in a number of ways. Most existing monitors obtain the sag magnitude from the rms voltages. But this situation might well change in the future. There are several alternative ways of quantifying the voltage level. Two obvious examples are the magnitude of the fundamental (power frequency) component of the voltage and the peak voltage over each cycle or half-cycle. As long as the voltage is sinusoidal, it does not matter whether rms voltage,

fundamental voltage, or peak voltage is used to obtain the sag magnitude. But especially during a voltage sag this is often not the case.

4.2.1.1 Rms Voltage. As voltage sags are initially recorded as sampled points in time, the rms voltage will have to be calculated from the sampled time-domain voltages. This is done by using the following equation:

$$V_{rms} = \sqrt{\frac{1}{N}\sum_{i=1}^{N} v_i^2} \tag{4.1}$$

where N is the number of samples per cycle and v_i are the sampled voltages in time domain.

The algorithm described by (4.1) has been applied to the sag shown in Fig. 4.1. The results are shown in Fig. 4.3 and in Fig. 4.4. In Fig. 4.3 the rms voltage has been calculated over a window of one cycle, which was 256 samples for the recording used. Each point in Fig. 4.3 is the rms voltage over the preceeding 256 points (the first 255 rms values have been made equal to the value for sample 256):

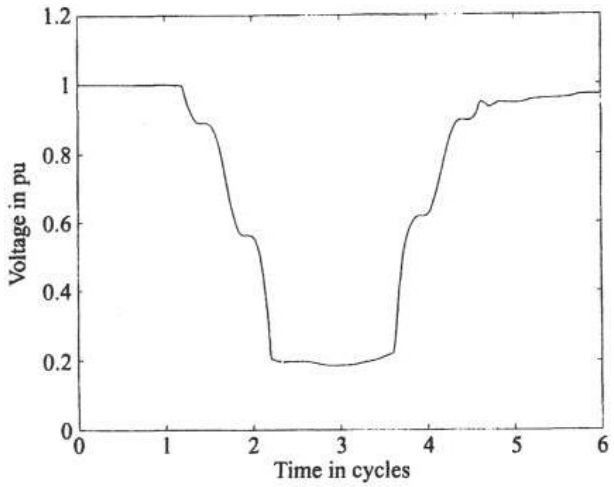

Figure 4.3 One-cycle rms voltage for the voltage sag shown in Fig. 4.1.

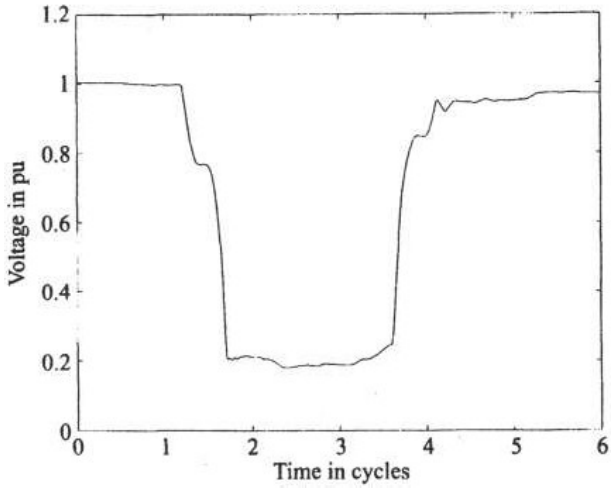

Figure 4.4 Half-cycle rms voltage for the voltage sag shown in Fig. 4.1.

$$V_{rms}(k) = \sqrt{\frac{1}{N}\sum_{i=k-N+1}^{i=k} v_i^2} \tag{4.2}$$

with $N = 256$. We see that the rms voltage does not immediately drop to a lower value but takes one cycle for the transition. We also see that the rms value during the sag is not completely constant and that the voltage does not immediately recover after the fault. A surprising observation is that the rms voltage immediately after the fault is only about 90% of the pre-sag voltage. We will come back to this phenomenon in Section 4.9. From Fig. 4.1 one can see that the voltage in time domain shows a small overvoltage instead. In Fig. 4.4 the rms voltage has been calculated over the preceeding 128 points, $N = 128$ in (4.2). The transition now takes place in one half-cycle. A shorter window than one half-cycle is not useful. The window length has to be an integer multiple of one half-cycle. Any other window length will produce an oscillation in the result with a frequency equal to twice the fundamental frequency. For both figures the rms voltage has been calculated after each sample. In power quality monitors, this calculation is typically made once a cycle:

$$V_{rms}(kN) = \sqrt{\frac{1}{N}\sum_{i=(k-1)N+1}^{i=kN} v_i^2} \tag{4.3}$$

It is thus very likely that the monitor will give one value with an intermediate magnitude before its rms voltage value settles down. We will come back to this when discussing sag duration.

4.2.1.2 Fundamental Voltage Component. Using the fundamental component of the voltage has the advantage that the phase-angle jump can be determined in the same way. The phase-angle jump will be discussed in detail in Section 4.5. The fundamental voltage component as a function of time may be calculated as

$$V_{fund}(t) = \frac{2}{T}\int_{t-T}^{t} v(\tau)e^{j\omega_0\tau}d\tau \tag{4.4}$$

where $\omega_0 = \frac{2\pi}{T}$ and T one cycle of the fundamental frequency. Note that this results in a complex voltage as a function of time. The absolute value of this complex voltage is the voltage magnitude as a function of time; its argument can be used to obtain the phase-angle jump. In a similar way we can obtain magnitude and phase angle of a harmonic voltage component as a function of time. This so-called "time-frequency analysis" is a well-developed area within digital signal processing with a large application potential in power engineering.

The fundamental component has been obtained for the voltage sag shown in Fig. 4.1. The absolute value of the fundamental component is shown in Fig. 4.5. Each point represents the magnitude of the (complex) fundamental component of the previous cycle (256 points). The fundamental component of the voltage has been obtained through a fast-Fourier transform (fft) algorithm [148]. A comparison with Fig. 4.3 shows that the behavior of the fundamental component is very similar to the behavior of the rms voltage.

The rms voltage has the advantage that it can be applied easily to a half-cycle window. Obtaining the fundamental voltage from a half-cycle window is more complicated. A possible solution is to take a half-cycle window and to calculate the second half-cycle by using

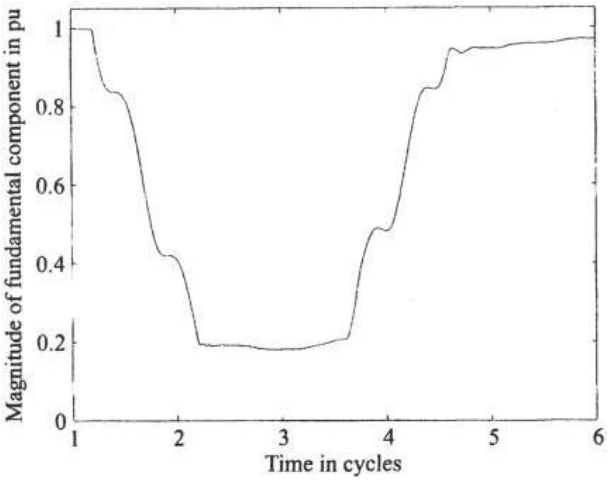

Figure 4.5 Magnitude of the fundamental component of the voltage sag in Fig. 4.1.

$$\cos(\omega t + \phi + \pi) = -\cos(\omega t + \phi) \tag{4.5}$$

Let $v_i, i = 1 \cdots \frac{N}{2}$ be the samples voltages over a half-cycle window. The fundamental voltage is obtained by taking the Fourier transform of the following series:

$$v_1 \cdots v_{\frac{N}{2}}, -v_1 \cdots - v_{\frac{N}{2}} \tag{4.6}$$

This algorithm has been applied to the voltage sag shown in Fig. 4.1, resulting in Fig. 4.6. The transition from pre-fault to during-voltage is clearly faster than in Fig. 4.5. Note that this method assumes that there is no dc voltage component present. The presence of a dc voltage component will lead to an error in the fundamental voltage.

An alternative method of obtaining the fundamental voltage component is discussed in Section 4.5.

4.2.1.3 Peak Voltage. The peak voltage as a function of time can be obtained by using the following expression:

$$V_{peak} = \max_{0 < \tau < T} |v(t - \tau)| \tag{4.7}$$

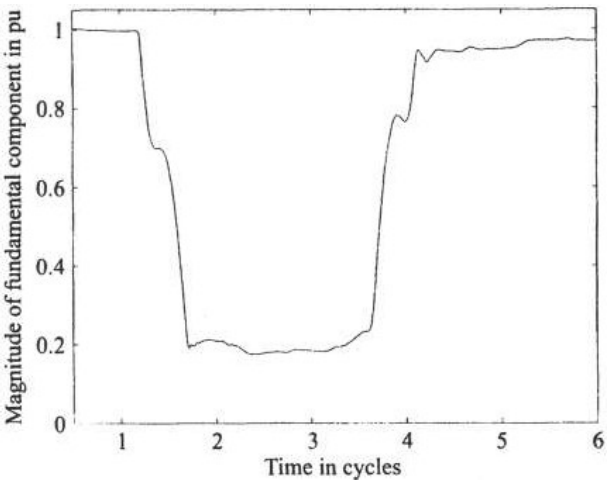

Figure 4.6 Magnitude of the fundamental component of the voltage sag in Fig. 4.1, obtained by using a half-cycle window.

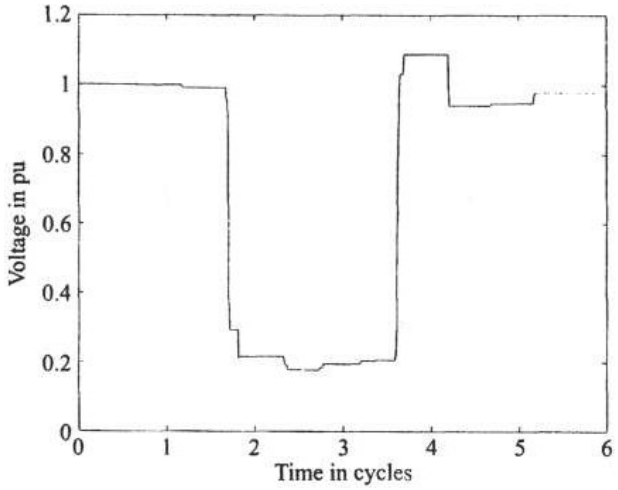

Figure 4.7 Half-cycle peak voltage for the voltage sag shown in Fig. 4.1.

with $v(t)$ the sampled voltage waveform and T an integer multiple of one half-cycle. In Fig. 4.7, for each sample the maximum of the absolute value of the voltage over the preceding half-cycle has been calculated. We see that this peak voltage shows a sharp drop and a sharp rise, although we will see later that they do not coincide with commencement and clearing of the sag. Contrary to the rms voltage, the peak voltage shows an overshoot immediately after the sag, which corresponds to the overvoltage in time domain. The two methods are compared in Fig. 4.8. We see that the peak voltage tends to be higher most of the time with the exception of the end of the deep part of the sag.

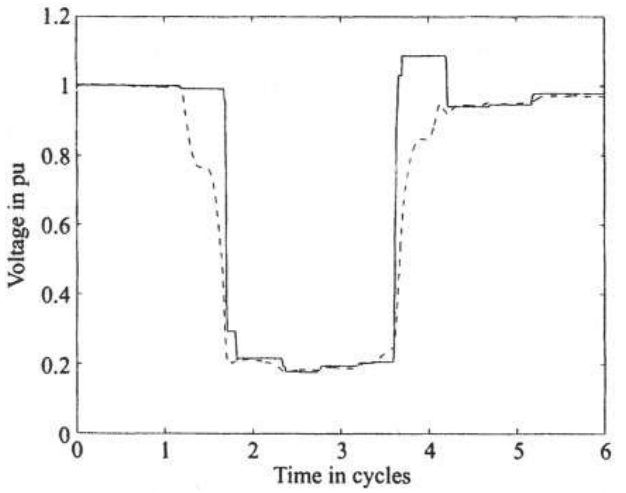

Figure 4.8 Comparison between half-cycle peak (solid line) and half-cycle rms voltage (dashed line) for the voltage sag shown in Fig. 4.1.

4.2.1.4 A One-Cycle Voltage Sag. Another example of a voltage sag is shown in Fig. 4.9; contrary to Fig. 4.1, all three phase voltages are shown. The voltage is low in one phase for about one cycle and recovers rather fast after that. The other two phases show some transient phenomenon, but no clear sag or swell. The latter is also evident from Fig. 4.10 which gives the half-cycle rms value for the sag shown in Fig. 4.9. We see in the latter figure that the voltage in the two non-faulted phases shows a small swell. Due to the short duration of the sag the rms voltage curve does not have a specific flat part. This makes the determination of the sag magnitude rather arbitrary. If the monitor takes one sample every half-cycle the resulting sag

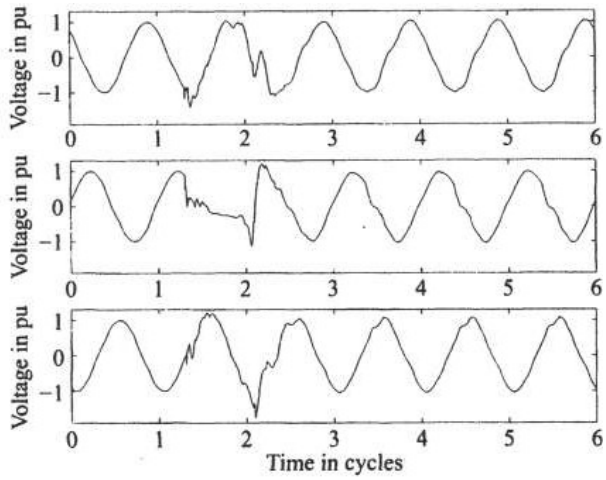

Figure 4.9 Time-domain plot of a one-cycle sag, plots of the three phase voltages. (Data obtained from [16].)

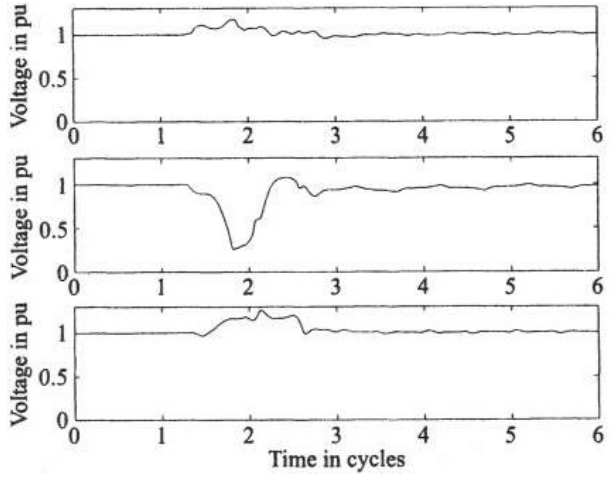

Figure 4.10 Half-cycle rms voltages for the voltage sag shown in Fig. 4.9.

magnitude can be anywhere between 26% and 70% depending on the moment at which the sample is taken. In case a one-cycle window is used to calculate the rms voltage, the situation becomes worse.

The two alternative methods for obtaining the sag magnitude versus time have also been applied to phase b of the event in Fig. 4.9. The half-cycle peak voltage is shown in Fig. 4.11, the half-cycle fundamental voltage component in Fig. 4.12. The shape of the latter is similar to the shape of the half-cycle rms. The half-cycle peak voltage again shows a much sharper transition than the other two methods.

4.2.1.5 Obtaining One Sag Magnitude. Until now, we have calculated the sag magnitude as a function of time: either as the rms voltage, as the peak voltage, or as the fundamental voltage component obtained over a certain window. There are various ways of obtaining one value for the sag magnitude from the magnitude as a function of time. Most monitors take the lowest value. Thinking about equipment sensitivity, this corresponds to the assumption that the equipment trips instantaneously when the voltage drops below a certain value. As most sags have a rather constant rms value during the deep part of the sag, using the lowest value appears an acceptable assumption.

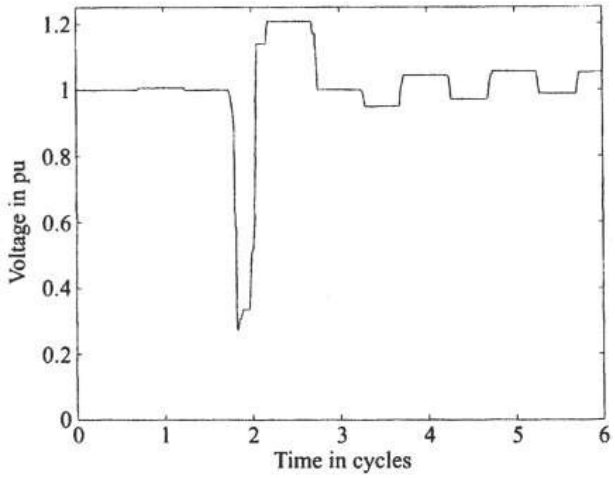

Figure 4.11 Half-cycle peak voltage for phase b of the sag shown in Fig. 4.9.

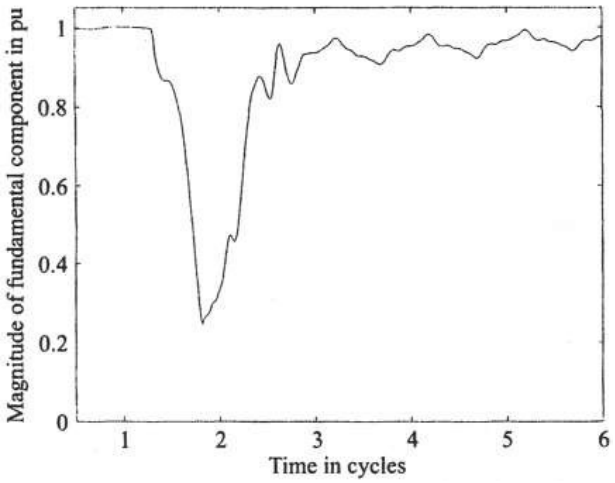

Figure 4.12 Half-cycle fundamental voltage for phase b of the sag shown in Fig. 4.9.

So far there is rather general agreement, both about using the rms value, and about taking the lowest rms value to determine the sag magnitude. But when the sag magnitude needs to be quantified in a number, the agreement is no longer there. One common practice is to characterize the sag through the remaining voltage during the sag. This is then given as a percentage of the nominal voltage. Thus, a 70% sag in a 120 volt system means that the voltage dropped to 84 V. This method of characterizing the sag is recommended in a number of IEEE standards (493–1998, 1159–1995, 1346–1998). The confusion with this terminology is clear. One could be tricked into thinking that a 70% sag refers to a drop of 70%, thus a remaining voltage of 30%. The recommendation is therefore to use the phrase "a sag down to 70%" [3]. The IEC has solved this ambiguity by characterizing the sag through the actual drop in the rms voltage [4]. This has somewhat become common practice in Europe. Characterizing a sag through its drop in voltage does not solve all problems however, because the next question will be: What is the reference voltage? There are arguments in favor of using the pre-fault voltage and there are arguments in favor of using the nominal voltage. The International Union of Producers and Distributors of Electrical Energy (Union International des Producteurs et Distributeurs d'Energie Electrique, UNIPEDE)

recommends to use the nominal voltage as a reference [5]. As several definitions are in use, it is important to clearly define the way in which the sag magnitude is defined. In this book sag magnitude is defined as the remaining voltage during the event.

Using the remaining voltage as the sag magnitude, leads to some obvious confusions. The main source of confusion is that a larger sag magnitude indicates a less severe event. In fact, a sag magnitude of 100% corresponds to no sag at all. The use of terms like "large sag" and "small sag" would be extremely confusing. Instead we will talk about a "deep sag" and a "shallow sag." A deep sag is a sag with a low magnitude; a shallow sag has a large magnitude. When referring to equipment behavior we will also use the terms "severe sag" and "mild sag." As far as magnitude is concerned, these terms correspond to "deep sag" and "shallow sag," respectively.

4.2.2 Theoretical Calculations

Consider the power system shown in Fig. 4.13, where the numbers (1 through 5) indicate fault positions and the letters (A through D) loads. A fault in the transmission network, fault position 1, will cause a serious sag for both substations bordering the faulted line. This sag is then transferred down to all customers fed from these two substations. As there is normally no generation connected at lower voltage levels, there is nothing to keep up the voltage. The result is that a deep sag is experienced by all customers A, B, C, and D. The sag experienced by A is likely to be somewhat less deep, as the generators connected to that substation will keep up the voltage. A fault at position 2 will not cause much voltage drop for customer A. The impedance of the transformers between the transmission and the sub-transmission system are large enough to considerably limit the voltage drop at high-voltage side of the transformer. The sag experienced by customer A is further mitigated by the generators feeding in to its local transmission substation. The fault at position 2 will, however, cause a deep sag at both subtransmission substations and thus for all customers fed from here (B, C, and D).

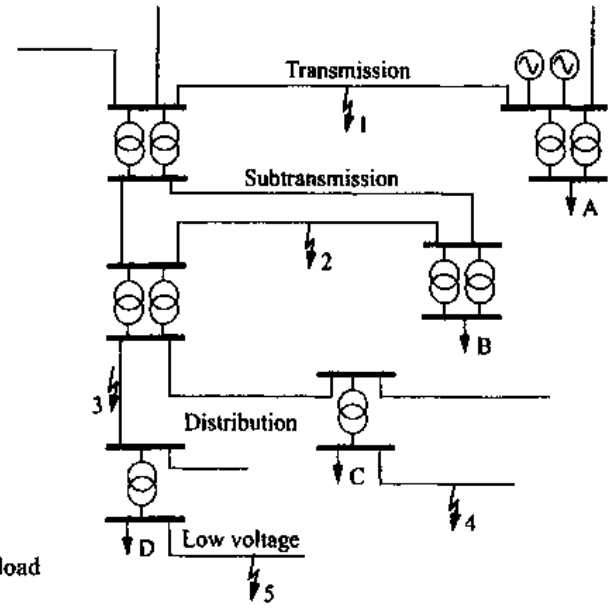

Figure 4.13 Distribution network with load positions and fault positions.

A fault at position 3 will cause a very deep sag for customer D, followed by a short or long interruption when the protection clears the fault. Customer C will only experience a deep sag. If fast reclosure is used in the distribution system, customer C will experience two or more sags shortly after each other for a permanent fault. Customer B will only experience a shallow sag due to the fault at position 3, again due to the transformer impedance. Customer A will probably not notice anything from this fault. Finally, fault 4 will cause a deep sag for customer C and a shallow one for customer D. For fault 5 the result is just the other way around: a deep sag for customer D and a shallow one for customer C. Customers A and B will not be influenced at all by faults 4 and 5.

To quantify sag magnitude in radial systems, the voltage divider model, shown in Fig. 4.14, can be used. This might appear a rather simplified model, especially for transmission systems. But as we will see in the course of this and further chapters, it has turned out to be a rather useful model to predict some of the properties of sags. In Fig. 4.14 we see two impedances: Z_S is the source impedance at the point-of-common coupling; and Z_F is the impedance between the point-of-common coupling and the fault. The point-of-common coupling is the point from which both the fault and the load are fed. In other words: it is the place where the load current branches off from the fault current. We will often abbreviate "point-of-common coupling" as pcc. In the voltage divider model, the load current before as well as during the fault is neglected. There is thus no voltage drop between the load and the pcc. The voltage at the pcc, and thus the voltage at the equipment terminals, can be found from

$$V_{sag} = \frac{Z_F}{Z_S + Z_F} E \tag{4.8}$$

In the remainder of this chapter, we will assume that the pre-event voltage is exactly 1 pu, thus $E = 1$. This results in the following expression for the sag magnitude

$$V_{sag} = \frac{Z_F}{Z_S + Z_F} \tag{4.9}$$

Any fault impedance should be included in the feeder impedance Z_F. We see from (4.9) that the sag becomes deeper for faults electrically closer to the customer (when Z_F becomes smaller), and for systems with a smaller fault level (when Z_S becomes larger).

Note that a single-phase model has been used here, whereas in reality the system is three-phase. That means that this equation strictly speaking only holds for three-phase faults. How the voltage divider model can be used for single-phase and phase-to-phase faults is discussed in Section 4.4.

Equation (4.9) can be used to calculate the sag magnitude as a function of the distance to the fault. Therefore we have to write $Z_F = z \times \mathcal{L}$, with z the impedance of the feeder per unit length and $\mathcal{L}$ the distance between the fault and the pcc, leading to

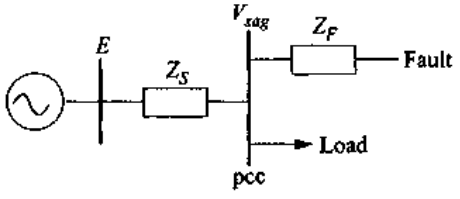

Figure 4.14 Voltage divider model for a voltage sag.

$$V_{sag} = \frac{z\mathcal{L}}{Z_S + z\mathcal{L}} \tag{4.10}$$

The sag magnitude as a function of the distance to the fault has been calculated for a typical 11 kV overhead line, resulting in Fig. 4.15. For the calculations a 150 mm^2 overhead line was used and fault levels of 750 MVA, 200 MVA, and 75 MVA. The fault level is used to calculate the source impedance at the pcc, the feeder impedance to calculate the impedance between the pcc and the fault. It was assumed that the source impedance is purely reactive, thus $Z_S = j0.161\,\Omega$ for the 750 MVA source. The impedance of the 150 mm^2 overhead line is $0.117 + j0.315\,\Omega$ per km [10].

As expected, the sag magnitude increases (i.e., the sag becomes less severe) for increasing distance to the fault and for increasing fault level. We also see that faults at tens of kilometers distance may still cause a severe sag.

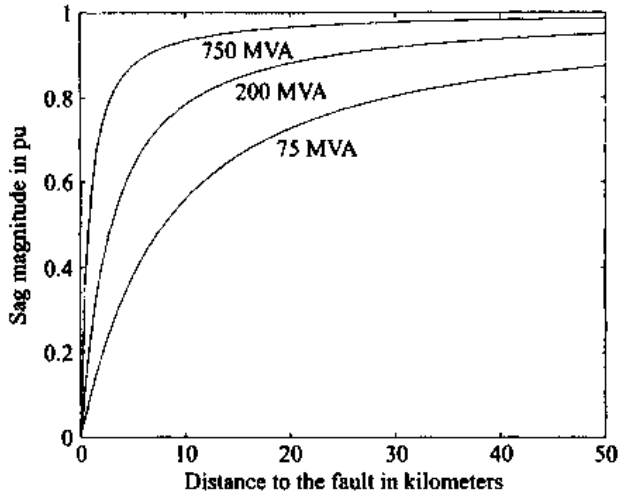

Figure 4.15 Sag magnitude as a function of the distance to the fault, for faults on an 11 kV, 150 mm^2 overhead line.

4.2.2.1 Influence of Cross Section. Overhead lines of different cross section have different impedance, and lines and cables also have different impedance. It is thus to be expected that the cross section of the line or cable influences the sag magnitude as well. To show this influence, Fig. 4.16 plots the sag magnitude at the pcc

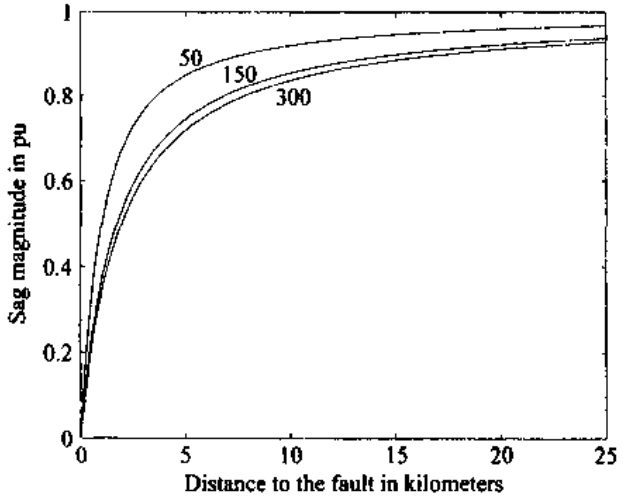

Figure 4.16 Sag magnitude versus distance, for 11 kV overhead lines with different cross sections.

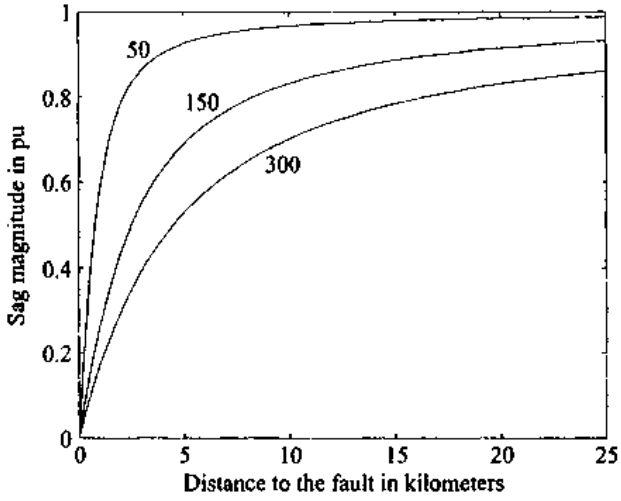

Figure 4.17 Sag magnitude versus distance, for 11 kV underground cables with different cross sections.

as a function of the distance between the fault and the pcc, for 11 kV overhead lines with three different cross sections: 50, 150, and 300 mm^2. A source impedance of 200 MVA has been used. The smaller the cross section, the higher the impedance of the feeder and thus the lower the voltage drop. For overhead lines, the influence is rather small as the reactance dominates the impedance. For underground cables, the influence is much bigger as shown in Fig. 4.17, again for cross sections of 50, 150, and 300 mm^2. The inductance of cables is significantly smaller than for overhead lines, so that the resistance has more influence on the impedance and thus on the sag magnitude. The impedance values used to obtain Fig. 4.16 and Fig. 4.17 are given in Table 4.1. All impedances are for an 11 kV voltage level.

TABLE 4.1 Line and Cable Impedances for 11 kV Feeders Used in Figs. 4.16 and 4.17

	Impedance	
Cross Section	Overhead Line	Cable
50 mm^2	$0.363 + j0.351\,\Omega$	$0.492 + j0.116\,\Omega$
150 mm^2	$0.117 + j0.315\,\Omega$	$0.159 + j0.097\,\Omega$
300 mm^2	$0.061 + j0.298\,\Omega$	$0.079 + j0.087\,\Omega$

Source: Data obtained from [10].

4.2.2.2 Faults behind Transformers. The impedance between the fault and the pcc in Fig. 4.14 not only consists of lines or cables but also of power transformers. As transformers have a rather large impedance, among others to limit the fault level on the low-voltage side, the presence of a transformer between the fault and the pcc will lead to relatively shallow sags.

To show the influence of transformers on the sag magnitude, consider the situation shown in Fig. 4.18: a 132/33 kV transformer is fed from the same bus as a 132 kV line. A 33 kV line is fed from the low-voltage side of the transformer. Fault levels are 3000 MVA at the 132 kV bus, and 900 MVA at the 33 kV bus. In impedance terms, the source impedance at the 132 kV bus is 5.81 Ω, and the transformer impedance is 13.55 Ω, both referred to the 132 kV voltage level. The sensitive load for which we

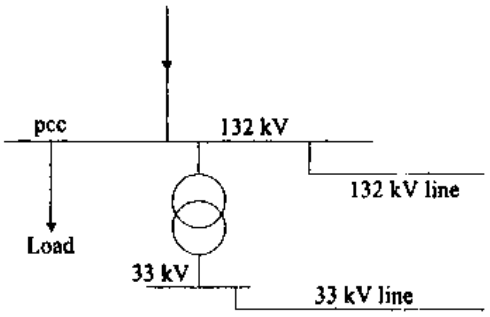

Figure 4.18 Power system with faults at two voltage levels.

want to calculate the sag magnitude is fed from the 132 kV bus via another 132/33 kV transformer. We can again use (4.9), where $Z_S = 5.81\,\Omega$, $Z_F = 13.55\,\Omega + z \times \mathcal{L}$, z is the feeder impedance per unit length, and $\mathcal{L}$ the distance between the fault and the transformer's secondary side terminals. The feeder impedance must also be referred to the 132 kV level: $z = \left(\frac{132kV}{33kV}\right)^2 \times 0.3\,\Omega/\text{km}$ when the feeder impedance is $0.3\,\Omega/\text{km}$ at 33 kV. The results of the calculations are shown in Fig. 4.19 for faults on the 33 kV line (upper curve) and for faults on the 132 kV line (lower curve). We see that sags due to 33 kV faults are less severe than sags due to 132 kV faults. Not only does the 33 kV curve start off at a higher level (due to the transformer impedance), it also rises much faster. The latter is due to the fact that the feeder impedance seen from the 132 kV level is $(132/33)^2 = 16$ times as high as that seen from the 33 kV level.

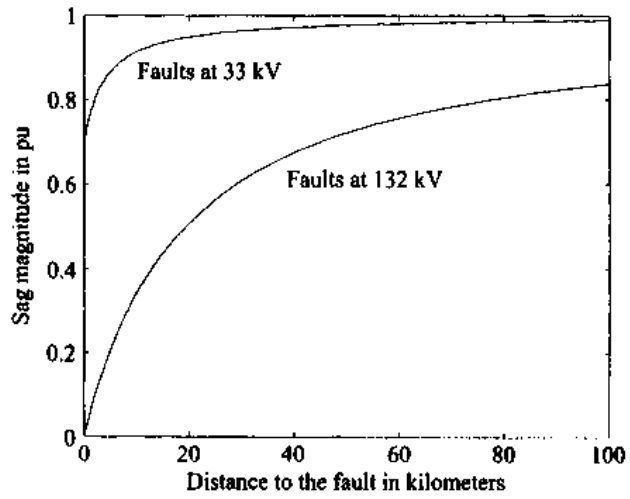

Figure 4.19 Comparison of sag magnitude for 132 kV and 33 kV faults.

4.2.2.3 Fault Levels. Often the source impedance at a certain bus is not immediately available, but instead the fault level is. One can of course translate the fault level into a source impedance and use (4.9) to calculate the sag magnitude. But one may calculate the sag magnitude directly if the fault levels both at the pcc and at the fault position are known. Let S_{FLT} be the fault level at the fault position and S_{pcc} at the point-of-common coupling. For a rated voltage V_n the relations between fault level and source impedance are as follows:

$$S_{FLT} = \frac{V_n^2}{Z_S + Z_F} \tag{4.11}$$

$$S_{pcc} = \frac{V_n^2}{Z_S} \tag{4.12}$$

With (4.9) the voltage at the pcc can be written as

$$V_{sag} = 1 - \frac{S_{FLT}}{S_{pcc}} \tag{4.13}$$

We use (4.13) to calculate the magnitude of sags behind transformers. For this we use typical fault levels in the U.K. power system [13]:

400 V	20 MVA
11 kV	200 MVA
33 kV	900 MVA
132 kV	3000 MVA
400 kV	17000 MVA

Consider a fault at a typical 11 kV bus, i.e., with a fault level of 200 MVA. The voltage sag at the high-voltage side of the 33/11 kV transformer is from (4.13)

$$V_{sag} = 1 - \frac{200\ \text{MVA}}{900\ \text{MVA}} = 78\%$$

In a similar way the whole of Table 4.2 has been filled. The zeros in this table indicate that the fault is at the same or at a higher voltage level. The voltage drops to a low value in such a case. We can see from Table 4.2 that sags are significantly damped when they propagate upwards in the power system. In a sag study we typically only have to take faults one voltage level down into account. And even those are seldom of serious concern. An exception here could be sags due to faults at 33 kV with a pcc at 132 kV. They could lead to sags down to 70%.

TABLE 4.2 Upward Propagation of Sags

	Point-of-Common Coupling			
Fault Point	11 kV	33 kV	132 kV	400 kV
400 V	90%	98%	99%	100%
11 kV	0	78%	93%	99%
33 kV	0	0	70%	95%
132 kV	0	0	0	82%

4.2.2.4 Critical Distance. Equation (4.10) gives the voltage magnitude as a function of the distance to the fault. From this equation we can obtain the distance at which a fault will lead to a sag of a certain magnitude. If we assume equal X/R ratio of source and feeder, we obtain

$$\mathcal{L}_{crit} = \frac{Z_S}{Z} \times \frac{V}{1 - V} \tag{4.14}$$

We refer to this distance as the critical distance for a voltage V. Suppose that a piece of equipment trips when the voltage drops below a certain level (the critical voltage). The

definition of critical distance is such that each fault within the critical distance will cause the equipment to trip. This concept will be used in Section 6.5 to estimate the expected number of equipment trips.

If we assume further that the number of faults is proportional to the line length within the critical distance, we would expect that the number of sags below a level V is proportional to $V/(1-V)$. Another assumption is needed to arrive at this conclusion. Every feeder connected to every pcc needs to be infinitely long without any branching off. Of course this is not the case in reality. Still this equation has been compared with a number of large power quality surveys. The results are shown in Fig. 4.20. Power quality survey results in the United States [11], [12], in the U.K. [13] and in Norway [16] are indicated as dots, the theoretical curve is shown as a solid line. The correspondence is good, despite the obviously serious approximations made.

Even though (4.14) only holds for radial systems, it gives a generally usable relation between the number of voltage sags and the voltage. The expression clearly shows that the majority of sags are shallow, a fact confirmed by most measurements.

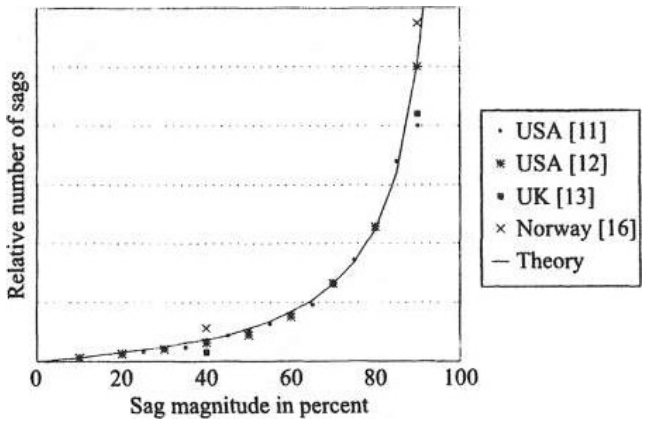

Figure 4.20 Number of sags versus magnitude: theoretical results (solid line) versus monitoring results (dots).

4.2.3 Example of Calculation of Sag Magnitude

We will apply the theoretical concepts developed in the previous sections to the supply shown schematically in Fig. 4.21. This same example will be used again in forthcoming parts of this book. The supply shown in Fig. 4.21 is the existing supply to an industrial customer somewhere in the North of England [15]. The sensitive load consists of several large ac and dc adjustable-speed drives. The dc drives are fed via dedicated transformers at 420 V, the more modern ac drives at 660 V. Most of the data used for the various calculations below have been obtained from the local utility. Where no data was available, data have been used which was considered "as typical as possible." Like often in these kind of studies, the collection of the data requires at least as much effort as the actual calculations. In the rest of this book it will always be assumed that all the required data is readily available.

The first step in a sag analysis is to recognize the possible pcc's. For any fault on one of the 11 kV feeders, the fault current will flow through the STU-11 bus, but not further towards the load. The STU-11 bus is thus the pcc for all faults within the 11 kV network. In the same way, the ROS-33 bus is the pcc for faults on any of the 33 kV feeders. The other possible pcc's are PAD-132 and PAD-400. To calculate the sag magnitude we need the source impedance and the feeder impedance. The source

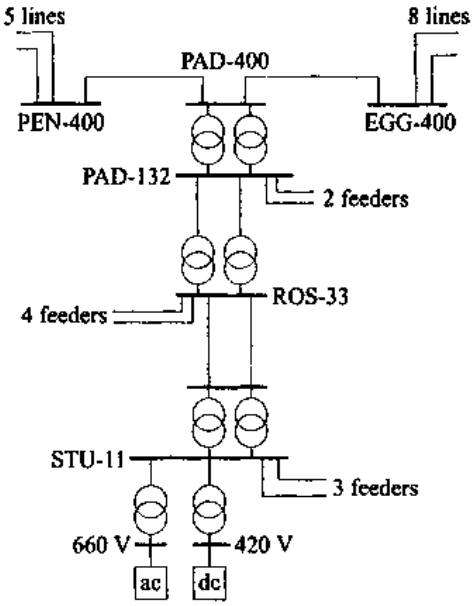

Figure 4.21 Example of power supply to be used for voltage sag calculations.

impedance is given in Table 4.3, the feeder impedance in Table 4.4. All impedances are given for a 100 MVA base. Finally, Table 4.5 gives the transformer connection and neutral grounding. This information is needed in later sections, when unbalanced sags are discussed.

For now we ignore the fact that the impedances are complex and use the absolute values for our calculations. We will come back to the complex impedances in Section 4.5 when phase-angle jumps are discussed. For faults at 11 kV we obtain for the impedances: $z = 27.75\%$ per km and $Z_S = 66.08\%$. The critical distance can be calculated from $\mathcal{L}_{crit} = 2.381 \times \frac{V}{1-V}$.

Calculations for the critical distances at 33 kV and 132 kV proceed in exactly the same way as for the 11 kV system. The results of these calculations are shown in Table 4.6. We see that there are two columns for the 400 kV system in Table 4.3 and in Table 4.6. This has to do with the fact that there are two possible sources for the short-circuit power. If the fault is somewhere between PAD-400 and PEN-400 the fault current will be delivered from the direction of EGG-400. Thus, for such a fault, the impedance Z_S is the source impedance as seen in the direction of EGG-400. The critical distances resulting from this source impedance are shown in Table 4.6 in the column labeled "toward PEN-400." Note that for this the source impedance in the direction of EGG-400 has been used. For faults in the direction of EGG-400, the source impedance in the direction of PEN-400 has been used. Those results are shown in the column labeled "toward EGG-400."

When interpreting Table 4.6 one should realize that these values hold for a radial system with infinitely long lines without any side branches. In reality all feeders have a finite length. In this system the maximum distance from the pcc for a fault at 11 kV is 5 km. The distance to the fault can thus not be more than 5 km and the magnitude of the most shallow sag due to a fault at 11 kV is

$$V_{sag} = \frac{Z_F}{Z_S + Z_F} = \frac{5 \times 0.2727}{5 \times 0.2727 + 0.6608} = 67\% \tag{4.15}$$

Figure 4.22 plots sag magnitude versus distance for faults at all the voltage levels in Fig. 4.21. The horizontal scale is determined by the maximum length of the feeders at that

TABLE 4.3 Source Impedance for the Supply Shown in Fig. 4.21, at a 100 MVA Base

	Zero Sequence	Positive and Negative Sequence
11 kV	787 + *j*220%	4.94 + *j*65.9%
33 kV	251%	1.23 + *j*18.3%
132 kV	0.047 + *j*2.75%	0.09 + *j*2.86%
400 kV		
From EGG	0.329 + *j*2.273%	0.084 + *j*1.061%
From PEN	0.653 + *j*5.124%	0.132 + *j*1.94%

TABLE 4.4 Feeder Data for the Supply Shown in Fig. 4.21

	Positive and Negative Sequence	Zero Sequence	Max Length
11 kV	9.7 + *j*26%/km	18.4 + *j*112%/km	5 km
33 kV	1.435 + *j*3.102%/km	2.795 + *j*15.256%/km	10 km
132 kV	0.101 + *j*0.257%/km	0.23 + *j*0.65%/km	2 km
400 kV	0.001 + *j*0.018%/km	0.007 + *j*0.050%/km	> 1000 km

TABLE 4.5 Transformer Connections and Neutral Grounding for the Supply Shown in Fig. 4.21

Voltage Level	Transformer Winding Connection	Neutral Grounding at LV Side
400 kV		solidly grounded
400/132 kV	YY autotransformer	solidly grounded
132/33 kV	Star – Delta	resistance grounded through zig-zag transformer
33/11 kV	Delta – Star	resistance grounded
11 kV/660 V and 11 kV/420 V	Delta – Star	solidly grounded

TABLE 4.6 Critical Distance Calculation for the Network Shown in Fig. 4.21, According to (4.14)

	11 kV	33 kV	132 kV	400 kV Toward PEN-400	400 kV Toward EGG-400
z	27.27%	3.418%	0.276%	0.018%	0.018%
Z_S	66.08%	18.34%	2.861%	1.064%	1.944%
$V = 10\%$	0.3 km	0.6 km	1.2 km	6.6 km	12.0 km
$V = 30\%$	1.0 km	2.3 km	4.4 km	25.3 km	46.3 km
$V = 50\%$	2.4 km	5.4 km	10.4 km	59.1 km	108 km
$V = 70\%$	5.6 km	12.5 km	24.2 km	138 km	252 km
$V = 90\%$	21.4 km	48.3 km	93.3 km	532 km	972 km

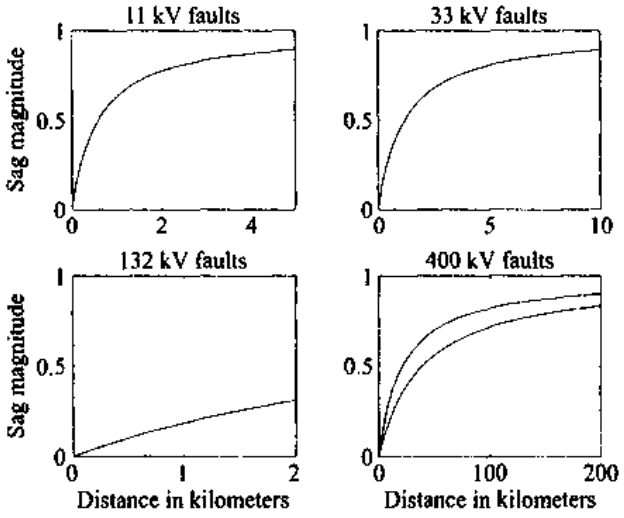

Figure 4.22 Magnitude versus distance for faults at various voltage levels in the supply in Fig. 4.21.

voltage level. For 400 kV a length of 200 km has been taken. The short length of the 132 kV feeders makes that sags due to faults at 132 kV are always very deep.

4.2.4 Sag Magnitude in Non-Radial Systems

In Section 4.2.2 we discussed sag magnitude versus distance in radial systems. Radial systems are common in low-voltage and medium-voltage networks. At higher voltage levels other supply arrangements are common. Some typical cases will be discussed below. We will also present a general way of calculating sag magnitudes in meshed systems.

4.2.4.1 Local Generators. The connection of a local generator to a distribution network, as shown in Fig. 4.23, mitigates voltage sags of the indicated load in two different ways. The generator increases the fault level at the distribution bus, which mitigates voltage sags due to faults on the distribution feeders. This especially holds for a weak system. For a strong system, the fault level cannot be increased much without the risk of exceeding the maximum-allowable short-circuit current of the switchgear. The installation of local generation requires a larger impedance of the feeding transformer.

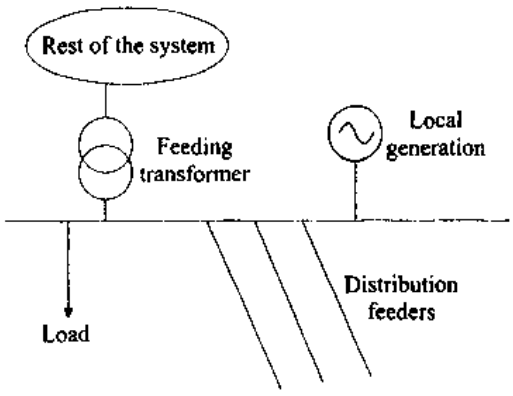

Figure 4.23 Connection of a local generator to a distribution bus.

A local generator also mitigates sags due to faults in the rest of the system. During such a fault the generator keeps up the voltage at its local bus by feeding into the fault. An equivalent circuit to quantify this effect has been drawn in Fig. 4.24: Z_4 is the impedance of the local generator during the fault (typically the transient impedance); Z_1 the source impedance at the pcc; Z_2 the impedance between the fault and the pcc; and Z_3 the impedance between the generator bus and the pcc. Note that the concept of point-of-common coupling strictly speaking no longer holds. This concept, which was introduced for radial networks, assumes one single flow of fault current. By adding a generator close to the load a second flow of fault current is introduced. The pcc as indicated in Fig. 4.24 is the point-of-common coupling before the introduction of the local generator. Without the local generator the voltage at the equipment terminals would be equal to the voltage at the pcc. When a local generator is present, the voltage at the equipment terminals during the sag equals the voltage on the generator bus. This voltage is related to the voltage at the pcc according to the following equation:

$$(1 - V_{sag}) = \frac{Z_4}{Z_3 + Z_4}(1 - V_{pcc}) \tag{4.16}$$

The voltage drop at the generator bus is $\frac{Z_4}{Z_3+Z_4}$ times the voltage drop at the pcc. The voltage drop becomes smaller for larger impedance to the pcc (weaker connection) and for smaller generation impedance (larger generator). The fault contribution of the rest of the system at the generator bus is often mainly determined by the impedance of the feeding transformer. In that case the reduction in voltage drop is approximately equal to the generator contribution to the fault level at the generator bus. Thus, if the generator delivers 50% of the fault current, a sag down to 40% at the pcc (60% voltage drop) will be reduced to a sag down to 70% (30% voltage drop) at the equipment terminals. From (4.16) we can also conclude that there is a non-zero minimum sag magnitude. Even a fault at the pcc will no longer cause a sag down to zero voltage but a sag of magnitude

$$V_{min} = \frac{Z_3}{Z_3 + Z_4} \tag{4.17}$$

For the above-mentioned system, where the local generator is responsible for 50% of the fault level at the generator bus, the lowest sag magnitude due to a fault at a higher voltage level is 50%. During a fault not only local generators contribute to the fault but also induction motors. Using the above reasoning we can conclude that the minimum voltage at the plant bus equals the relative fault level contribution of the induction motors. We will discuss induction motors in more detail in Section 4.8.

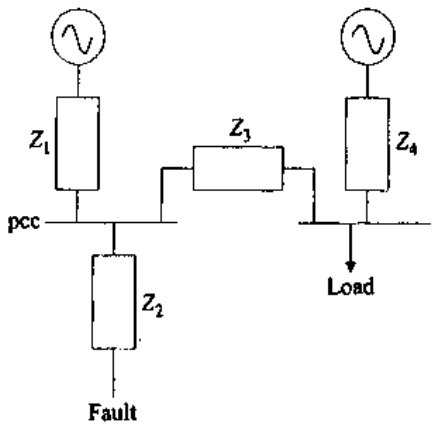

Figure 4.24 Equivalent circuit for system with local generation.

EXAMPLE An example of a system with on-site generation is given in Fig. 4.25: the industrial system is fed from a 66 kV, 1700 MVA substation via two 66/11 kV transformers in parallel. The fault level at the 11 kV bus is 720 MVA, which includes the contribution of two 20 MVA on-site generators with a transient reactance of 17%. The actual industrial load is fed from the 11 kV bus, for which we will calculate the sag magnitude due to faults at 66 kV. The feeder impedance at 66 kV is 0.3 Ω/km.

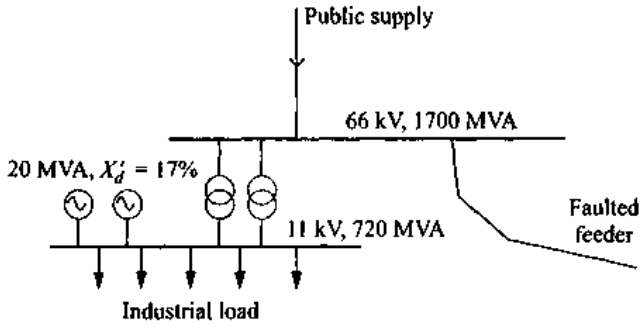

Figure 4.25 Industrial distribution system with on-site generation.

With reference to (4.16) and Fig. 4.24, we get the following impedance values for this system (referred to 66 kV):

$$Z_1 = 2.56\,\Omega$$
$$Z_2 = 0.3\,\Omega/\text{km} \times \mathcal{L}$$
$$Z_3 = 6.42\,\Omega$$
$$Z_4 = 18.5\,\Omega$$

The calculation results are shown in Fig. 4.26. The bottom curve gives the sag magnitude at the 11 kV bus for faults at a 66 kV feeder, when the 11 kV generator is not in operation. In that case the sag magnitude at 11 kV equals the sag magnitude at 66 kV because all load currents have been neglected. The top curve gives the sag magnitude at the 11 kV bus with on-site generator connected. Due to the generator keeping up the voltage at the 11 kV bus, the sag magnitude never drops below 26%. There are two methods to further improve the supply. One can increase the number or size of the generators, which corresponds to decreasing Z_4 in (4.16). Alternatively one can increase Z_3, which leads to a lower fault level at the 11 kV bus.

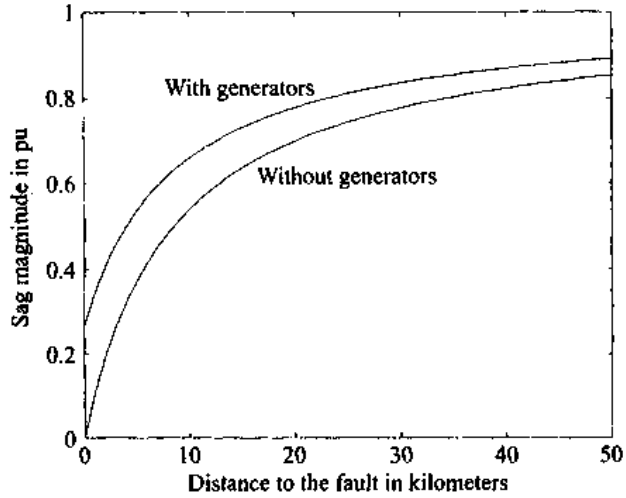

Figure 4.26 Sag magnitude versus distance, with and without on-site generator.

EXAMPLE Another example of the use of (4.16) is given by means of Fig. 4.27. This figure represents half of the transmission system part of the example in Fig. 4.21, containing the substations PAD-400 and EGG-400, plus 30 km of overhead 400 kV line in between them. The impedances have the following values (in % at a 100 MVA base), with $\mathcal{L}$ the distance between EGG-400 and the fault:

$$Z_1 = 1.4\%$$
$$Z_2 = 0.018\%/\text{km} \times \mathcal{L}$$
$$Z_3 = 0.54\%$$
$$Z_4 = 1.94\%$$

The impedance Z_4 represents the source contribution from PEN-400 at PAD-400; Z_3 represents the impedance of 30 km line (0.018%/km); Z_2 the impedance between EGG-400 and the fault, and Z_1 the contribution through the non-faulted lines at EGG-400 (excluding the contribution from PAD-400) during the fault. The latter impedance is likely to be different for faults on different lines. In this study we assumed it to be simply equal to the contribution of all lines at EGG-400 minus the line to PAD-400. As there are a total of nine lines connected to EGG-400 the error made will not be very big.

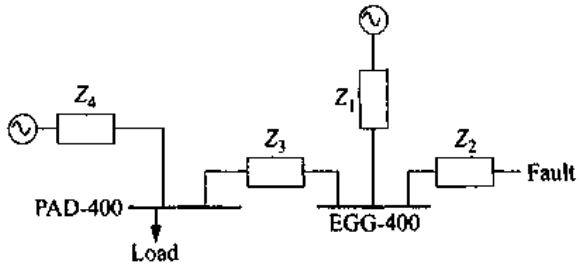

Figure 4.27 Circuit diagram representation of two transmission substations. The sensitive load is fed from the substation on the left.

For faults to the right of EGG-400 we can use (4.16) to calculate the voltage at PAD-400, knowing the voltage at EGG-400. The latter can be obtained from the voltage divider equation with the source impedance formed by the parallel connection of Z_1 and $Z_3 + Z_4$. Note that we still neglect all load currents, so that both source voltages are equal in magnitude and in phase and can be replaced by one source. For faults between PAD-400 and EGG-400 the voltage divider model will give the required voltage directly. The source impedance is now formed by Z_4; the feeder impedance is 0.018%/km × $\mathcal{L}$, with $\mathcal{L}$ the distance between PAD-400 and the fault. The resulting sag magnitude as a function of the distance to the fault is shown in Fig. 4.28. For

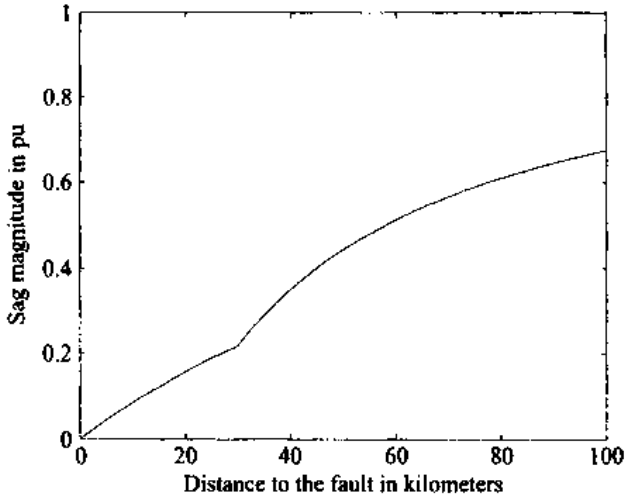

Figure 4.28 Sag magnitude as a function of the distance to the fault, for transmission systems.

distances up to 30 km the sag magnitude changes with distance like in a radial system; for larger distances the magnitude increases faster. Thus, the sag is less severe than for a fault at the same distance in a radial system.

4.2.4.2 Subtransmission Loops. At subtransmission level, the networks often consist of several loops—a typical example is shown in Fig. 4.29. The transmission system is connected to the subtransmission system through two or three transformers. From the busses at the low-voltage side of these transformers a number of substations are fed via a loop. Such a network configuration is also found in industrial power systems. Often the loop only consists of two branches in parallel. The mathematical expressions that will be derived below can also be used to calculate voltage sags due to faults on parallel feeders.

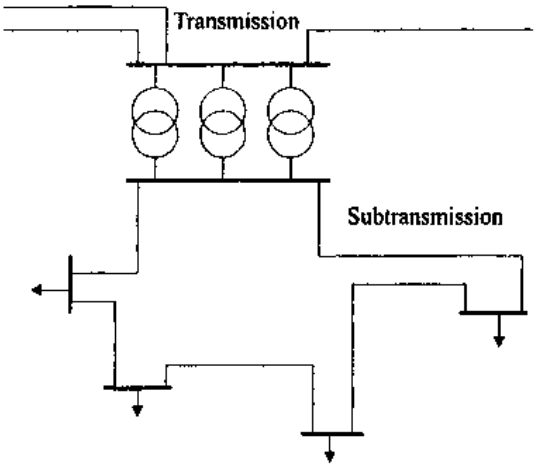

Figure 4.29 Example of subtransmission loop.

To calculate the sag magnitude we need to identify the load bus, the faulted branch, and the non-faulted branch. Knowing these the equivalent scheme in Fig. 4.30 is obtained, where Z_0 is the source impedance at the bus from which the loop is fed; Z_1 is the impedance of the faulted branch of the loop; Z_2 is the impedance of the non-faulted branch; and p is the position of the fault on the faulted branch ($p = 0$ corresponds to a fault at the bus from which the load is fed, $p = 1$ corresponds to a fault at the load bus).

From Fig. 4.30 the voltage at the load bus can be calculated, resulting in the following expression:

$$V_{sag} = \frac{p(1-p)Z_1^2}{Z_0(Z_1+Z_2)+pZ_1Z_2+p(1-p)Z_1^2} \tag{4.18}$$

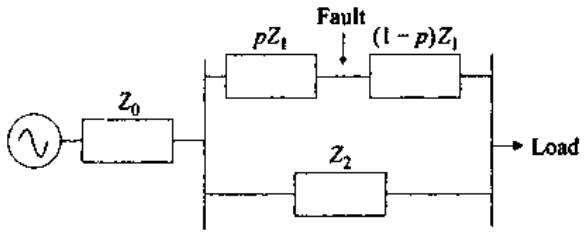

Figure 4.30 Equivalent circuit for subtransmission loop.

The voltage is zero for $p = 0$ (fault at the main subtransmission bus) and for $p = 1$ (fault at the load bus) and has a maximum somewhere in between.

EXAMPLE Consider the system shown in Fig. 4.31: a 125-km 132 kV loop connecting a number of substations. Only the substation feeding the load of interest is shown in the figure. This substation is located at 25 km from the main substation. The fault level at the point-of-supply is 5000 MVA and the feeder impedance 0.3 Ω/km. Faults occur both in the 25 km part and in the 100 km part of the loop, so that both may form the faulted branch. For a fault on the 25 km branch we substitute in (4.18): $Z_1 = 25z$ and $Z_2 = 100z$, with z the feeder impedance per km. For a fault on the 100 km branch, we get $Z_1 = 100z$ and $Z_2 = 25z$.

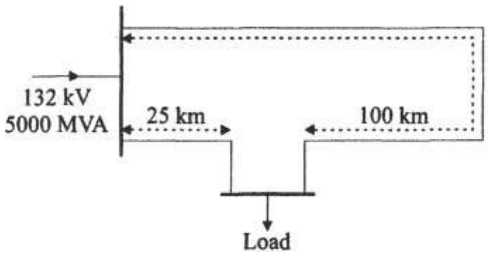

Figure 4.31 Loop system operating at 132 kV.

Figure 4.32 gives the magnitudes of sags due to faults in the 132 kV subtransmission loop. The dashed (top) curve gives the sag magnitude for faults on the 100 km branch, the solid (bottom) curve holds for the 25 km branch. Note that the horizontal scale corresponds to 25 km for the bottom curve and to 100 km for the top curve. Figure 4.33 gives the sag magnitudes for the 100 km and 25 km feeder as a function of the actual distance between the fault and the main 132 kV bus. For comparison, the magnitude is also given for sags due to faults at a radial feeder from the same main 132 kV bus (dotted curve).

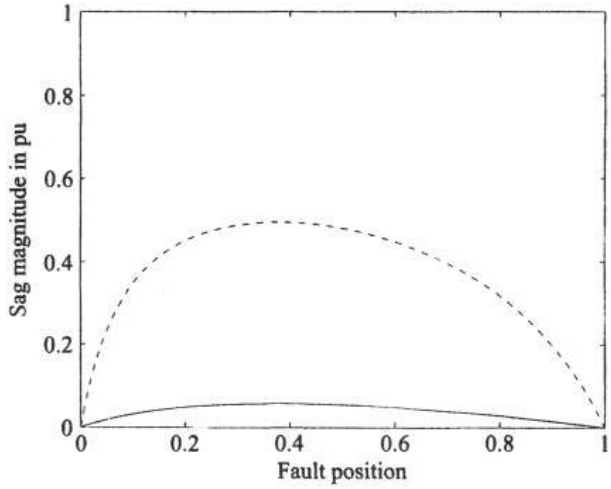

Figure 4.32 Sag magnitudes for faults on a 132 kV loop.

We see from Fig. 4.32 and Fig. 4.33 that each fault on the loop will cause the voltage to drop below 50% of the nominal voltage. A sag due to a fault on a loop is always lower than due to a fault on a radial feeder. Faults close to the point-of-supply will lead to a deep sag. Faults close to the load too. Somewhere in between there is a

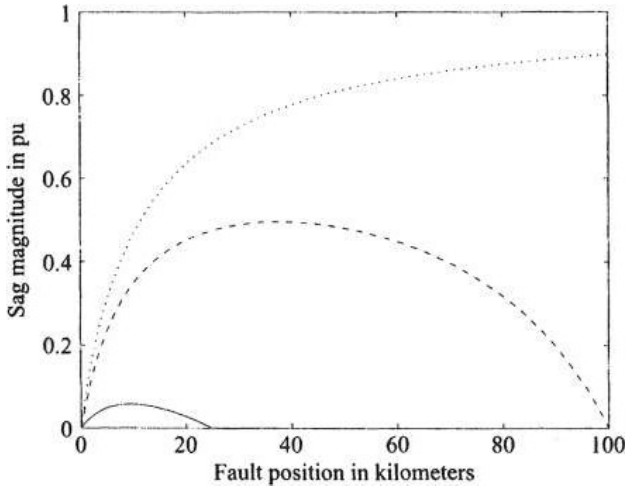

Figure 4.33 Sag magnitude versus distance, for faults on loops (solid and dashed lines) and on a radial feeder (dotted line).

maximum magnitude of the voltage sag due to a fault. The longer the line the higher the maximum. We see from the figure that this maximum is not necessarily in the middle of the branch. The maximum voltage has been calculated as a function of the system parameters. The results are shown in Fig. 4.34 and in Fig. 4.35. To obtain these graphs (4.18) has been rewritten as a function of $z_1 = \frac{Z_1}{Z_0}$ and $z_2 = \frac{Z_2}{Z_0}$; z_1 is the relative impedance of the faulted branch and z_2 of the non-faulted branch. Figure 4.34 gives the maximum voltage as a function of z_2 for various values of z_1 and Fig. 4.35 the other way around. From both figures it follows that the sags become less severe (higher maximum) when the faulted branch becomes longer (higher impedance) and when the non-faulted branch becomes shorter. This can be explained as follows. A longer faulted branch means that the fault can be further away from both busses. A shorter non-faulted branch gives stronger voltage support at the load bus. These relations can easily be understood by considering a fault in the middle of the faulted branch.

The range of values used for both z_1 and z_2 is between 1 and 10. For smaller values of z_1 the sag magnitude becomes very small. Larger values do not give realistic systems. One has to realize that $\frac{1}{Z_0}$ is proportional to the fault level at the point-of-supply. Thus, z_1 and z_2 indicate the variation in fault level for different points in the system. A value of 10 implies that there is at least a factor of six between the highest and the lowest fault level. (Note that the two branches are operated in parallel.) Such a large

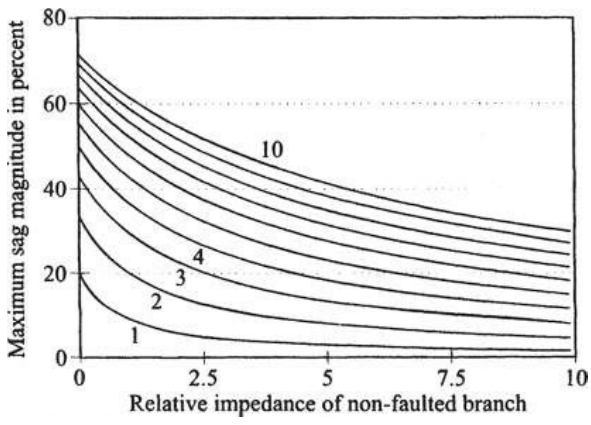

Figure 4.34 Most shallow sag for a fault in a loop, as a function of the impedance of the non-faulted branch for various values of the impedance of the faulted branch.

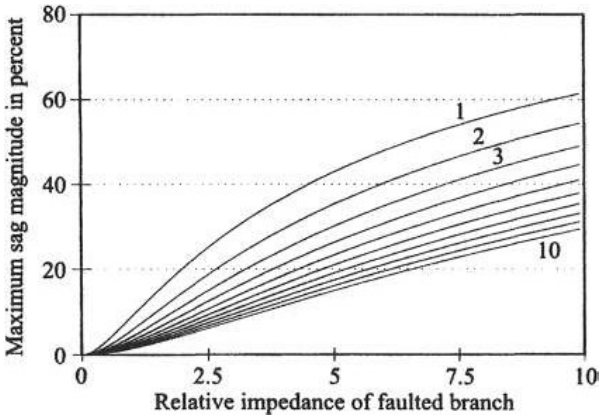

Figure 4.35 Most shallow sag for a fault in a loop, as a function of the impedance of the faulted branch, for various values of the impedance of the non-faulted branch.

range in fault level is rather unlikely in subtransmission systems, as it will lead to large variations in voltage due to load variations.

The general conclusion from Figs. 4.34 and 4.35 is that faults on a loop lead to sags with a magnitude well below 50%, irrespective of the voltage levels. As mentioned before a parallel feeder is a special case of a loop: one in which $z_1 = z_2$. For these we can conclude that the most shallow sag has a magnitude between 20% and 30% for most systems.

4.2.4.3 Branches from Loops. When a load is fed from a loop, like the ones discussed above, a fault on a branch away from that loop will also cause a sag. In that case it is often possible to model the system as shown in Fig. 4.36. The feeder to the fault does not necessarily have to be a single feeder, but could, e.g., represent the effective impedance of another loop. The equivalent circuit for the system in Fig. 4.36 is shown in Fig. 4.37: Z_1 is the source impedance at the main subtransmission bus; Z_2 is the impedance between that bus and the bus from which the load is fed; Z_3 is the impedance between the bus from which the load is fed and the bus from which the fault is fed; Z_4 and Z_5 are the impedances between the latter bus and the main subtransmission bus and the fault, respectively. The voltage at the load bus is found from

$$V_{sag} = \frac{Z_5Z_2 + Z_5Z_3 + Z_5Z_4 + Z_4Z_3}{Z_1Z_2 + Z_1Z_3 + Z_1Z_4 + Z_5Z_2 + Z_5Z_3 + Z_5Z_4 + Z_4Z_2 + Z_4Z_3} \tag{4.19}$$

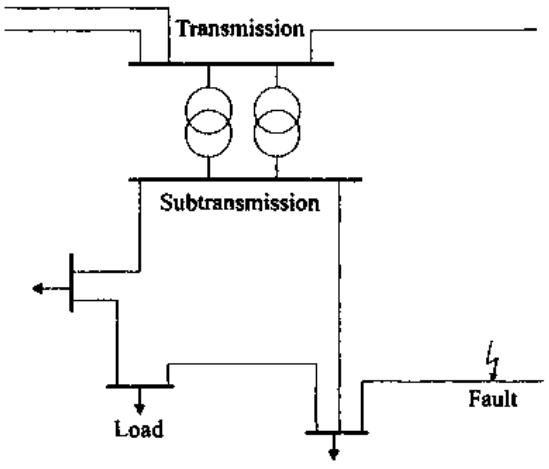

Figure 4.36 System with a branch away from a loop.

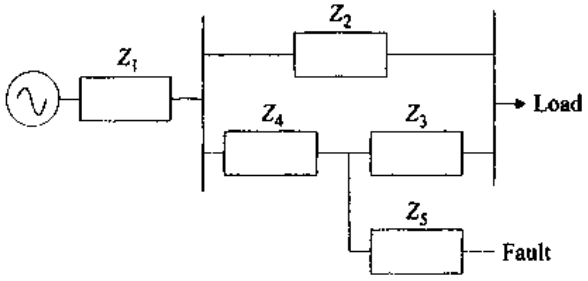

Figure 4.37 Equivalent circuit for system with a branch away from a loop, as in Fig. 4.36.

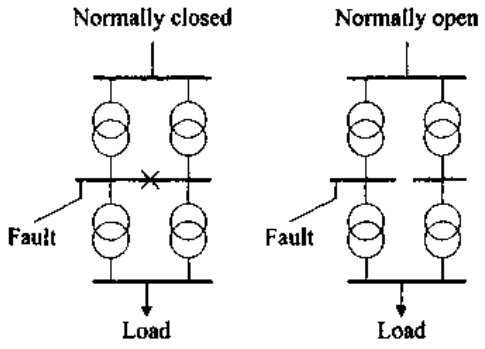

Figure 4.38 Industrial system with breaker at intermediate voltage level closed (left) and open (right).

The same expression can be used to assess an industrial system in which bus splitting is used at an intermediate voltage level. An example of the supply configuration in a large industrial network is shown in Fig. 4.38. In the left example, two transformers are operated in parallel. Typically both transformers feed into a different part of the substation bus, separated through a circuit breaker. This enables an uninterrupted supply after a bus fault. In the network on the right the substation consists of two separate busses, typically with a normally open breaker in between. In case the breaker at an intermediate voltage level is closed, the sag due to a fault at this voltage level will be experienced fully by the load. In case the breaker is open the sag will be mitigated according to (4.19). On the one hand, the source impedance will be less when the breaker is open, leading to a deeper sag at the intermediate voltage level. But on the other hand, the sag at the load bus will be less deep than at the faulted intermediate voltage level.

EXAMPLE Consider the system shown in Fig. 4.38 with the following voltages and fault levels: 2500 MVA at 66 kV, 500 MVA at 11 kV (with the breaker closed), and 50 MVA at 660 V. When the breaker connecting the two 11 kV busses is open, the circuit diagram in Fig. 4.37 can be used to calculate the sag magnitude at the 660 V bus for a fault at an 11 kV feeder. From the fault levels given, the values of various impedances can be calculated (all referred to 11 kV):

$$Z_1 = 0.048\,\Omega$$
$$Z_2 = 4.75\,\Omega$$
$$Z_3 = 4.36\,\Omega$$
$$Z_4 = 0.388\,\Omega$$
$$Z_5 = 0.3\,\Omega/\text{km} \times \mathcal{L}$$

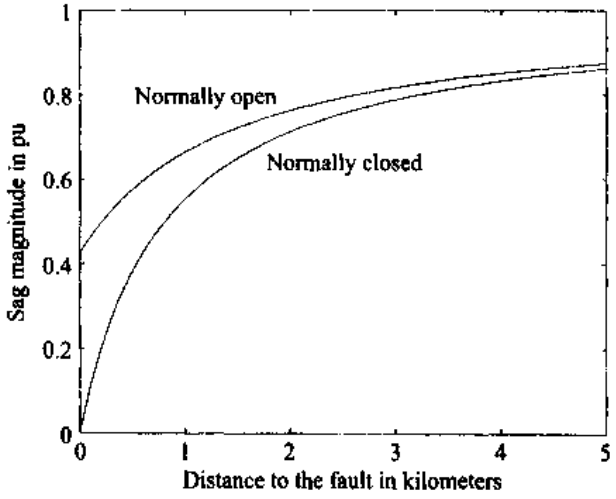

Figure 4.39 Sag magnitude versus distance to the fault, for an industrial system with and without bus-splitting applied to the 11 kV bus.

with $\mathcal{L}$ the distance between the 11 kV bus and the fault, and a feeder impedance of 0.3 Ω/km. When the 11 kV breaker is closed, the system can be treated like a radial system with a source impedance equal to $Z_1 + \frac{1}{2}Z_4$ and a feeder impedance equal to Z_5. A comparison between these two ways of system operation is given in Fig. 4.39. Bus-splitting (operating the system with the 11 kV breaker normally open) clearly limits the influence of 11 kV faults on the load. The improvement is especially large for nearby faults. For faults further away from the 11 kV substation the effect becomes smaller. But industrial medium-voltage systems are seldom larger than a few kilometers. We will come back to this and other ways of mitigating sags through system design and operation in Chapter 7.

4.2.4.4 Parallel Operation across Voltage Levels. In many countries the subtransmission system is not fed from the transmission system at one point but at a number of points, resulting in a system structure similar to the one shown in Fig. 4.40. The number of supply points for the subtransmission system varies from country to country. The 275 kV systems in the U.K. are fed like this; also the 130 kV system in Sweden and the 150 kV system in Belgium [23].

This type of configuration can be treated like a loop that extends over two voltage levels. For a fault within the loop we can apply (4.18), for a fault on a feeder away from the loop (4.19) can be used. The equations remain the same independent of the voltage level at which the fault takes place. The only thing that changes are the impedance values.

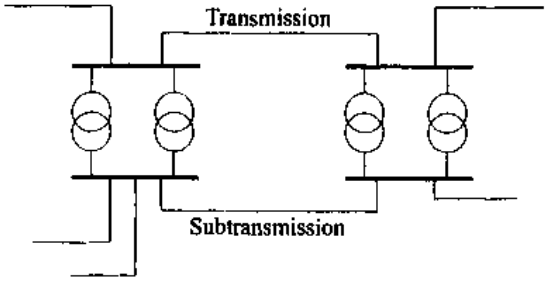

Figure 4.40 Parallel operation of transmission and subtransmission systems.

4.2.5 Voltage Calculations in Meshed Systems

When the system becomes more complicated than the examples discussed previously, closed expressions for the voltage during the sag get very complicated and unfeasible to handle. For meshed systems, matrix calculations have proven to be very efficient for computer-based analysis. The calculation of the voltages during a fault is based on two principles from circuit theory: Thevenin's superposition theorem; and the node impedance matrix. Both are discussed in detail in many books on power systems. Here we will only give a brief description.

- According to Thevenin's superposition theorem voltages and currents in the system during a sag are the sum of two contributions: currents and voltages before the event, and currents and voltages due to the change in voltage at the fault position. Currents and voltages before the fault are due to all generators across the system. Currents and voltages due to the fault originate at a voltage source at the fault position. All other voltage sources are considered short-circuited during the calculation of the latter contribution.
- The node impedance matrix $\mathbf{Z}$ relates node voltages and node currents:

$$V = \mathbf{Z}I \tag{4.20}$$

with V the vector of (complex) node voltages and I the vector of (complex) node currents. The node voltage is the voltage between a node and the reference node (typically ground). The node current is equal to the sum of all currents flowing toward a node. For most nodes the node current is zero according to Kirchhoff's current law. The only exception are generator nodes, where the node current is the current flowing from the generator into the system.

Consider a system with N nodes plus a reference node. The voltages before the fault are denoted as $V_k^{(0)}$. A short-circuit fault occurs at node f. According to Thevenin's superposition theorem we can write the voltage during the fault at any node k as

$$V_k = V_k^{(0)} + \Delta V_k \tag{4.21}$$

where ΔV_k is the change in voltage at node k due to the fault. This latter term is due to a voltage source $-V_f^{(0)}$ at the fault position. To calculate ΔV_k all other voltage sources in the system are short-circuited, so that node f is the only node with a non-zero node current. After using the information, (4.20) becomes

$$\Delta V_k = Z_{kf} I_f \tag{4.22}$$

At the fault position ($k = f$) we know that $\Delta V_f = -V_f^{(0)}$ so that

$$I_f = -\frac{V_f^{(0)}}{Z_{ff}} \tag{4.23}$$

and

$$V_k = V_k^{(0)} - \frac{Z_{kf}}{Z_{ff}} V_f^{(0)} \tag{4.24}$$

The pre-fault voltages are normally close to unity, so that (4.24) can be approximated by

$$V_k = 1 - \frac{Z_{kf}}{Z_{ff}} \tag{4.25}$$

The moment the node impedance matrix is known, calculating sag magnitudes becomes very easy. The drawback with this method is that the node impedance matrix needs to be calculated. This can be done through a recursive procedure where the matrix is updated for each new branch added. Alternatively one can first calculate the node admittance matrix from the branch impedances. The node impedance matrix is the inverse of the node admittance matrix.

EXAMPLE Consider the circuit diagram shown in Fig. 4.41. This circuit represents a 275/400 kV system, with nodes 1 and 2 representing 400 kV substations; nodes 3, 4, and 5 representing 275 kV substations; the branches between 1 and 3 and between 2 and 4 representing transformers (the latter two transformers in parallel). The impedance values indicated in the figure are in percent at a 100 MVA base.

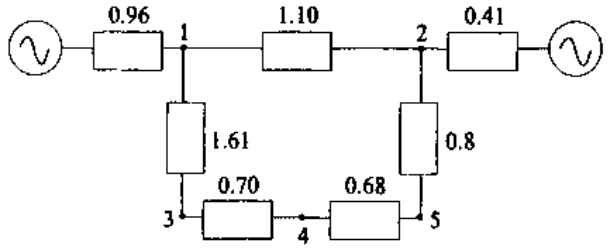

Figure 4.41 Circuit diagram representation of part of a 400/275 kV system.

The node admittance matrix can be built easily from the branch admittances or impedances. An off-diagonal element Y_{kl} of the node admittance matrix is equal to minus the admittance of the branch between nodes k and l. The element is zero if there is no branch between these two nodes. The diagonal element Y_{kk} equals the sum of all admittances of branches to node k including any branch between node k and the reference node. For the circuit in Fig. 4.41 this calculation leads to the node admittance matrix

$$Y = \begin{bmatrix} 2.5719 & -0.9091 & -0.6211 & 0 & 0 \\ -0.9091 & 4.5981 & 0 & -1.25 & 0 \\ -0.6211 & 0 & 2.0497 & 0 & -1.4286 \\ 0 & -1.25 & 0 & 2.7206 & -1.4706 \\ 0 & 0 & -1.4286 & -1.4706 & 2.8992 \end{bmatrix} \tag{4.26}$$

The node impedance matrix is obtained by inverting the node admittance matrix

$$Z = Y^{-1} = \begin{bmatrix} 0.5453 & 0.1771 & 0.3889 & 0.2548 & 0.3209 \\ 0.1771 & 0.3344 & 0.2439 & 0.3012 & 0.2730 \\ 0.3889 & 0.2439 & 1.2534 & 0.6144 & 0.9292 \\ 0.2548 & 0.3012 & 0.6144 & 0.9225 & 0.7707 \\ 0.3209 & 0.2730 & 0.9292 & 0.7707 & 1.1937 \end{bmatrix} \tag{4.27}$$

The voltage at node 5 due to a fault at node 2 is

$$V_5 = 1 - \frac{Z_{52}}{Z_{22}} = 1 - \frac{0.2730}{0.3344} = 0.1836 \tag{4.28}$$

TABLE 4.7 Voltage Sags in the System Shown in Fig. 4.41

	Fault at Node				
Voltage at Node	1	2	3	4	5
1	0	0.4704	0.6897	0.7238	0.7312
2	0.6753	0	0.8054	0.6735	0.7713
3	0.2869	0.2706	0	0.3340	0.2216
4	0.5327	0.0993	0.5098	0	0.3544
5	0.4116	0.1837	0.2586	0.1646	0

Table 4.7 gives the voltage at any node due to a fault at any other node. We see, e.g., that for node 5 a fault at node 2 is more severe than a fault at node 1. This is understandable as the source at node 2 is stronger than the source at node 1.

4.3 VOLTAGE SAG DURATION

4.3.1 Fault-Clearing Time

We have seen in Section 4.2 that the drop in voltage during a sag is due to a short circuit being present in the system. The moment the short-circuit fault is cleared by the protection, the voltage can return to its original value. The duration of a sag is mainly determined by the fault-clearing time, but it may be longer than the fault-clearing time. We will come back to this further on in this section.

Generally speaking faults in transmission systems are cleared faster than faults in distribution systems. In transmission systems the critical fault-clearing time is rather small. Thus, fast protection and fast circuit breakers are essential. Also transmission and subtransmission systems are normally operated as a grid, requiring distance protection or differential protection, both of which are rather fast. The principal form of protection in distribution systems is overcurrent protection. This requires often some time-grading which increases the fault-clearing time. An exception are systems in which current-limiting fuses are used. These have the ability to clear a fault within one half-cycle [6], [7].

An overview of the fault-clearing time of various protective devices is given in reference [8].

- current-limiting fuses: less than one cycle
- expulsion fuses: 10–1000 ms
- distance relay with fast breaker: 50–100 ms
- distance relay in zone 1: 100–200 ms
- distance relay in zone 2: 200–500 ms
- differential relay: 100–300 ms
- overcurrent relay: 200–2000 ms

Some typical fault-clearing times at various voltage levels for a U.S. utility are given in reference [9].

Voltage Level	Best Case	Typical	Worse Case
525 kV	33 ms	50 ms	83 ms
345 kV	50 ms	67 ms	100 ms
230 kV	50 ms	83 ms	133 ms
115 kV	83 ms	83 ms	167 ms
69 kV	50 ms	83 ms	167 ms
34.5 kV	100 ms	2 sec	3 sec
12.47 kV	100 ms	2 sec	3 sec

From this list it becomes clear that the sag duration will be longer when a sag originates at a lower voltage level. Many utilities operate their distribution feeders in such a way that most faults are cleared within a few cycles. Such a way of operation was discussed in detail in Chapter 3. But even for those feeders, a certain percentage of faults will lead to long sags. The difference between the two ways of operation is discussed in more detail in Section 7.1.3.

4.3.2 Magnitude-Duration Plots

Knowing the magnitude and duration of a voltage sag, it can be presented by a point in a magnitude-duration plane. This way of sag characterization has been shown to be extremely useful for various types of studies. We will use it in forthcoming chapters to describe both equipment and system performance. Various types of magnitude-duration plots will be discussed in Section 6.2. The magnitude-duration plot will also be used in Chapter 6 to present the results of power quality surveys. An example of a magnitude-duration plot is shown in Fig. 4.42. The numbers in Fig. 4.42 refer to the following sag origins:

1. Transmission system faults
2. Remote distribution system faults
3. Local distribution system faults
4. Starting of large motors
5. Short interruptions
6. Fuses

Consider the general system configuration shown in Fig. 4.43. A short-circuit fault in the local distribution network will typically lead to a rather deep sag. This is

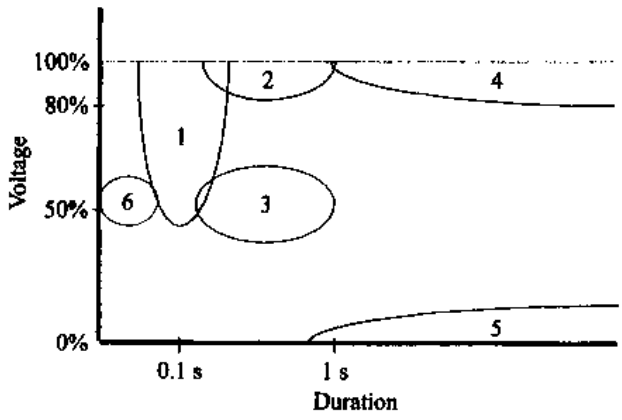

Figure 4.42 Sags of different origin in a magnitude-duration plot.

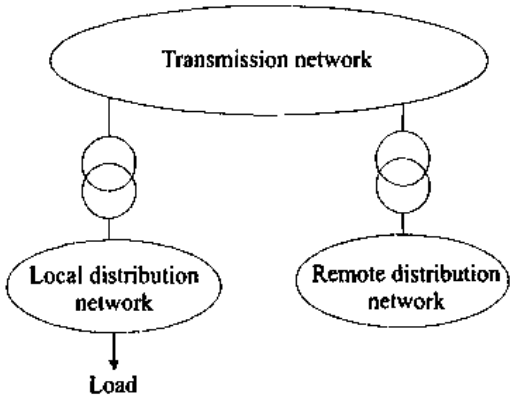

Figure 4.43 General structure of power system, with distribution and transmission networks.

due to the limited length of distribution feeders. When the fault occurs in a remote distribution network, the sag will be much more shallow due to the transformer impedance between the fault and the pcc. For a fault in any distribution network, the sag duration may be up to a few seconds.

Transmission system faults are typically cleared within 50 to 100 ms, thus leading to short-duration sags. Current-limiting fuses lead to sag durations of one cycle or less, and rather deep sags if the fault is in the local distribution or low-voltage network. Faults in remote networks, cleared by current-limiting fuses, lead to short and shallow sags, not indicated in the figure. Finally the figure contains voltage sags due to motor starting, shallow and long duration (see Section 4.9) and short interruptions, deep and long duration (see Chapter 3).

4.3.3 Measurement of Sag Duration

Measurement of sag duration is much less trivial than it might appear from the previous section. For a sag like in Fig. 4.1 it is obvious that the duration is about $2\frac{1}{2}$ cycles. However, to come up with an automatic way for a power quality monitor to obtain the sag duration is no longer straightforward. A commonly used definition of sag duration is the number of cycles during which the rms voltage is below a given threshold. This threshold will be somewhat different for each monitor but typical values are around 90%. A power quality monitor will typically calculate the rms value once every cycle. This gives an overestimation of the sag duration as shown in Fig. 4.44. The

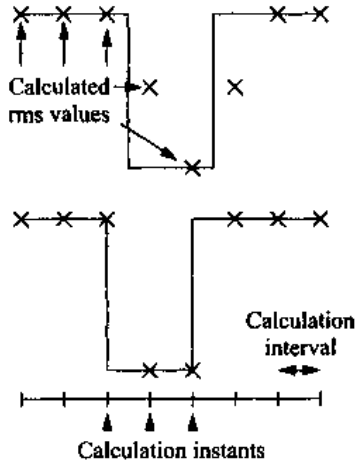

Figure 4.44 Estimation of sag duration by power quality monitor for a two-cycle sag: overestimation by one cycle (upper graph); correct estimation (lower graph).

normal situation is shown in the upper figure. The rms calculation is performed at regular instants in time and the voltage sag starts somewhere in between two of those instants. As there is no correlation between the calculation instants and the sag commencement, this is the most likely situation. We see that the rms value is low for three samples in a row. The sag duration according to the monitor will be three cycles. Here it is assumed that the sag is deep enough for the intermediate rms value to be below the threshold. For shallow sags both intermediate values might be above the threshold and the monitor will record a one-cycle sag. The bottom curve of Fig. 4.44 shows the rare situation where the sag commencement almost coincides with one of the instants on which the rms voltage is calculated. In that case the monitor gives the correct sag duration.

Calculating the rms voltage once a cycle, it is obvious that the resulting sag duration will be an integer number of cycles. For a $2\frac{1}{2}$-cycle sag the computed duration will be either two or three cycles. But even when a sliding window is used to calculate the rms voltage as a function of time, an erroneous sag duration might result. To show this possible error for a measured sag, we have plotted in Fig. 4.45 the half-cycle rms of the sag shown in Fig. 4.1, together with the absolute value of the measured voltage. The "actual sag duration" obtained from the sudden drop and rise in the voltage is 2.4 cycles. For large thresholds the recorded sag duration will be an overestimation. A 90% threshold gives a 2.8 cycle sag duration, and 80% threshold a 2.5 cycles duration. For lower thresholds the recorded sag duration is an underestimation: a 60% threshold gives a 2.1 cycle duration and a 40% threshold a 2.0 cycle duration. In reality, thresholds this low will not be used, but the same effect will be obtained when the depth of the sag is varied and the threshold is kept constant. The duration of deep sags will be overestimated, and the duration of shallow ones underestimated.

As the shortest-duration window for calculating the sag magnitude is one half-cycle, an error up to one half-cycle must be accepted. Several methods have been suggested to measure sag initiation and voltage recovery more accurately. These methods also give a more accurate value of sag duration [134], [201], [202]. Using the fundamental voltage component results in a similar transition between pre-sag and during-sag voltage, thus similar errors in sag duration. Using the half-cycle peak voltage will give a much sharper transition, as long as sag initiation and voltage recovery are close to voltage maximum. Sag initiation and voltage recovery around the voltage zero-crossing will give a smoother transition and a larger uncertainly in sag duration.

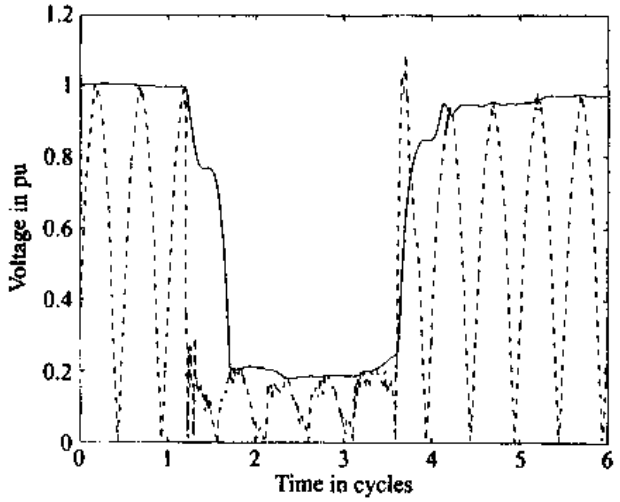

Figure 4.45 Half-cycle rms voltage together with absolute value of the voltage (dashed line) of the sag shown in Fig. 4.1.

The above-mentioned error in sag duration is only significant for short-duration sags. For longer sags it does not really matter. But for longer sags the so-called post-fault sag will give a serious uncertainty in sag duration. When the fault is cleared the voltage does not recover immediately. Some of this effect can be seen in Fig. 4.3 and Fig. 4.4. The rms voltage after the sag is slightly lower than before the sag. The effect can be especially severe for sags due to three-phase faults. The explanation for this effect is as follows [17], [18]. Due to the drop in voltage during the sag, induction motors will slow down. The torque produced by an induction motor is proportional to the square of the voltage, so even a rather small drop in voltage can already produce a large drop in torque and thus in speed. The moment the fault is cleared and the voltage comes back, the induction motors start to draw a large current: up to 10 times their nominal current. Immediately after the sag, the air-gap field will have to be built up again. In other words, the induction motor behaves like a short-circuited transformer. After the flux has come back into the air gap, the motor can start re-accelerating which also requires a rather large current. It is this post-fault inrush current of induction motors which leads to an extended sag. The post-fault sag can last several seconds, much longer than the actual sag.

Such a post-fault sag will cause uncertainty in the sag duration as obtained by a power quality monitor: different monitors can give different results. This is shown schematically in Fig. 4.46. Assume that monitor 1 has a setting as indicated, and monitor 2 a slightly higher setting. Both monitors will record a sag duration much longer than the fault-clearing time. The fault-clearing time can be estimated from the duration of the deep part of the sag. We see that monitor 2 will record a significantly longer duration than monitor 1.

A measured sag with a long post-fault component is shown in Fig. 4.47. The three phases are shown in the same figure to better indicate the post-fault voltage sag. Note that the sag is unbalanced during the fault, but balanced after the fault.

The rms voltage versus time for the sag shown in Fig. 4.47 is plotted in Fig. 4.48. We see a large drop in voltage in two phases and a small one in the third phase. The fault-clearing time is about four cycles; the fault leading to this sag took place at 132 kV, the voltages were measured at 11 kV. The sag duration has been determined as the time during which the rms voltage is below a certain threshold. Figure 4.49 plots this duration as a function of the threshold, for the three phases. One of the phases only drops to 88% so that any threshold setting below 88% will give zero sag duration for that phase. The sag duration obtained for the other two phases is about four cycles for thresholds below 90%, increasing fast for higher threshold settings.

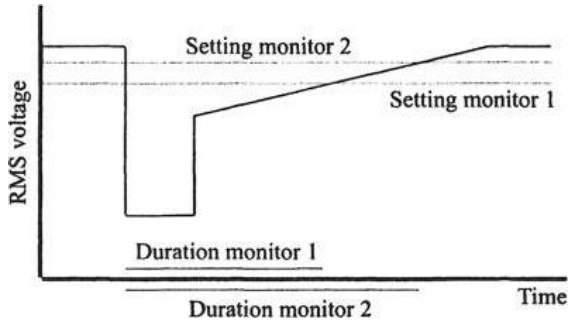

Figure 4.46 Error in sag duration due to post-fault sag.

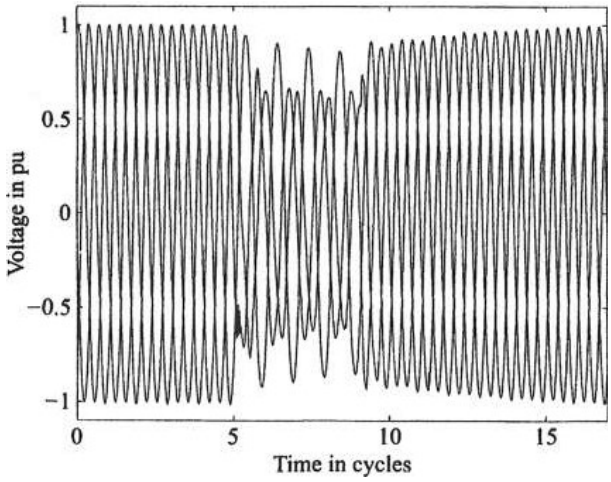

Figure 4.47 Measured sag with a clear post-fault component (Data obtained from Scottish Power.)

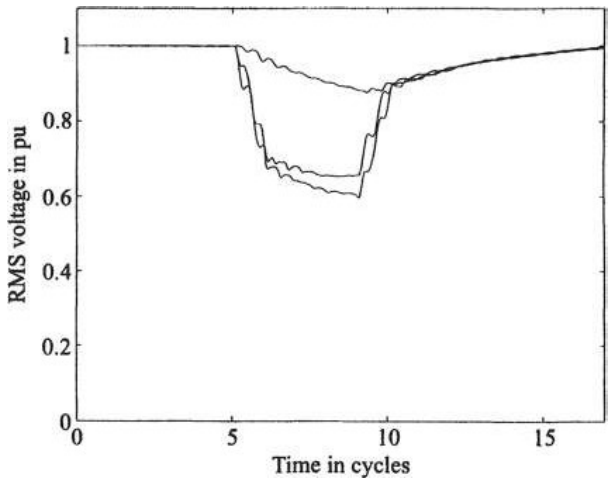

Figure 4.48 The rms voltages versus time for the sag shown in Fig. 4.47.

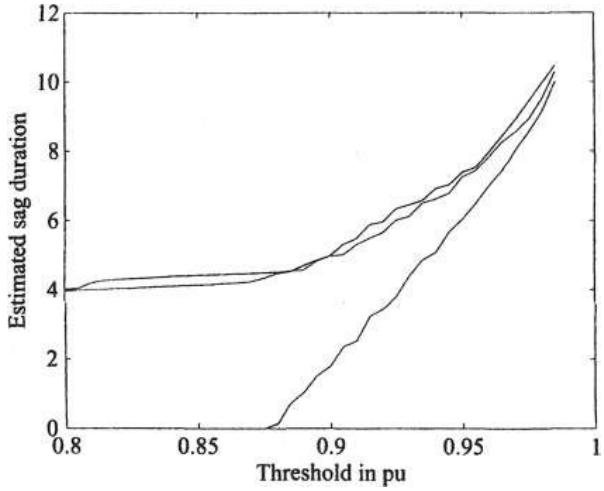

Figure 4.49 Sag duration versus threshold setting for the three phases of the sag shown in Figs. 4.47 and 4.48.

4.4 THREE-PHASE UNBALANCE

The analysis of sag magnitude presented in the previous sections considers only one phase. For example, the voltage divider model in Fig. 4.14 was introduced for three-phase faults: the impedances used in that figure are the positive-sequence values. But most short circuits in power systems are single phase or two phase. In that case we need to take all three phases into account or use the symmetrical component theory. A good and detailed description of the use of symmetrical components theory for the analysis of non-symmetrical faults is given in reference [24] and in several other books on power system analysis and is not repeated here. We will only use the results of the theory to calculate the voltages in the three phases due to a non-symmetrical short circuit.

For non-symmetrical faults the voltage divider in Fig. 4.14 can still be used but it has to be split into its three components: a positive-sequence network, a negative-sequence network, and a zero-sequence network. The three component networks are shown in Fig. 4.50, where V_1, V_2, and V_0 represent positive-, negative-, and zero-sequence voltage, respectively, at the pcc; Z_{S1}, Z_{S2}, and Z_{S0} are the source impedance values and Z_{F1}, Z_{F2}, and Z_{F0} the feeder impedance values in the three components. The three components of the fault current are denoted by I_1, I_2, and I_0. The positive-sequence source is denoted by E. There is no source in the negative and zero-sequence networks. The three component networks have to be connected into one equivalent circuit at the fault position. The connection of the component networks depends on the fault type. For a three-phase fault all three networks are shorted at the fault position. This leads to the standard voltage divider model for the positive sequence, and zero voltage and current for the negative and zero sequences.

4.4.1 Single-Phase Faults

For a single-phase fault, the three networks shown in Fig. 4.50 should be connected in series at the fault position. The resulting circuit for a single-phase fault in

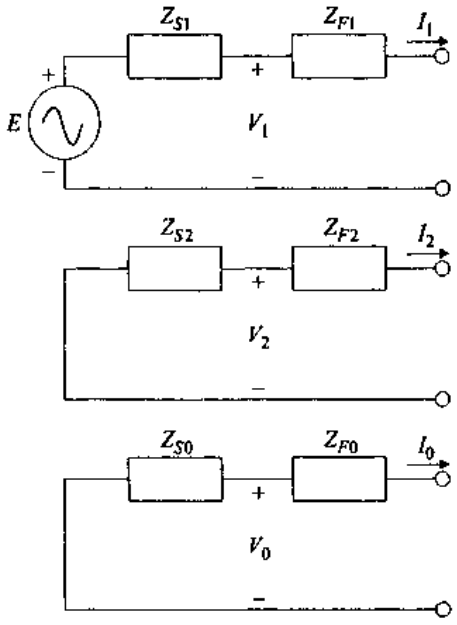

Figure 4.50 Positive- (top), negative- (center), and zero- (bottom) sequence networks for the voltage divider shown in Fig. 4.14.

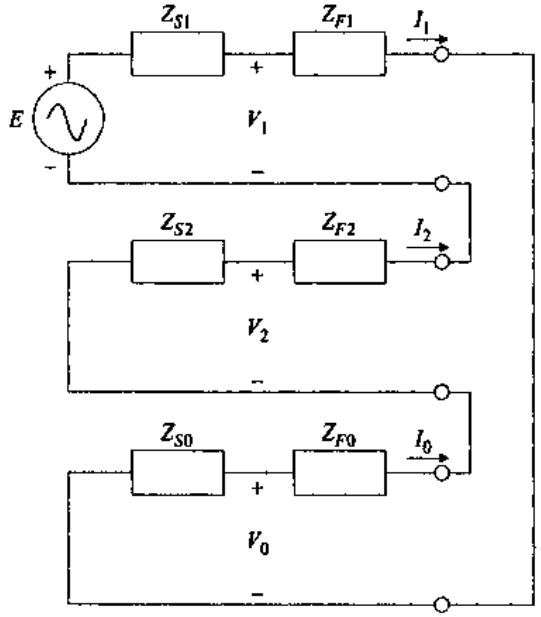

Figure 4.51 Equivalent circuit for a single-phase fault.

phase a, is shown in Fig. 4.51. If we again make $E = 1$, like in the single-phase model in Fig. 4.14, the following expressions are obtained for the component voltages at the pcc:

$$V_1 = \frac{Z_{F1} + Z_{S2} + Z_{F2} + Z_{S0} + Z_{F0}}{(Z_{F1} + Z_{F2} + Z_{F0}) + (Z_{S1} + Z_{S2} + Z_{S0})} \tag{4.29}$$

$$V_2 = \frac{Z_{S2}}{(Z_{F1} + Z_{F2} + Z_{F0}) + (Z_{S1} + Z_{S2} + Z_{S0})} \tag{4.30}$$

$$V_0 = \frac{Z_{S0}}{(Z_{F1} + Z_{F2} + Z_{F0}) + (Z_{S1} + Z_{S2} + Z_{S0})} \tag{4.31}$$

The voltages in the three phases at the pcc during the fault are obtained by transforming back from sequence domain to phase domain:

$$\begin{aligned} V_a &= V_1 + V_2 + V_0 \\ V_b &= a^2 V_1 + aV_2 + V_0 \\ V_c &= aV_1 + a^2 V_2 + V_0 \end{aligned} \tag{4.32}$$

For the faulted phase voltage V_a we get

$$V_a = \frac{Z_{F1} + Z_{F2} + Z_{F0}}{(Z_{F1} + Z_{F2} + Z_{F0}) + (Z_{S1} + Z_{S2} + Z_{S0})} \tag{4.33}$$

We can obtain the original voltage divider equation (4.9) by defining $Z_F = Z_{F1} + Z_{F2} + Z_{F0}$ and $Z_S = Z_{S1} + Z_{S2} + Z_{S0}$. Thus, the voltage divider model of Fig. 4.14 and (4.9) still holds for single-phase faults. The condition thereby is that the resulting voltage is the voltage in the faulted phase, and that the impedance values used are the sum of the positive-, negative-, and zero-sequence impedances. From (4.29) through (4.32) we can calculate the voltages in the non-faulted phases, which results into the following expressions for the three voltages:

$$V_a = 1 - \frac{Z_{S1} + Z_{S2} + Z_{S0}}{(Z_{F1} + Z_{F2} + Z_{F0}) + (Z_{S1} + Z_{S2} + Z_{S0})}$$
$$V_b = a^2 - \frac{a^2 Z_{S1} + aZ_{S2} + Z_{S0}}{(Z_{F1} + Z_{F2} + Z_{F0}) + (Z_{S1} + Z_{S2} + Z_{S0})} \tag{4.34}$$
$$V_c = a - \frac{aZ_{S1} + a^2 Z_{S2} + Z_{S0}}{(Z_{F1} + Z_{F2} + Z_{F0}) + (Z_{S1} + Z_{S2} + Z_{S0})}$$

Note that the expression for V_a has been slightly rewritten to explicitly obtain the voltage drop as a separate term.

These voltages are shown as a phasor diagram in Fig. 4.52. The voltage drop in the non-faulted phases consists of three terms:

- a voltage drop proportional to the positive-sequence source impedance, along the direction of the pre-fault voltage.
- a voltage drop proportional to the negative-sequence source impedance, along the direction of the pre-fault voltage in the other non-faulted phase.
- a voltage drop proportional to the zero-sequence source impedance, along the direction of the pre-fault voltage in the faulted phase.

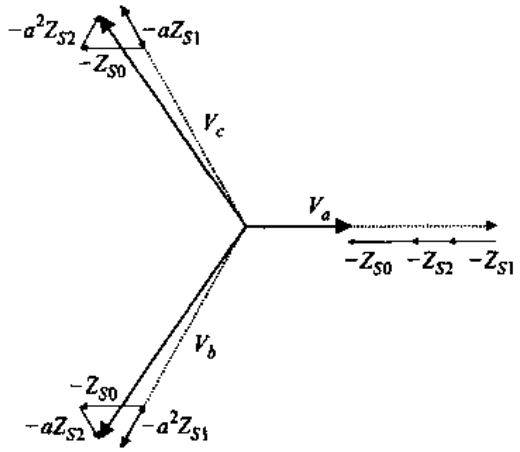

Figure 4.52 Phase-to-ground voltages during a single-phase fault.

The voltage between the two non-faulted phases is

$$V_b - V_c = (a^2 - a)\left[1 - \frac{Z_{S1} - Z_{S2}}{(Z_{F1} + Z_{F2} + Z_{F0}) + (Z_{S1} + Z_{S2} + Z_{S0})}\right] \tag{4.35}$$

We see that the change in this voltage is only due to the difference between positive-sequence and negative-sequence source impedances. As these two are normally about equal, the voltage between the non-faulted phases is normally not influenced by the fault. Below we will simplify the expressions (4.34) and (4.35) for two cases:

- Positive-, negative-, and zero-sequence source impedances are equal.
- Positive- and negative-sequence source and feeder impedances are equal.

4.4.1.1 Solidly-Grounded Systems. In a solidly-grounded system, the source impedances in the three sequence components are often about equal. The three voltage drops in the non-faulted phases now cancel, resulting in the following voltages during the fault:

$$\begin{aligned} V_a &= -\frac{Z_{S1}}{\frac{1}{3}(Z_{F1}+Z_{F2}+Z_{F0})+Z_{S1}} \\ V_b &= a^2 \\ V_c &= a \end{aligned} \tag{4.36}$$

The voltage in the faulted phase is the same as during a three-phase fault, the voltages in the non-faulted phase are not affected.

4.4.1.2 Impedance-Grounded Systems. In a resistance or high-impedance grounded system, the zero-sequence source impedance differs significantly from the positive and negative-sequence source impedances. We can, however, assume that the latter two are equal. Also in systems where the source impedance consists for a large part of line or cable impedances (e.g., in transmission systems) positive- and zero-sequence impedances can be significantly different. The resulting expressions for the voltages at the pcc during a single-phase fault are, when $Z_{S1} = Z_{S2}$ and $Z_{F1} = Z_{F2}$:

$$\begin{aligned} V_a &= 1 - \frac{Z_{S0}+2Z_{S1}}{(2Z_{F1}+Z_{F0})+(2Z_{S1}+Z_{S0})} \\ V_b &= a^2 - \frac{Z_{S0}-2Z_{S1}}{(2Z_{F1}+Z_{F0})+(2Z_{S1}+Z_{S0})} \\ V_c &= a - \frac{Z_{S0}-2Z_{S1}}{(2Z_{F1}+Z_{F0})+(2Z_{S1}+Z_{S0})} \end{aligned} \tag{4.37}$$

The voltage drop in the non-faulted phases only contains a zero-sequence component (it is the same in both phases). We will see later that the zero-sequence component of the voltage is rarely of importance for the voltage sag as experienced at equipment terminals. Sags at the same voltage level as the equipment terminals are rare. During the transfer of the sag down to lower voltage levels, the transformers normally block the zero-sequence component of the voltage. Even if the fault occurs at the same voltage level as the equipment terminals, the equipment is normally connected in delta so it will not notice the zero-sequence component of the voltage. Thus the voltage drop in the non-faulted phases is not of importance from an equipment point of view. We can therefore add a zero-sequence voltage to (4.37) such that the voltage drop in the non-faulted phases disappears. The resulting expressions are

$$\begin{aligned} V'_a &= V_a + \frac{Z_{S0}-Z_{S1}}{(2Z_{F1}+Z_{F0})+(2Z_{S1}+Z_{S0})} = 1 - \frac{3Z_{S1}}{(2Z_{F1}+Z_{F0})+(2Z_{S1}+Z_{S0})} \\ V'_b &= V_b + \frac{Z_{S0}-Z_{S1}}{(2Z_{F1}+Z_{F0})+(2Z_{S1}+Z_{S0})} = a^2 \\ V'_c &= V_c + \frac{Z_{S0}-Z_{S1}}{(2Z_{F1}+Z_{F0})+(2Z_{S1}+Z_{S0})} = a \end{aligned} \tag{4.38}$$

The expression for the voltage in the faulted phase is somewhat rewritten, to enable a comparison with (4.36):

$$V'_a = 1 - \frac{Z_{S1}}{\frac{1}{3}(Z_{F1}+Z_{F2}+Z_{F0})+\frac{1}{3}(Z_{S0}-Z_{S1})+Z_{S1}} \tag{4.39}$$

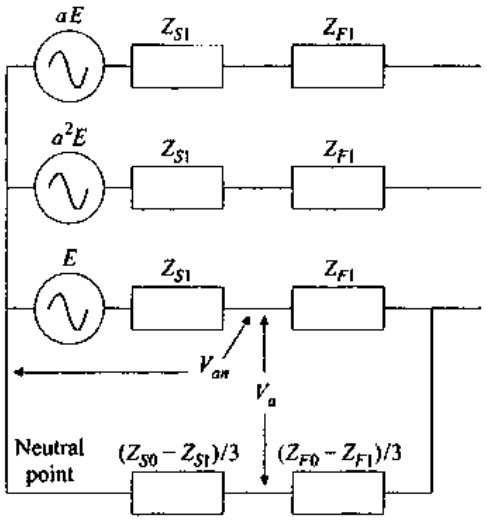

Figure 4.53 Three-phase voltage divider model.

The denominator contains an additional term $\frac{1}{3}(Z_{S0} - Z_{S1})$ compared to (4.36). This can be interpreted as an additional impedance between the pcc and the fault. When this impedance is positive, thus when $Z_{S0} > Z_{S1}$, the sag becomes more shallow. In resistance and reactance-grounded systems, $Z_{S0} \gg Z_{S1}$, so that even a terminal fault, $Z_{F1} + Z_{F2} + Z_{F0} = 0$, will lead to a shallow sag.

Note that in solidly-grounded systems, the zero-sequence source impedance may be less than the positive-sequence one, $Z_{S0} < Z_{S1}$, so that the additional impedance is negative. For nearby faults, we will thus obtain a negative voltage V_a'.

All this might look like a mathematical trick to get rid of the voltage drop in the non-faulted phases. There is, however, some physical significance to this. To show this, the three-phase voltage divider is drawn in a commonly used way [24] in Fig. 4.53. From this model we can calculate the phase-to-neutral voltages at the pcc; with $E = 1$ the calculation results into

$$\begin{aligned} V_{an} &= 1 - \frac{3Z_{S1}}{(2Z_{F1} + Z_{F0}) + (2Z_{S1} + Z_{S0})} \\ V_{bn} &= a^2 \\ V_{cn} &= a \end{aligned} \tag{4.40}$$

The correspondence between (4.40) and (4.38) is obvious. The voltages in (4.38) thus correspond to the phase-to-neutral voltages. Note that the "neutral" in Fig. 4.53 is not a physical neutral but a kind of mathematical neutral. In resistance- or high-impedance grounded systems the physical neutral (i.e., the star point of the transformer) is a good approximation of this "mathematical neutral." The expressions derived not only hold for resistance-grounded systems, but for each system in which we can assume positive- and negative-sequence impedances equal.

EXAMPLE Consider again the system shown in Fig. 4.21, and assume that a single-phase fault occurs on one of the 132 kV feeders. The 132 kV system is solidly grounded, therefore the positive- and zero-sequence source impedances are similar. For the feeders, the zero-sequence impedance is about twice the positive- and negative- sequence impedance. Positive- and negative-sequence impedance are assumed equal.

$$\begin{aligned} Z_{S1} &= Z_{S2} = 0.09 + j2.86\% \\ Z_{S0} &= 0.047 + j2.75\% \\ Z_{F1} &= Z_{F2} = 0.101 + j0.257\%/\text{km} \\ Z_{F0} &= 0.23 + j0.65\%/\text{km} \end{aligned}$$

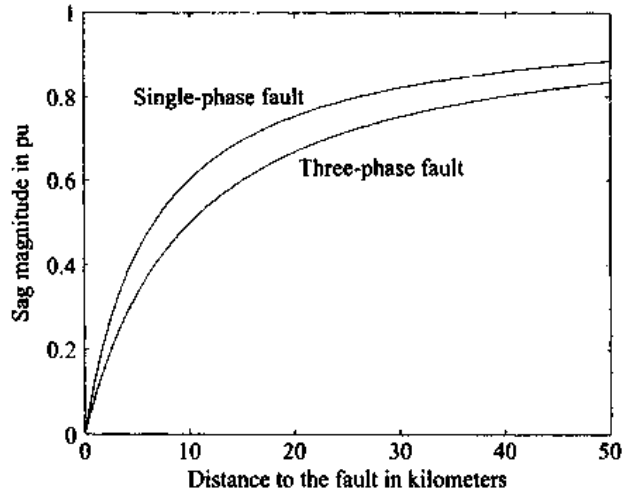

Figure 4.54 Voltage in the faulted phase for single-phase and three-phase faults on a 132 kV feeder in Fig. 4.21.

By using the above-given equations, the voltages in the three phases have been calculated for single-phase as well as for three-phase faults. The results for the faulted phase are shown in Fig. 4.54. The difference is mainly due to the difference in feeder impedance. Note that it is assumed here that the feeders are at least 50 km long, where they are in reality only 2 km long. The zero-sequence feeder impedance increases faster than the positive-sequence impedance, with increasing distance to the fault. Therefore single-phase faults lead to slightly smaller voltage drops than three-phase faults. As we saw from the equations above, it is the average of the three sequence impedances which determines the voltage drop due to single-phase faults. The voltages in the non-faulted phases showed only a very small change due to the single-phase fault.

EXAMPLE The voltages due to single-phase faults have been calculated for the 11 kV system in Fig. 4.21. As this system is resistance grounded, the zero-sequence source impedance is considerably larger than the positive-sequence impedance.

$$Z_{S1} = Z_{S2} = 4.94 + j65.9\%$$
$$Z_{S0} = 787 + j220\%$$
$$Z_{F1} = Z_{F2} = 9.7 + j26\%/\text{km}$$
$$Z_{F0} = 18.4 + j112\%/\text{km}$$

Note the large zero-sequence source impedance, especially its resistive part. The voltage in the faulted phase for three-phase and single-phase faults is shown in Fig. 4.55 as a function of the distance to the fault. The larger source impedance for single-phase faults more than compensates the larger feeder impedance, which makes that single-phase faults cause deeper sags than three-phase faults.

In a solidly-grounded system the voltage in a non-faulted phase stays about the same during a single-phase fault. In a resistance-grounded system the voltage in the non-faulted phases increases. This effect is shown in Figs. 4.56 and 4.57. Figure 4.56 shows the voltage magnitude versus distance to the fault and Fig. 4.57 the path of the voltages in the complex plane. The circles and the arrows indicate the complex voltages during normal operation. The curves indicate the path of the complex voltages with varying distance to the fault. Where the faulted phase shows a drop in voltage, the non-faulted phases show a large increase in voltage, for one phase even increasing 170% of the nominal voltage. From Fig. 4.57 we see that all three voltages are shifted over a

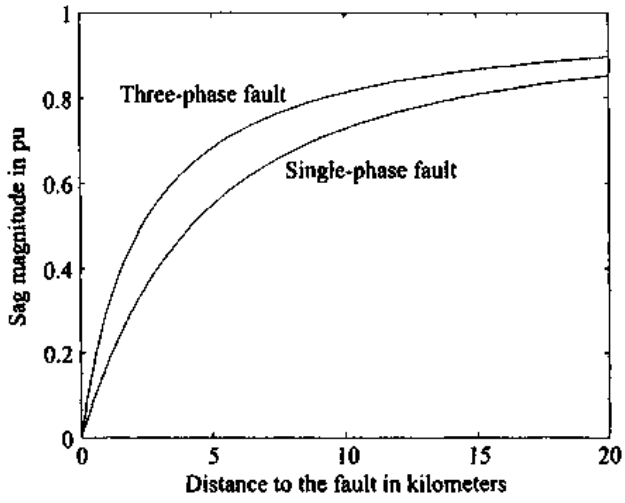

Figure 4.55 Voltage in the faulted phase for single-phase and three-phase faults on an 11 kV feeder in Fig. 4.21.

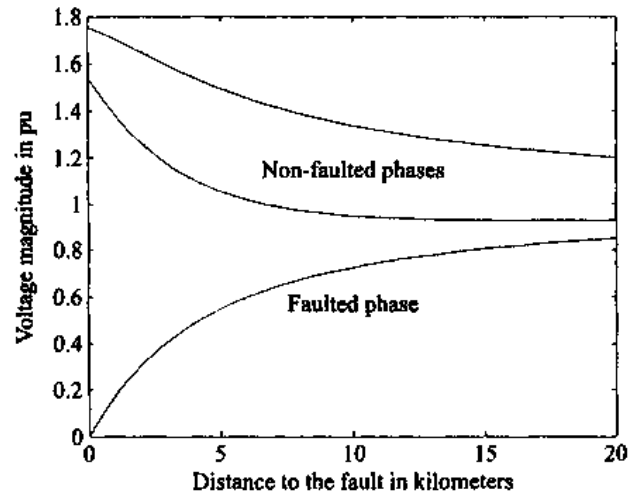

Figure 4.56 Voltage in the faulted and non-faulted phases for a single-phase fault on an 11 kV feeder in Fig. 4.21, as a function of the distance to the fault.

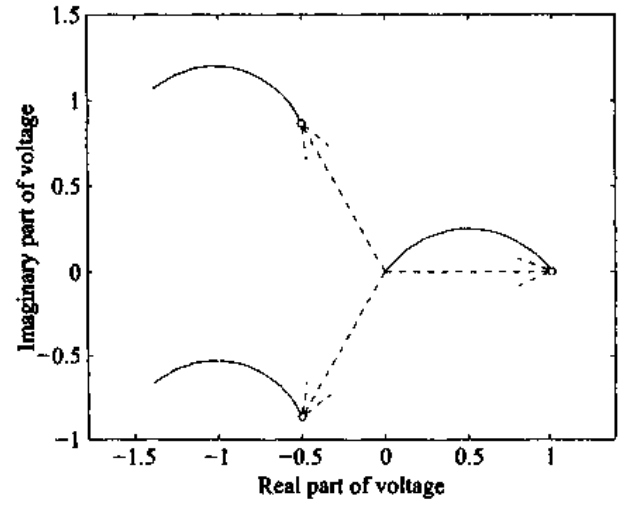

Figure 4.57 Complex voltages due to a fault on an 11 kV feeder in Fig. 4.21.

similar distance in the complex plane. The effect of this common shift (a zero-sequence component) is that the phase-to-phase voltages do not change much.

The phase-to-phase voltages have been calculated from the complex phase voltages by using the following expressions:

$$V_{ab} = \frac{V_a - V_b}{\sqrt{3}}$$
$$V_{bc} = \frac{V_b - V_c}{\sqrt{3}} \tag{4.41}$$
$$V_{ca} = \frac{V_c - V_a}{\sqrt{3}}$$

The factor $\sqrt{3}$ is needed to ensure that the pre-fault phase-to-phase voltages are 1 pu. The resulting voltage magnitudes are shown in Fig. 4.58: note the difference in vertical scale compared to the previous figures. We see that the phase-to-phase voltages are not much influenced by single-phase faults. The lowest voltage magnitude is 89%, the highest 101%.

Figure 4.59 compares phase-to-ground voltage, according to (4.37), and phase-to-neutral voltage, according to (4.40). We see that the drop in phase-to-neutral voltage is

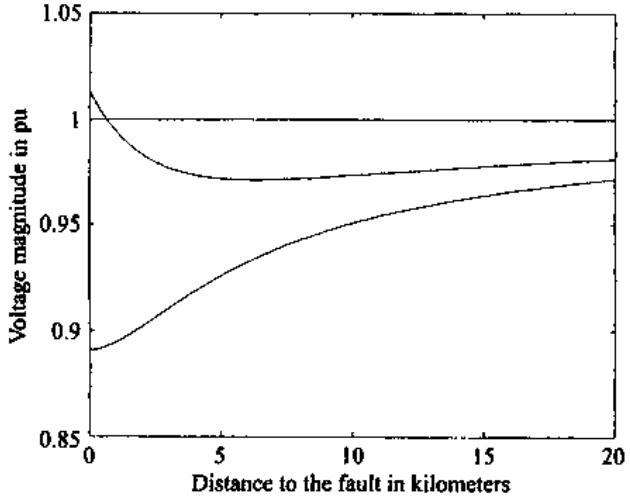

Figure 4.58 Phase-to-phase voltages due to a single-phase fault on an 11 kV feeder in Fig. 4.21, as a function of the distance to the fault.

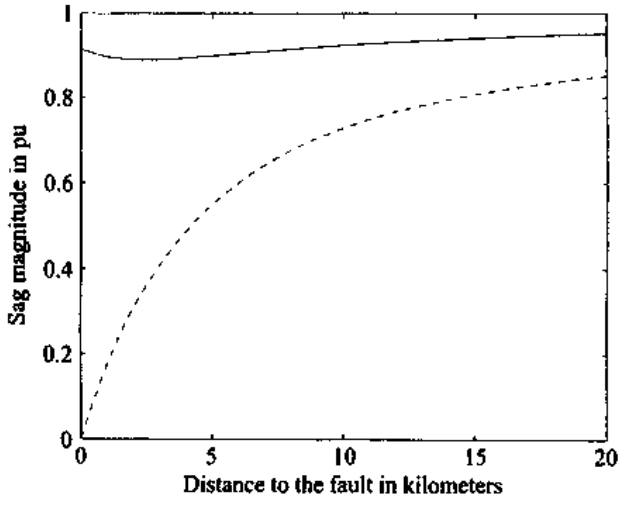

Figure 4.59 Phase-to-ground (dashed) and phase-to-neutral (solid) voltages due to single-phase faults on an 11 kV feeder in Fig. 4.21.

very small. As explained before, this is due to the large zero-sequence source impedance. Also note that the lowest phase-to-neutral voltage occurs for a non-zero distance to the fault.

4.4.2 Phase-to-Phase Faults

For a phase-to-phase fault the positive- and negative-sequence networks are connected in parallel, as shown in Fig. 4.60. The zero-sequence voltages and currents are zero for a phase-to-phase fault.

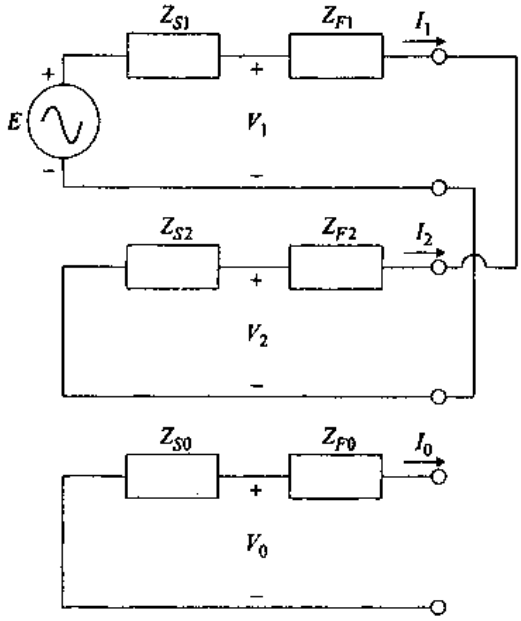

Figure 4.60 Equivalent circuit for a phase-to-phase fault.

The sequence voltages at the pcc are

$$\begin{aligned} V_1 &= E - E\frac{Z_{S1}}{(Z_{S1}+Z_{S2})+(Z_{F1}+Z_{F2})} \\ V_2 &= \frac{Z_{S2}}{(Z_{S1}+Z_{S2})+(Z_{F1}+Z_{F2})} \\ V_0 &= 0 \end{aligned} \tag{4.42}$$

The phase voltages can be found from (4.42) by using (4.32). This results in the following expressions, again with $E = 1$:

$$\begin{aligned} V_a &= 1 - \frac{Z_{S1}-Z_{S2}}{(Z_{S1}+Z_{S2})+(Z_{F1}+Z_{F2})} \\ V_b &= a^2 - \frac{a^2Z_{S1}-aZ_{S2}}{(Z_{S1}+Z_{S2})+(Z_{F1}+Z_{F2})} \\ V_c &= a - \frac{aZ_{S1}-a^2Z_{S2}}{(Z_{S1}+Z_{S2})+(Z_{F1}+Z_{F2})} \end{aligned} \tag{4.43}$$

In the calculation of the component voltages and currents, it has been assumed that the fault is between the phases b and c. Thus a is the non-faulted phase, and b and c are the

faulted phases. From (4.43) we see that the voltage drop in the non-faulted phase depends on the difference between the positive and negative-sequence source impedances. As these are normally equal, the voltage in the non-faulted phase will not be influenced by the phase-to-phase fault. Under the assumption, $Z_{S1} = Z_{S2}$ (4.43) becomes

$$\begin{aligned} V_a &= 1 \\ V_b &= a^2 - \frac{(a^2 - a)Z_{S1}}{2Z_{S1} + 2Z_{F1}} \\ V_c &= a + \frac{(a^2 - a)Z_{S1}}{2Z_{S1} + 2Z_{F1}} \end{aligned} \tag{4.44}$$

We see that the voltage drop in the faulted phases is equal in magnitude $\frac{Z_{S1}}{2Z_{S1}+2Z_{F1}}$ but opposite in direction. The direction in which the two phase voltages drop is along the pre-fault phase-to-phase voltage between the faulted phases, $V_b - V_c$.

From (4.43) we can derive the following expression for the voltage between the faulted phases

$$V_b - V_c = \frac{Z_{F1} + Z_{F2}}{(Z_{S1} + Z_{S2}) + (Z_{F1} + Z_{F2})}(a^2 - a) \tag{4.45}$$

When we realize that $(a^2 - a)$ is the pre-fault voltage between the two faulted phases, the resemblance with the single-phase voltage divider of Fig. 4.14 and (4.9) becomes immediately clear. The same expressions as for the three-phase fault can be used, but for the voltages between the faulted phases; the impedances in the expression are the sum of positive and negative sequence values.

EXAMPLE Consider phase-to-phase faults on one of the 33 kV feeders in the system shown in Fig. 4.21. The impedance values needed to calculate the voltages during a phase-to-phase fault are as follows:

$$\begin{aligned} Z_{S1} &= Z_{S2} = 1.23 + j18.3\% \\ Z_{F1} &= Z_{F2} = 1.435 + j3.102\%/\text{km} \end{aligned}$$

The resulting complex voltages are shown in Fig. 4.61. The circles and the arrows indicate the pre-fault voltages; the cross indicates the voltages in the faulted phases for a fault at the 33 kV bus.

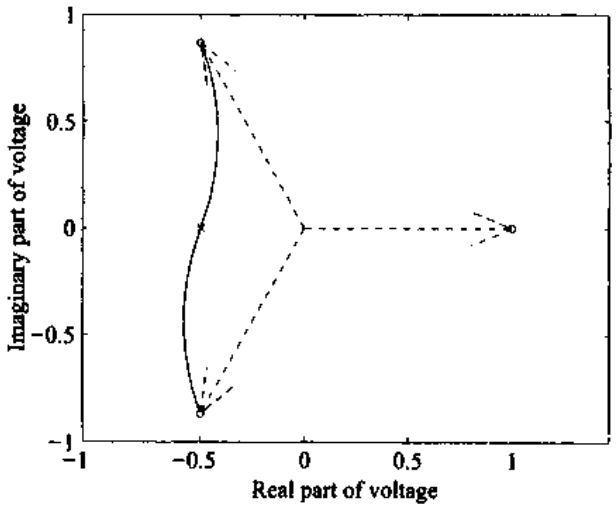

Figure 4.61 Complex voltages due to a phase-to-phase fault (solid line).

We see how the voltages in the two faulted phases move toward each other. The deviation of their path from a straight line is due to the difference in X/R ratio between source and feeder impedance. This is a subject to be discussed in further detail in Section 4.5.

4.4.3 Two-Phase-to-Ground Faults

Single-phase and phase-to-phase faults have been discussed in the two previous sections. The only asymmetrical fault type remaining is the two-phase-to-ground fault. For a two-phase-to-ground fault the three sequence networks are connected in parallel, as shown in Fig. 4.62. It is again possible to calculate component voltages and from these calculate voltages in the three phases in the same way as done for the single-phase and phase-to-phase faults.

The sequence voltages at the pcc for a fault between phases b and c and ground are given by the following expressions:

$$\begin{aligned} V_1 &= 1 - \frac{Z_{S1}(Z_{S0} + Z_{F0} + Z_{S2} + Z_{F2})}{D} \\ V_2 &= \frac{Z_{S2}(Z_{S0} + Z_{F0})}{D} \\ V_0 &= \frac{Z_{S0}(Z_{S2} + Z_{F2})}{D} \end{aligned} \tag{4.46}$$

with

$$D = (Z_{S0} + Z_{F0})(Z_{S1} + Z_{F1} + Z_{S2} + Z_{F2}) + (Z_{S1} + Z_{F1})(Z_{S2} + Z_{F2}) \tag{4.47}$$

From (4.46) it is possible to calculate the phase-to-ground voltages in the three phases

$$\begin{aligned} V_a &= 1 + \frac{(Z_{S2} - Z_{S1})(Z_{S0} + Z_{F0})}{D} + \frac{(Z_{S0} - Z_{S1})(Z_{S2} + Z_{F2})}{D} \\ V_b &= a^2 + \frac{(aZ_{S2} - a^2Z_{S1})Z_0}{D} + \frac{(Z_{S0} - a^2Z_{S1})Z_2}{D} \\ V_c &= a + \frac{(a^2Z_{S2} - aZ_{S1})Z_0}{D} + \frac{(Z_{S0} - aZ_{S1})Z_2}{D} \end{aligned} \tag{4.48}$$

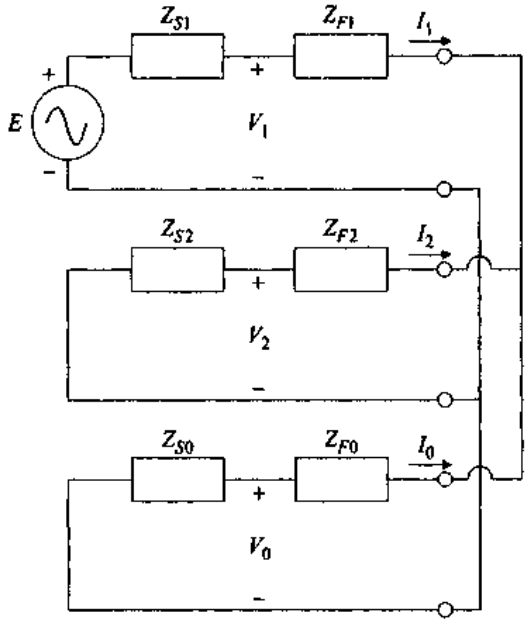

Figure 4.62 Equivalent circuit for a two-phase-to-ground fault.

There are two effects which cause a change in voltage in the non-faulted phase (V_a): the difference between the positive- and the negative-sequence source impedance; and the difference between the positive- and the zero-sequence source impedance. For both effects the non-faulted phase voltage drops when the positive-sequence impedance increases. Negative- and positive-sequence impedance are normally rather close, so that the second term in (4.48) may be neglected. The third term, which depends on the difference between zero- and positive-sequence source impedance, could cause a serious change in voltage. As the zero-sequence source impedance is often larger than the positive-sequence one, we expect a rise in voltage in the non-faulted phase. Like with single-phase faults we can eliminate this term by considering phase-to-neutral voltages instead of phase-to-ground voltages.

Looking at the voltages in the faulted phases and realizing that Z_{S1} is close to Z_{S2} we see that the second term is a voltage drop in the direction of the other faulted phase; $(a - a^2)$ is the pre-fault voltage between the faulted phases. For $Z_{S0} = Z_{S1}$ the third term in (4.48) is a voltage drop towards the non-faulted phase pre-fault voltage, for $Z_{S0} \ll Z_{S1}$ the third term is a drop along the positive real axis, as shown in Fig. 4.63. The voltage drop according to A in Fig. 4.63 is the same drop as for a phase-to-phase fault. The ground-connection causes an additional drop in the voltage in the two faulted phases, somewhere in between directions B and C. It is assumed here that all impedances have the same X/R ratio.

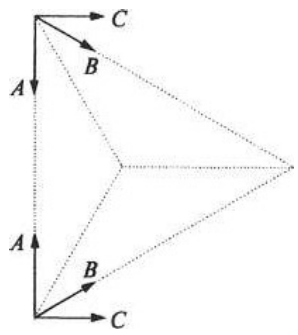

Figure 4.63 Voltage drops in the faulted phase during a two-phase-to-ground fault. A: second term in (4.48); B: third term for $Z_{S1} = Z_{S0}$; C: third term for $Z_{S1} \ll Z_{S0}$.

As said before, positive- and negative-sequence impedances are normally very close. In that case we can simplify the expressions by substituting $Z_{S1} = Z_{S2}$ and $Z_{F1} = Z_{F2}$. But when we are only interested in phase-to-neutral voltages it is easier to use the three-phase voltage divider model introduced in Fig. 4.53 for single-phase faults. For two-phase-to-ground faults the equivalent circuit is redrawn in Fig. 4.64.

Without any further calculation we can see from Fig. 4.64 that the phase-to-neutral voltage in the non-faulted phase is not influenced by the two-phase-to-ground fault. The phase-to-neutral voltage at the fault point, V_{FN}, is found from applying Kirchhoff's current law to the fault point:

$$\frac{a^2 - V_{FN}}{Z_{S1} + Z_{F1}} + \frac{a - V_{FN}}{Z_{S1} - Z_{F1}} = \frac{V_{FN}}{\frac{1}{3}(Z_{S0} - Z_{S1}) + \frac{1}{3}(Z_{F0} - Z_{F1})} \tag{4.49}$$

Solving (4.49) leads to the following expression for the voltage at the fault point:

$$V_{FN} = -\frac{(Z_{S0} + Z_{F0}) - (Z_{S1} + Z_{F1})}{2(Z_{S0} + Z_{F0}) + (Z_{S1} + Z_{F1})} \tag{4.50}$$

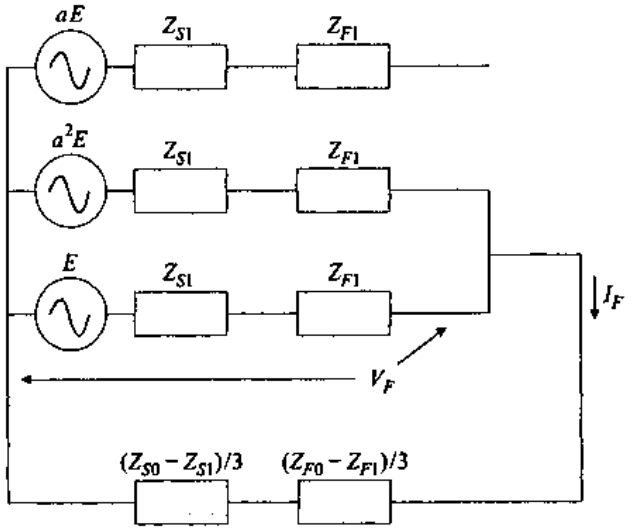

Figure 4.64 Three-phase voltage divider model for a two-phase-to-ground fault.

If zero-sequence and positive-sequence impedances are equal, $Z_{S0} = Z_{S1}$ and $Z_{F0} = Z_{F1}$, we find that

$$V_{FN} = 0 \tag{4.51}$$

If the zero-sequence impedance becomes large, like in a resistance-grounded system, the fault-point voltage is

$$V_{FN}^{\text{li}} = -\frac{1}{2} \tag{4.52}$$

The latter expression corresponds to the expression obtained for phase-to-phase faults. This is rather obvious if we realize that a large zero-sequence impedance implies that the fault current through the earth return is very small. Thus, the presence of a connection with earth during the fault does not influence the voltages.

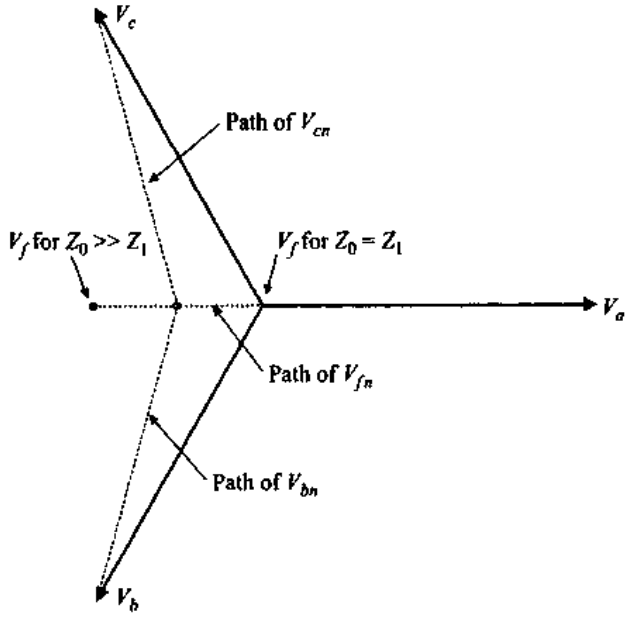

Figure 4.65 Phase-to-neutral voltages in the faulted phases for a two-phase-to-ground fault.

The intermediate case, where $Z_{S1} < Z_{S0} < \infty$, gives a voltage at the fault point somewhere in between these two extremes:

$$-\frac{1}{2} < V_{FN} < 0 \tag{4.53}$$

This voltage and the resulting voltages at the pcc can be obtained from Fig. 4.65. The voltage at the fault point is located between the origin and the point $-\frac{1}{2}$: the former for equal positive- negative-, and zero-sequence impedances, the latter for very large zero-sequence impedance. The voltage at the pcc for a faulted phase is somewhere between the voltage at the fault point and the pre-fault voltage in that phase. This knowledge will later be used for the classification of three-phase unbalanced sags. For calculating sag magnitudes this construction is not of practical use, as the fault-to-neutral voltage V_{FN} depends on the fault position.

4.4.4 Seven Types of Three-Phase Unbalanced Sags

The voltage sags due to the various types of faults have been discussed in the previous sections: three-phase faults in Section 4.2, single-phase faults in Section 4.4.1, phase-to-phase faults in Section 4.4.2, and finally two-phase-to-ground faults in Section 4.4.3. For each type of fault, expressions have been derived for the voltages at the pcc. But as already mentioned, this voltage is not equal to the voltage at the equipment terminals. Equipment is normally connected at a lower voltage level than the level at which the fault occurs. The voltages at the equipment terminals, therefore, not only depend on the voltages at the pcc but also on the winding connection of the transformers between the pcc and the equipment terminals. The voltages at the equipment terminals further depend on the load connection. Three-phase load is normally connected in delta but star-connection is also used. Single-phase load is normally connected in star (i.e., between one phase and neutral) but sometimes in delta (between two phases). Note that we consider here the voltage sag as experienced at the terminals of end-user equipment, not the voltage as measured by monitoring equipment. The latter is typically located at distribution or even at transmission level.

In this section we will derive a classification for three-phase unbalanced voltage sags, based on the following assumptions:

- Positive- and negative-sequence impedances are identical.
- The zero-sequence component of the voltage does not propagate down to the equipment terminals, so that we can consider phase-to-neutral voltages.
- Load currents, before, during, and after the fault, can be neglected.

4.4.4.1 Single-Phase Faults. The phase-to-neutral voltages due to a single-phase-to-ground fault are, under the assumptions mentioned,

$$\begin{aligned} V_a &= V \\ V_b &= -\frac{1}{2} - \frac{1}{2}j\sqrt{3} \\ V_c &= -\frac{1}{2} + \frac{1}{2}j\sqrt{3} \end{aligned} \tag{4.54}$$

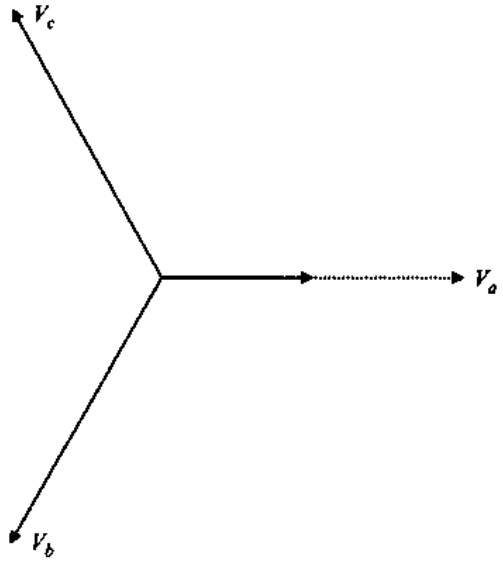

Figure 4.66 Phase-to-neutral voltages before (dashed line) and during (solid line) a phase-to-ground fault.

The resulting phasor diagram is shown in Fig. 4.66. If the load is connected in star, these are the voltages at the equipment terminals. If the load is connected in delta, the equipment terminal voltages are the phase-to-phase voltages. These can be obtained from (4.54) by the following transformation:

$$\begin{aligned} V_a' &= j\frac{V_b - V_c}{\sqrt{3}} \\ V_b' &= j\frac{V_c - V_a}{\sqrt{3}} \\ V_c' &= j\frac{V_a - V_b}{\sqrt{3}} \end{aligned} \tag{4.55}$$

This transformation will be an important part of the classification. The factor $\sqrt{3}$ is aimed at changing the base of the pu values, so that the normal operating voltage remains at 100%. The 90° rotation by using a factor j aims at keeping the axis of symmetry of the sag along the real axis. We will normally omit the primes from (4.55). Applying transformation (4.55) results in the following expression for the three-phase unbalanced voltage sag experienced by a delta-connected load, due to a single-phase fault:

$$\begin{aligned} V_a &= 1 \\ V_b &= -\frac{1}{2} - \left(\frac{1}{6} + \frac{1}{3}V\right)j\sqrt{3} \\ V_c &= -\frac{1}{2} + \left(\frac{1}{6} + \frac{1}{3}V\right)j\sqrt{3} \end{aligned} \tag{4.56}$$

The phasor diagram for the equipment terminal voltages is shown in Fig. 4.67: two voltages show a drop in magnitude and change in phase angle; the third voltage is not influenced at all. Delta-connected equipment experiences a sag in two phases due to a single-phase fault.

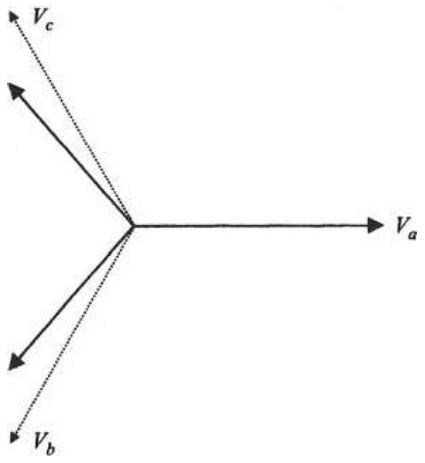

Figure 4.67 Phase-to-phase voltages before (dashed line) and during (solid line) a phase-to-ground fault.

4.4.4.2 Phase-to-Phase Faults. For a phase-to-phase fault the voltages in the two faulted phases move toward each other. The expressions for the phase-to-neutral voltages during a phase-to-phase fault read as follows:

$$\begin{aligned} V_a &= 1 \\ V_b &= -\frac{1}{2} - \frac{1}{2} V j\sqrt{3} \\ V_c &= -\frac{1}{2} + \frac{1}{2} V j\sqrt{3} \end{aligned} \tag{4.57}$$

Like before, (4.55) can be used to calculate the voltages experienced by a phase-to-phase connected load, resulting in

$$\begin{aligned} V_a &= V \\ V_b &= -\frac{1}{2} V - \frac{1}{2} j\sqrt{3} \\ V_c &= -\frac{1}{2} V + \frac{1}{2} j\sqrt{3} \end{aligned} \tag{4.58}$$

The corresponding phasor diagrams are shown in Figs. 4.68 and 4.69. Due to a phase-to-phase fault a star-connected load experiences a drop in two phases, a delta-

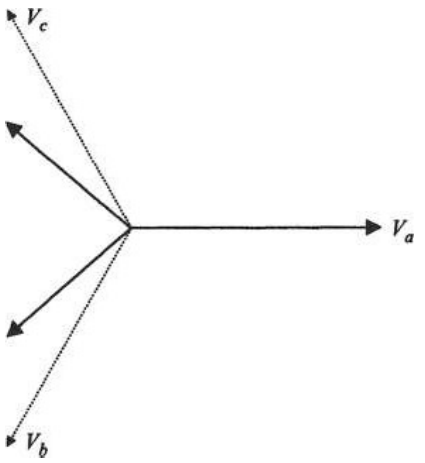

Figure 4.68 Phase-to-neutral voltages before (dashed line) and during (solid line) a phase-to-phase fault.

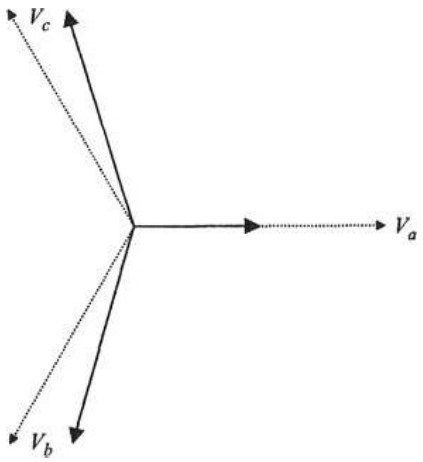

Figure 4.69 Phase-to-phase voltages before (dashed line) and during (solid line) a phase-to-phase fault.

connected load experiences a drop in three phases. For the star-connected load the maximum drop is 50%, for $V = 0$. But for the delta-connected load one phase could drop all the way down to zero. The conclusion that load could therefore best be connected in star is wrong, however. Most sags do not originate at the same voltage level as the equipment terminals. We will see later that the sag at the equipment terminals could be either of the two types shown in Figs. 4.68 and 4.69, depending on the transformer winding connections.

4.4.4.3 Transformer Winding Connections. Transformers come with many different winding connections, but a classification into only three types is sufficient to explain the transfer of three-phase unbalanced sags from one voltage level to another.

1. Transformers that do not change anything to the voltages. For this type of transformer the secondary-side voltages (in pu) are equal to the primary-side voltages (in pu). The only type of transformer for which this holds is the star-star connected one with both star points grounded.
2. Transformers that remove the zero-sequence voltage. The voltages on the secondary side are equal to the voltages on the primary side minus the zero-sequence component. Examples of this transformer type are the star-star connected transformer with one or both star points not grounded, and the delta-delta connected transformer. The delta-zigzag (Dz) transformer also fits into this category.
3. Transformers that swap line and phase voltages. For these transformers each secondary-side voltage equals the difference between two primary-side voltages. Examples are the delta-star (Dy) and the star-delta (Yd) transformer as well as the star-zigzag (Yz) transformer.

Within each of these three categories there will be transformers with different clock number (e.g., Yd1 and Yd11) leading to a different phase shift between primary- and secondary-side voltages. This difference is not of any importance for the voltage sags as experienced by the equipment. All that matters is the change between the pre-fault voltages and the during-fault voltages, in magnitude and in phase-angle. The whole phasor diagram, with pre-fault and during-fault phasors, can be rotated without any influence on the equipment. Such a rotation can be seen as a shift in the zero point on

the time axis which of course has no influence on equipment behavior. The three transformer types can be defined mathematically by means of the following transformation matrices:

$$T_1 = \begin{bmatrix} 1 & 0 & 0 \\ 0 & 1 & 0 \\ 0 & 0 & 1 \end{bmatrix} \tag{4.59}$$

$$T_2 = \frac{1}{3}\begin{bmatrix} 2 & -1 & -1 \\ -1 & 2 & -1 \\ -1 & -1 & 2 \end{bmatrix} \tag{4.60}$$

$$T_3 = \frac{j}{\sqrt{3}}\begin{bmatrix} 0 & 1 & -1 \\ -1 & 0 & 1 \\ 1 & -1 & 0 \end{bmatrix} \tag{4.61}$$

Equation (4.59) is straightforward: matrix T_1 is the unity matrix. Equation (4.60) removes the zero-sequence component of the voltage. The matrix T_2 can be understood easily by realizing that the zero-sequence voltage equals $\frac{1}{3}(V_a + V_b + V_c)$. Matrix T_3 in (4.61) describes exactly the same transformation as expression (4.55). The additional advantage of the 90° rotation is that twice applying matrix T_3 gives the same results as once applying matrix T_2. Thus, $T_3^2 = T_2$; in engineering terms: two Dy transformers in cascade have the same effect on the voltage sag as one Dd transformer.

4.4.3.4 Transfer of Voltage Sags across Transformers. The three types of transformers can be applied to the sags due to single-phase and phase-to-phase faults. To get an overview of the resulting sags, the different combinations will be systematically treated below.

- *Single-phase fault, star-connected load, no transformer.*
  This case has been discussed before, resulting in (4.54) and Fig. 4.66. We will refer to this sag as sag X1. Transformer type 1 gives the same results of course.
- *Single-phase fault, delta-connected load, no transformer.*
  The voltage sag for this case is given in (4.56) and shown in Fig. 4.67. This sag will be referred to as sag X2.
- *Single-phase fault, star-connected load, transformer type 2.*
  Transformer type 2 removes the zero-sequence component of the voltage. The zero-sequence component of the phase voltages due to a single-phase fault is found from (4.54) to be equal to $\frac{1}{3}(V - 1)$. This gives the following expressions for the voltages:

$$\begin{aligned} V_a &= \frac{1}{3} + \frac{2}{3}V \\ V_b &= -\frac{1}{6} - \frac{1}{3}V - \frac{1}{2}j\sqrt{3} \\ V_c &= -\frac{1}{6} - \frac{1}{3}V + \frac{1}{2}j\sqrt{3} \end{aligned} \tag{4.62}$$

  This looks like a new type of sag, but we will see later that it is identical to the one experienced by a delta-connected load during a phase-to-phase fault. But for now it will be referred to as sag X3.

- *Single-phase fault, delta-connected load, transformer type 2.*
  The phase-to-phase voltages experienced by a delta-connected load do not contain any zero-sequence component. Thus transformer type 2 does not have any influence on the sag voltages. The sag is thus still of type X2.
- *Single-phase fault, star-connected load, transformer type 3.*
  Transformer type 3 changes phase voltages into line voltages. Thus star-connected load on secondary side experiences the same sag as delta-connected load on primary side. In this case that is sag X2.
- *Single-phase fault, delta-connected load, transformer type 3.*
  There are now two transformations: from star- to delta-connected load, and from primary to secondary side of the transformer. Each of these transformations can be described through matrix T_3 defined in (4.61). Two of those transformations in cascade have the same effect as transformation T_2. Thus, the sag experienced by this delta-connected load is the same as by the star-connected load behind a transformer of type 2; thus, sag type X3.
- *Phase-to-phase fault, star-connected load, no transformer.*
  This case was treated before resulting in (4.57) and Fig. 4.68. This will be sag type X4.
- *Phase-to-phase fault, delta-connected load, no transformer.*
  The expression for the sag voltages reads as (4.58) and is shown in Fig. 4.69. This type will be referred to as X5.
- *Phase-to-phase fault, star-connected load, transformer type 2.*
  As phase-to-phase faults do not result in any zero-sequence voltage, transformer type 2 (which removes the zero-sequence voltage) does not have any effect. The sag thus remains of type X4.
- *Phase-to-phase fault, delta-connected load, transformer type 2.*
  Like before, the sag is still of type X5.
- *Phase-to-phase fault, star-connected load, transformer type 3.*
  Star-connected load on secondary side of transformer type 2 experiences the same sag as delta-connected load on primary side. This results in type X5.
- *Phase-to-phase fault, delta-connected load, transformer type 3.*
  This gives again two identical transformations T_3 in cascade, resulting in one transformation T_2. But that one only removes the zero-sequence component and has thus no influence on sags due to phase-to-phase faults. The result is, thus, again X4.

The effect of a second transformer on sags X1 through X5 is shown in Table 4.8. These results can be obtained by following the same reasoning as above. It becomes clear that

TABLE 4.8 Further Propagation of Sags

	Transformer Type		
Sag Type	1	2	3
X1	X1	X3	X2
X2	X2	X2	X3
X3	X3	X3	X2
X4	X4	X4	X5
X5	X5	X5	X4

the number of combinations is limited: at most five different sag types are possible due to single-phase and phase-to-phase faults.

4.4.4.5 The Basic Types of Sags. We saw that single-phase faults lead to three types of sags, designated sag X1, sag X2, and sag X3. Phase-to-phase faults lead to sag X4 and sag X5. We saw already from the phasor diagrams in Figs. 4.67 and 4.68 that single-phase and phase-to-phase faults lead to similar sags. The sag voltages for sag type X2 are

$$\begin{aligned} V_a &= 1 \\ V_b &= -\frac{1}{2} - \left(\frac{1}{6} + \frac{1}{3}V\right)j\sqrt{3} \\ V_c &= -\frac{1}{2} + \left(\frac{1}{6} + \frac{1}{3}V\right)j\sqrt{3} \end{aligned} \tag{4.63}$$

For sag type X4 the voltages are

$$\begin{aligned} V_a &= 1 \\ V_b &= -\frac{1}{2} - \frac{1}{2}Vj\sqrt{3} \\ V_c &= -\frac{1}{2} + \frac{1}{2}Vj\sqrt{3} \end{aligned} \tag{4.64}$$

Comparing these two sets of equations shows that (4.63) can be obtained by replacing V in (4.64) by $\frac{1}{3} + \frac{2}{3}V$. If we define the magnitude of sag X4 as V, then sag X2 is a sag of type X4 with magnitude $\frac{1}{3} + \frac{2}{3}V$.

In the same way we can compare sag X3:

$$\begin{aligned} V_a &= \frac{1}{3} + \frac{2}{3}V \\ V_b &= -\frac{1}{6} - \frac{1}{3}V - \frac{1}{2}j\sqrt{3} \\ V_c &= -\frac{1}{6} - \frac{1}{3}V + \frac{1}{2}j\sqrt{3} \end{aligned} \tag{4.65}$$

and sag X5:

$$\begin{aligned} V_a &= V \\ V_b &= -\frac{1}{2}V - \frac{1}{2}j\sqrt{3} \\ V_c &= -\frac{1}{2}V + \frac{1}{2}j\sqrt{3} \end{aligned} \tag{4.66}$$

Again we obtain (4.65) by replacing V in (4.66) by $\frac{1}{3} + \frac{2}{3}V$. The result is that only three types remain: X1, X4, and X5. A fourth type of sag is the sag due to three-phase faults, with all three voltages down the same amount. The resulting classification is shown in Table 4.9 in equation form and in Fig. 4.70 in phasor form. All sags in Fig. 4.70 have a magnitude of 50%. From the discussion about sags due to single-phase and phase-to-phase faults, together with the definition of the four types, the origin and the propagation of the sags becomes straightforward. The results are summarized in Table 4.10 for the origin of sags and in Table 4.11 for their propagation to lower voltage levels. The superscript (*) behind the sag type in Tables 4.10 and

TABLE 4.9 Four Types of Sags in Equation Form

Type A	Type B
$V_a = V$	$V_a = V$
$V_b = -\frac{1}{2}V - \frac{1}{2}jV\sqrt{3}$	$V_b = -\frac{1}{2} - \frac{1}{2}j\sqrt{3}$
$V_c = -\frac{1}{2}V + \frac{1}{2}jV\sqrt{3}$	$V_c = -\frac{1}{2} + \frac{1}{2}j\sqrt{3}$
Type C	**Type D**
$V_a = 1$	$V_a = V$
$V_b = -\frac{1}{2} - \frac{1}{2}jV\sqrt{3}$	$V_b = -\frac{1}{2}V - \frac{1}{2}j\sqrt{3}$
$V_c = -\frac{1}{2} + \frac{1}{2}jV\sqrt{3}$	$V_c = -\frac{1}{2}V + \frac{1}{2}j\sqrt{3}$

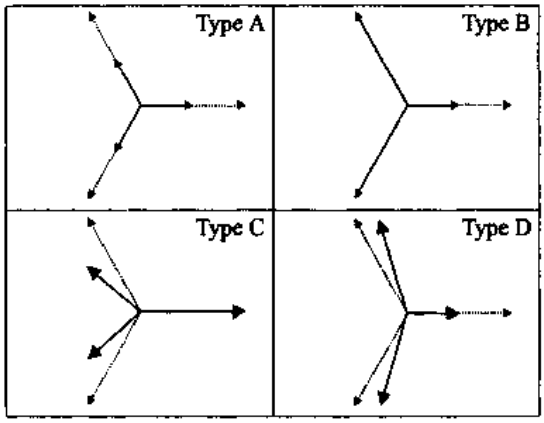

Figure 4.70 Four types of sag in phasor-diagram form.

TABLE 4.10 Fault Type, Sag Type, and Load Connection

Fault Type	Star-connected Load	Delta-connected Load
Three-phase	sag A	sag A
Phase-to-phase	sag C	sag D
Single-phase	sag B	sag C*

TABLE 4.11 Transformation of Sag Type to Lower Voltage Levels

Transformer Connection	Sag Type A	Sag Type B	Sag Type C	Sag Type D
YNyn	type A	type B	type C	type D
Yy, Dd, Dz	type A	type D*	type C	type D
Yd, Dy, Yz	type A	type C*	type D	type C

4.11 indicates that the sag magnitude is not equal to V but equal to $\frac{1}{3} + \frac{2}{3}V$, with V the voltage in the faulted phase or between the faulted phases in Table 4.10 and the magnitude of the sag on primary side in Table 4.11. Note that in effect these two definitions of V are the same.

4.4.4.6 Two-Phase-to-Ground Faults. Two-phase-to-ground faults can be treated in the same way as single-phase and phase-to-phase faults. We will assume that the voltage in the non-faulted phase is not influenced by the fault. As we have seen in Section 4.4.3 this corresponds to the situation in which positive-, negative-, and zero-sequence impedances are equal. This can be seen as an extreme case. A zero-sequence impedance larger than the positive-sequence impedance will shift the resulting voltages toward those for a phase-to-phase fault.

The phase-to-ground voltages at the pcc due to a two-phase-to-ground fault are

$$\begin{aligned} V_a &= 1 \\ V_b &= -\frac{1}{2}V - \frac{1}{2}Vj\sqrt{3} \\ V_c &= -\frac{1}{2}V + \frac{1}{2}Vj\sqrt{3} \end{aligned} \tag{4.67}$$

After a Dy transformer or any other transformer of type 3, the voltages are

$$\begin{aligned} V_a &= V \\ V_b &= -\frac{1}{3}j\sqrt{3} - \frac{1V}{2} - \frac{1}{6}Vj\sqrt{3} \\ V_c &= +\frac{1}{3}j\sqrt{3} - \frac{1}{2}V + \frac{1}{6}Vj\sqrt{3} \end{aligned} \tag{4.68}$$

After two transformers of type 3 or after one transformer of type 2, we get

$$\begin{aligned} V_a &= \frac{2}{3} + \frac{1}{3}V \\ V_b &= -\frac{1}{3} - \frac{1}{6}V - \frac{I}{2}Vj\sqrt{3} \\ V_c &= -\frac{1}{3} - \frac{1}{6}V + \frac{I}{2}Vj\sqrt{3} \end{aligned} \tag{4.69}$$

These three sags are different from the four types found earlier. It is not possible to translate one into the other. Two-phase-to-ground faults lead to three more types of sags, resulting in a total of seven. The three new types are shown in phasor-diagram form in Fig. 4.71 and in equation form in Table 4.12. Sags due to two-phase-to-ground faults and sags due to phase-to-phase faults are compared in Fig. 4.72. For a type C sag the voltages change along the imaginary axis only, for type D along the real axis only.

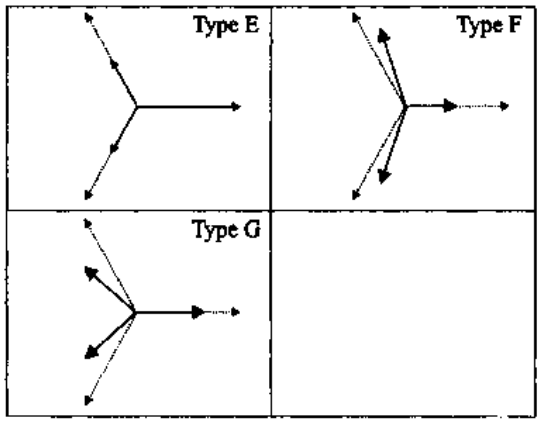

Figure 4.71 Three-phase unbalanced sags due to two-phase-to-ground faults.

TABLE 4.12 Sags Due to Two-Phase-to-Ground Faults

Type E	Type F
$V_a = 1$	$V_a = V$
$V_b = -\frac{1}{2}V - \frac{1}{2}Vj\sqrt{3}$	$V_b = -\frac{1}{3}j\sqrt{3} - \frac{1}{2}V - \frac{1}{6}Vj\sqrt{3}$
$V_c = -\frac{1}{2}V + \frac{1}{2}Vj\sqrt{3}$	$V_c = +\frac{1}{3}j\sqrt{3} - \frac{1}{2}V + \frac{1}{6}Vj\sqrt{3}$

Type G

$V_a = \frac{2}{3} + \frac{1}{3}V$

$V_b = -\frac{1}{3} - \frac{1}{6}V - \frac{1}{2}Vj\sqrt{3}$

$V_c = -\frac{1}{3} - \frac{1}{6}V + \frac{1}{2}Vj\sqrt{3}$

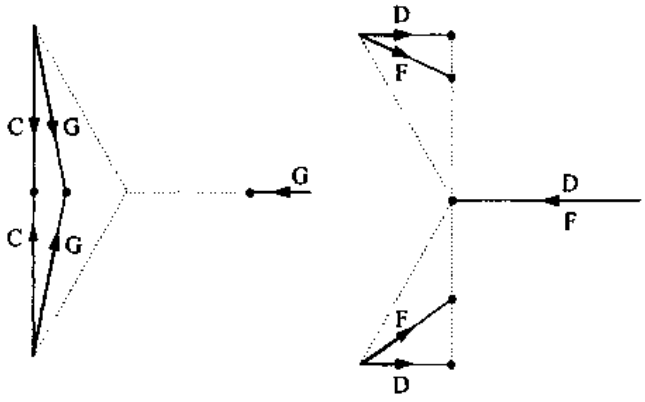

Figure 4.72 Comparison of three-phase unbalanced sags due to two-phase-to-ground faults (F and G) with three-phase unbalanced sags due to phase-to-phase and single-phase-to-ground faults (C and D). The arrows indicate the direction of change in the three complex voltages for the different sag types.

For types F and G the voltages drop along both axis. The resulting voltages at the equipment terminals are lower during a two-phase-to-ground fault. An additional difference is that all three voltages drop in magnitude for a type G sag. Note also that for a type D and type F sag the drop in the worst-affected phase is the same, whereas for a type C and a type G sag the drop in voltage between the two worst-affected phases is the same. This property will be used when defining the magnitude of measured three-phase unbalanced sags.

Sag types F and G have been derived by assuming that positive-, negative-, and zero-sequence impedances are the same. If the zero-sequence impedance is larger than the positive-sequence impedance, the resulting sag will be somewhere in between type C and type G, or in between type D and type F.

4.4.4.7 Seven Types of Three-Phase Unbalanced Sags. Origin of sags and transformation to lower voltage levels for all seven types of three-phase unbalanced sags are summarized in Tables 4.13 and 4.14. An example of the sag transformation to

TABLE 4.13 Origin of Three-Phase Unbalanced Sags

Fault Type	Star-connected Load	Delta-connected Load
Three-phase	Type A	Type A
Two-phase-to-ground	Type E	Type F
Phase-to-phase	Type C	Type D
Single-phase	Type B	Type C*

Note: Asterisk defined as in Tables 4.10 and 4.11.

TABLE 4.14 Transformation of Sag Type to Lower Voltage Levels

Transformer Connection	Sag on Primary Side						
	Type A	Type B	Type C	Type D	Type E	Type F	Type G
YNyn	A	B	C	D	E	F	G
Yy, Dd, Dz	A	D*	C	D	G	F	G
Yd, Dy, Yz	A	C*	D	C	F	G	F

lower voltage levels is shown in Fig. 4.73. A fault at 33 kV causes the voltage at the pcc to drop to 50% of the nominal voltage. For a three-phase fault the situation is easy: at any level and for any load connection the sag is of type A and with a magnitude of 50%. For a phase-to-phase fault the voltage between the faulted phases at the pcc drops to 50%. For star-connected load the resulting sags are type C, 50% at 33 kV; type D, 50% at 11 kV; and again type C, 50% at 660 V. In case the fault is a single-phase one, the voltage in the faulted phase drops to 50% at the pcc. This corresponds to a sag of type B and magnitude 50% at 33 kV. After the first Dy transformer the zero-sequence component of the voltages has been removed. Star-connected load at 11 kV will experience a sag of type C with a magnitude of 67%. Delta-connected load will experience a sag of type D with a magnitude of 67%. For load fed at 660 V the situation is just the other way around: star-connected load experiences a sag of type D; delta-connected load one of type C.

4.4.4.8 Overview. In the beginning of this section we assumed that the zero-sequence component of the voltages did not propagate down to the equipment terminals. We used this assumption to obtain an expression for the voltages during a single-phase-to-ground fault. Under this same assumption we find that three-phase unbalanced sags of type B or type E cannot occur at the equipment terminals. At the equipment terminals we only find the following five types of three-phase unbalanced sags:

- type A due to three-phase faults.
- type C and type D due to single-phase and phase-to-phase faults.
- type F and type G due to two-phase-to-ground faults.

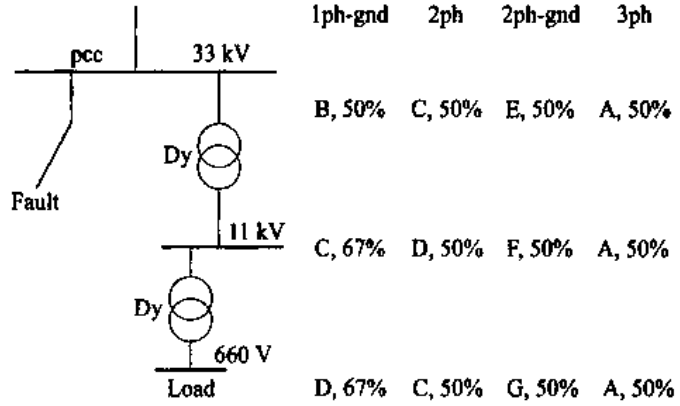

Figure 4.73 Example of sag transformation, for star-connected load.

The latter two types can be considered as distorted versions of type C and D. Sags of type C and D are also distorted by the presence of induction motor load. The presence of induction motor load makes that positive- and negative-sequence source impedances are no longer equal. One of the effects of this is that the voltage in the "non-faulted phase" for a type C sag is no longer equal to 100%. This has been the basis for a classification and characterization of three-phase unbalanced sags into three types, corresponding to our types A, C, and D [203], [204].

4.5 PHASE-ANGLE JUMPS

A short circuit in a power system not only causes a drop in voltage magnitude but also a change in the phase angle of the voltage. In a 50 Hz or 60 Hz system, voltage is a complex quantity (a phasor) which has magnitude and phase angle. A change in the system, like a short circuit, causes a change in voltage. This change is not limited to the magnitude of the phasor but includes a change in phase angle as well. We will refer to the latter as the phase-angle jump associated with the voltage sag. The phase-angle jump manifests itself as a shift in zero crossing of the instantaneous voltage. Phase-angle jumps are not of concern for most equipment. But power electronics converters using phase-angle information for their firing instants may be affected. We will come back to the effect of phase-angle jumps on equipment in Chapter 5.

Figure 4.74 shows a voltage sag with a phase-angle jump of +45°: the during-fault voltage leads the pre-fault voltage. A sag with a phase-angle jump of −45° is shown in Fig. 4.75: the during-fault voltage lags the pre-fault voltage. Both sags have a magnitude of 70%. In both figures, the pre-fault voltages have been continued as a dashed curve. Note that these are synthetic sags, not measurement results.

The origin of phase-angle jumps will be explained for a three-phase fault, as that enables us to use the single-phase model. Phase-angle jumps during three-phase faults are due to the difference in X/R ratio between the source and the feeder. A second cause of phase-angle jumps is the transformation of sags to lower voltage levels. This phenomenon has already been mentioned when unbalanced sags were discussed in Section 4.4.

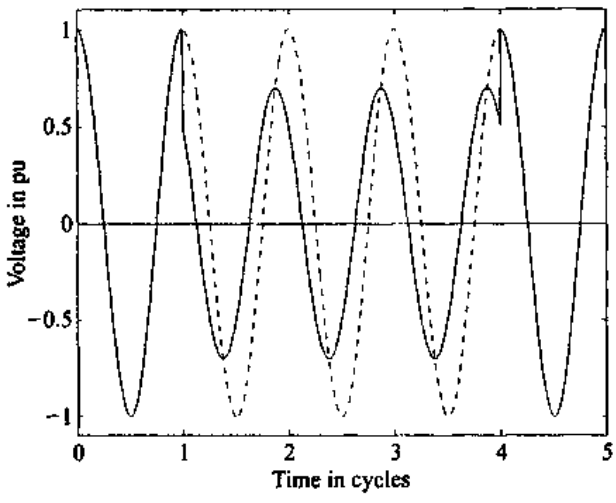

Figure 4.74 Synthetic sag with a magnitude of 70% and a phase-angle jump of +45°.

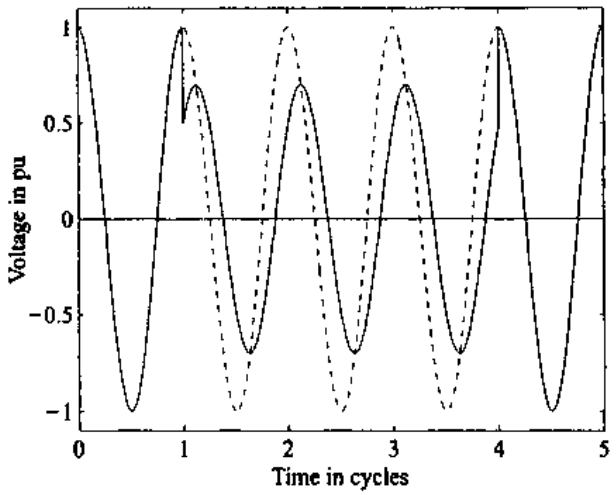

Figure 4.75 Synthetic sag with a magnitude of 70% and a phase-angle jump of −45°.

4.5.1 Monitoring

To obtain the phase-angle jump of a measured sag, the phase-angle of the voltage during the sag must be compared with the phase-angle of the voltage before the sag. The phase-angle of the voltage can be obtained from the voltage zero-crossing or from the phase of the fundamental component of the voltage. The complex fundamental voltage can be obtained by doing a Fourier transform on the signal. This enables the use of Fast-Fourier Transform (FFT) algorithms.

To explain an alternative method, consider the following voltage signal:

$$v(t) = X\cos(\omega_0 t) - Y\sin(\omega_0 t) = Re\left\{(X + jY)e^{j\omega_0 t}\right\} \tag{4.70}$$

with ω_0 the fundamental (angular) frequency. Two new signals are obtained from this signal, as follows:

$$v_d(t) = 2v(t) \times \cos(\omega_0 t) \tag{4.71}$$

$$v_q(t) = 2v(t) \times \sin(\omega_0 t) \tag{4.72}$$

which we can write as

$$v_d(t) = X + X\cos(2\omega_0 t) + Y\sin(2\omega_0 t) \tag{4.73}$$

$$v_q(t) = -Y + Y\cos(2\omega_0 t) + X\sin(2\omega_0 t) \tag{4.74}$$

Averaging the two resulting signals over one half-cycle of the fundamental frequency gives the required fundamental voltage.

$$X + jY = \overline{v}_d(t) - j\overline{v}_q(t) \tag{4.75}$$

Knowing the values of X and Y, the sag magnitude can be calculated as $\sqrt{X^2 + Y^2}$ and the phase-angle jump as $\arctan\frac{Y}{X}$.

This algorithm has been applied to the recorded sag in Fig. 4.1. The resulting sag magnitude is shown in Fig. 4.76 and the phase-angle jump in Fig. 4.77. The effect of averaging $v_d(t)$ and $v_q(t)$ over one full cycle of the fundamental frequency is shown in Fig. 4.78 for the sag magnitude and in Fig. 4.79 for the phase-angle jump. The effect of a larger window is that the transition is slower, but the overshoot in phase-angle is less. Which window length needs to be chosen depends on the application.

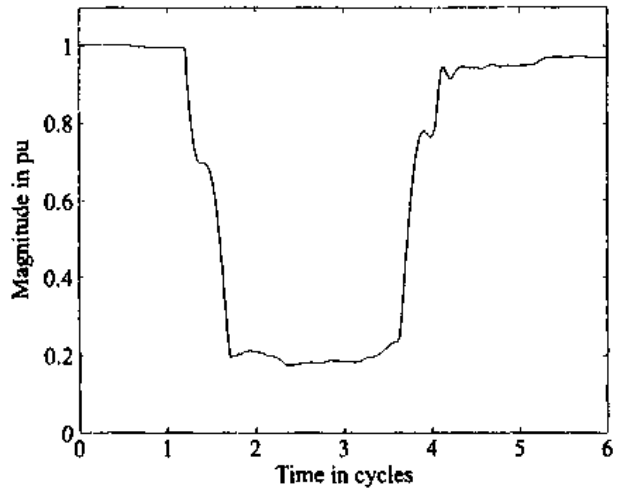

Figure 4.76 Amplitude of the fundamental voltage versus time for the voltage sag shown in Fig. 4.1—a half-cycle window has been used.

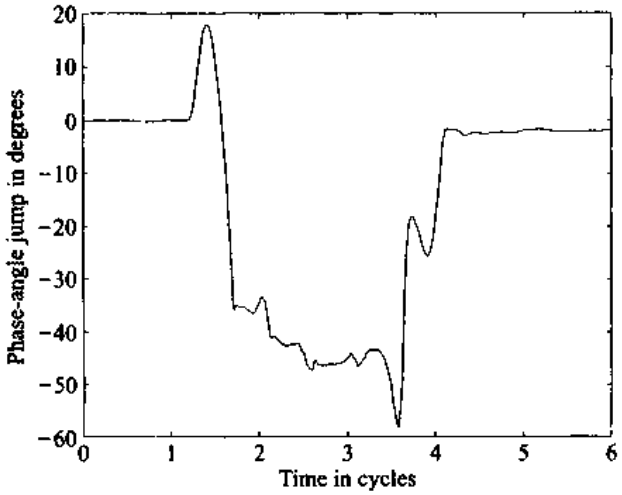

Figure 4.77 Argument of the fundamental voltage versus time for the voltage sag shown in Fig. 4.1—a half-cycle window has been used.

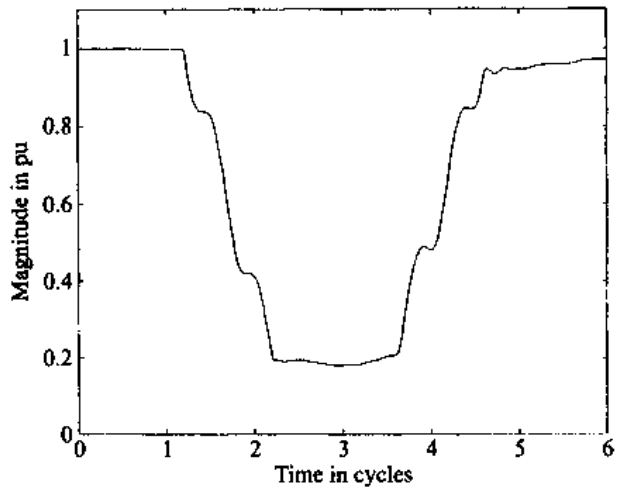

Figure 4.78 Amplitude of the fundamental voltage versus time for the voltage sag shown in Fig. 4.1—a one-cycle window has been used.

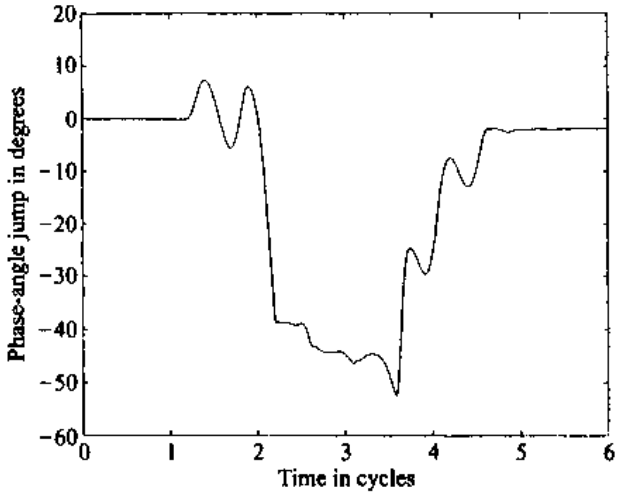

Figure 4.79 Argument of the fundamental voltage versus time for the voltage sag shown in Fig. 4.1—a one-cycle window has been used.

4.5.2 Theoretical Calculations

4.5.2.1 Origin of Phase-Angle Jumps. To understand the origin of phase-angle jumps associated with voltage sags, the single-phase voltage divider model of Fig. 4.14 can be used again, with the difference that Z_S and Z_F are complex quantities which we will denote as $\overline{Z}_S$ and $\overline{Z}_F$. Like before, we neglect all load currents and assume $E = 1$. This gives for the voltage at the point-of-common coupling (pcc):

$$\overline{V}_{sag} = \frac{\overline{Z}_F}{\overline{Z}_S + \overline{Z}_F} \tag{4.76}$$

Let $\overline{Z}_S = R_S + jX_S$ and $\overline{Z}_F = R_F + jX_F$. The argument of $\overline{V}_{sag}$, thus the phase-angle jump in the voltage, is given by the following expression:

$$\Delta\phi = \arg(\overline{V}_{sag}) = \arctan\left(\frac{X_F}{R_F}\right) - \arctan\left(\frac{X_S + X_F}{R_S + R_F}\right) \tag{4.77}$$

If $\frac{X_S}{R_S} = \frac{X_F}{R_F}$, expression (4.77) is zero and there is no phase-angle jump. The phase-angle jump will thus be present if the X/R ratios of the source and the feeder are different.

4.5.2.2 Influence of Source Strength. Consider again the power system used to obtain Fig. 4.15. Instead of the sag magnitude we calculated the phase-angle jump, resulting in Fig. 4.80. We again see that a stronger source makes the sag less severe: less drop in magnitude as well as a smaller phase-angle jump. The only exception is for terminal faults. The phase-angle jump for zero distance to the fault is independent of the source strength. Note that this is only of theoretical value as the phase-angle jump for zero distance to the fault, and thus for zero voltage magnitude, has no physical meaning.

4.5.2.3 Influence of Cross Section. Figure 4.81 plots phase-angle jump versus distance for 11 kV overhead lines of different cross sections. The resistance of the source has been neglected in these calculations: $R_S = 0$. The corresponding sag magnitudes were shown in Fig. 4.16. From the overhead line impedance data shown in Table 4.1 we can calculate the X/R ratio of the feeder impedances: 1.0 for the

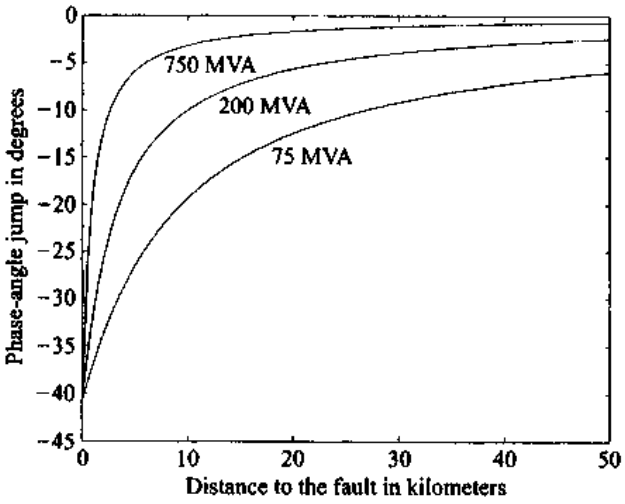

Figure 4.80 Phase-angle jump versus distance, for faults on a 150 mm^2 11 kV overhead feeder, with different source strength.

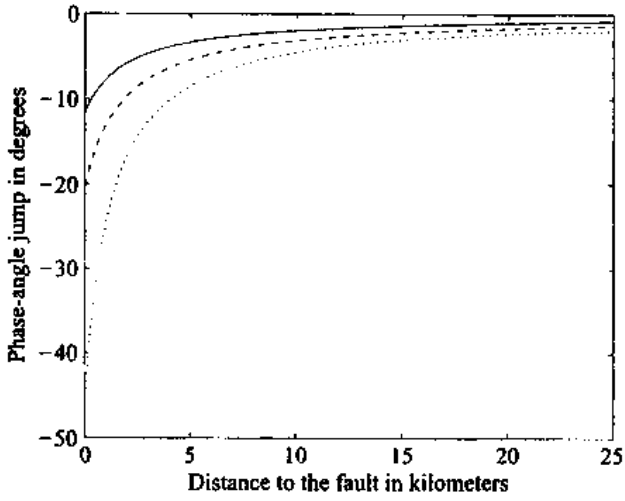

Figure 4.81 Phase-angle jump versus distance, for overhead lines with cross section 300 mm^2 (solid line), 150 mm^2 (dashed line), and 50 mm^2 (dotted line).

50 mm^2 line, 2.7 for the 150 mm^2, and 4.9 for the 300 mm^2; the phase-angle jump decreases for larger X/R ratio of the feeder.

The results for underground cables are shown in Fig. 4.82. Cables with a smaller cross section have a larger phase-angle jump for small distances to the fault, but the phase-angle jump also decays faster for increasing distance. This is due to the (in absolute value) larger impedance per unit length. The corresponding sag magnitudes were shown in Fig. 4.17.

Sag magnitude and phase-angle jump, i.e., magnitude and argument of the complex during-fault voltage, can be plotted in one diagram. Figure 4.83 shows the voltage paths in the complex plane, where the pre-sag voltage is in the direction of the positive real axis. The further the complex voltage is from $1+j0$, the larger the change in complex voltage due to the fault. The difference between the pre-sag voltage and the actual voltage is referred to as the missing voltage. We will come back to the concept of missing voltage in Section 4.7.2.

Instead of splitting the disturbance into real and imaginary parts one may plot magnitude against phase-angle jump as done in Fig. 4.84. From the figure we can conclude that the phase-angle jump increases (in absolute value) when the drop in voltage increases (thus, when the sag magnitude decreases). Both an increase in

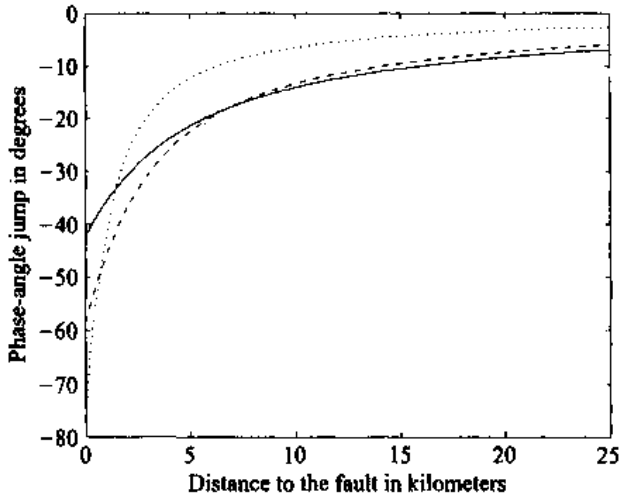

Figure 4.82 Phase-angle jump versus distance, for underground cables with cross section 300 mm^2 (solid line), 150 mm^2 (dashed line), and 50 mm^2 (dotted line).

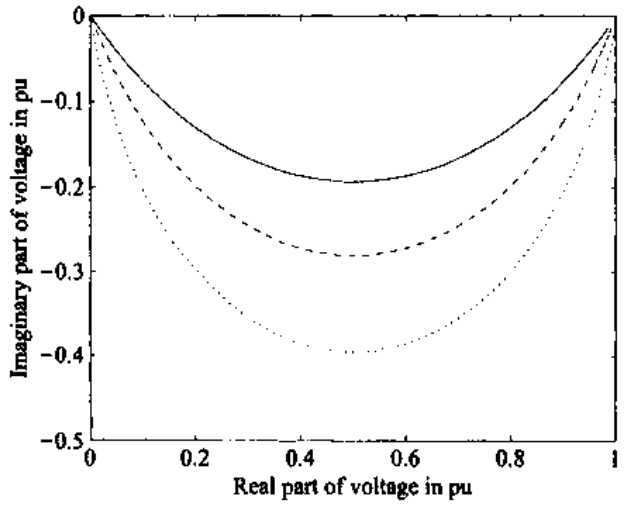

Figure 4.83 Path of the voltage in the complex plane when the distance to the fault changes, for underground cables with cross section 300 mm^2 (solid line), 150 mm^2 (dashed line), and 50 mm^2 (dotted line).

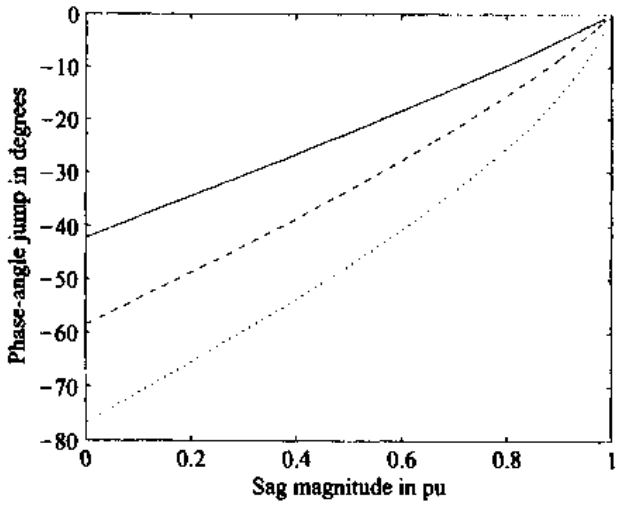

Figure 4.84 Magnitude versus phase-angle jump, for underground cables with cross section 300 mm^2 (solid line), 150 mm^2 (dashed line), and 50 mm^2 (dotted line).

phase-angle jump and a decrease in magnitude can be described as a more severe event. Knowing that both voltage drop and phase-angle jump increase when the distance to the fault increases, we can conclude that a fault leads to a more severe event the closer it is to the point-of-common coupling. We will later see that this only holds for three-phase faults. For single-phase and phase-to-phase faults this is not always the case.

4.5.2.4 Magnitude and Phase-Angle Jump Versus Distance. To obtain expressions for magnitude and phase-angle jump as a function of the distance to the fault we substitute $\overline{Z}_F = \overline{z}\mathcal{L}$ in (4.76) with $\overline{z}$ the complex feeder impedance per unit length, resulting in

$$\overline{V}_{sag} = \frac{\overline{z}\mathcal{L}}{\overline{Z}_S + \overline{z}\mathcal{L}} \tag{4.78}$$

The phase-angle jump is found from

$$\arg(\overline{V}_{sag}) = \arg(\overline{z}\mathcal{L}) - \arg(\overline{Z}_S + \overline{z}\mathcal{L}) \tag{4.79}$$

The phase-angle jump is thus equal to the angle in the complex plane between $\overline{z}\mathcal{L}$ and $\overline{Z}_S + \overline{z}\mathcal{L}$. This is shown in Fig. 4.85, where ϕ is the phase-angle jump and α is the angle between source impedance $\overline{Z}_S$ and feeder impedance $\overline{z}$.

$$\alpha = \arctan\left(\frac{X_F}{R_F}\right) - \arctan\left(\frac{X_S}{R_S}\right) \tag{4.80}$$

We will refer to α as the "impedance angle;" it is positive when the X/R-ratio of the feeder is larger than that of the source. Note that this is a rare situation: the impedance angle is in most cases negative. Using the cosine rule twice in the lower triangle in Fig. 4.85 gives the two expressions

$$|\overline{Z}_S + \overline{z}\mathcal{L}|^2 = |\overline{z}\mathcal{L}|^2 + |\overline{Z}_S|^2 - 2|\overline{z}\mathcal{L}||\overline{Z}_S|\cos(180° + \alpha) \tag{4.81}$$

$$|\overline{Z}_S|^2 = |\overline{Z}_S + \overline{z}\mathcal{L}|^2 + |\overline{z}\mathcal{L}|^2 - 2|\overline{Z}_S + \overline{z}\mathcal{L}||\overline{z}\mathcal{L}|\cos(-\phi) \tag{4.82}$$

Substituting (4.81) into (4.82) and some rewriting gives an expression for the phase-angle jump as a function of distance

$$\cos(\phi) = \frac{\lambda + \cos\alpha}{\sqrt{1 + \lambda^2 + 2\lambda\cos\alpha}} \tag{4.83}$$

where $\lambda = z\mathcal{L}/Z_S$ is a measure of the "electrical" distance to the fault and α the impedance angle. Note that it is not so much the difference in X/R ratio which deter-

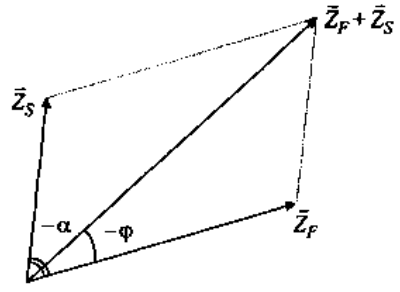

Figure 4.85 Phasor diagram for calculation of magnitude and phase-angle jump.

mines the size of the phase-angle jump but the actual angle between source and feeder impedance. For example, a source with $X_S/R_S = 40$ and a feeder with $X_F/R_F = 2$ gives an impedance angle of

$$\alpha = \arctan(2) - \arctan(40) = 63.4° - 88.6° = -25.2° \tag{4.84}$$

where a source with $X_S/R_S = 3$ and a feeder with $X_F/R_F = 1$ gives an impedance angle of $\alpha = -26.6°$. The latter will result in more severe phase-angle jumps.

The maximum angular difference occurs for underground cables in distribution systems. For a source X/R of 10 and a cable X/R of 0.5 we obtain an impedance angle of about $-60°$. In the forthcoming sections the value of $-60°$ is used as the worst case. Although this is a rather rare case, it assists in showing the various relationships. Small positive phase-angle jumps may occur in transmission systems where X/R ratio of source and feeder impedance are similar. Impedance angles exceeding $+10°$ are very unlikely. For most of the forthcoming studies we will assume that the impedance angle varies between 0 and $-60°$.

From (4.83) we can conclude that the maximum phase-angle jump occurs for $\mathcal{L} = 0$, $\lambda = 0$ and that it is equal to the impedance angle α.

The magnitude of the sag is obtained from (4.79) as

$$V_{sag} = \frac{|\overline{z}\mathcal{L}|}{|\overline{z}\mathcal{L} + \overline{Z}_S|} \tag{4.85}$$

With (4.81) the following expression for the sag magnitude as a function of the distance to the fault is obtained:

$$V_{sag} = \frac{\lambda}{(1+\lambda)} \frac{1}{\sqrt{1 - \frac{2\lambda(1-\cos\alpha)}{(1+\lambda)^2}}} \tag{4.86}$$

Note that the first factor in the right-hand side of (4.86) gives the sag magnitude when the difference in X/R ratio is neglected ($\alpha = 0$). This is the same expression as (4.9) in Section 4.2. The error in making this approximation is estimated by approximating the second factor in (4.86) for small values of α:

$$\frac{1}{\sqrt{1 - \frac{2\lambda(1-\cos\alpha)}{(1+\lambda)^2}}} \approx \frac{1}{1 - \frac{\lambda(1-\cos\alpha)}{(1+\lambda)^2}} \approx 1 + \frac{\lambda}{(1+\lambda)^2}(1-\cos\alpha) \approx 1 + \frac{\lambda}{(1+\lambda)^2}\alpha^2 \tag{4.87}$$

The error is proportional to α^2. Thus, for moderate values of α the simple expression without considering phase-angle jumps can be used to calculate the sag magnitude.

4.5.2.5 Range of Magnitude and Phase-Angle Jump. The relation between magnitude and phase-angle jump is plotted for four values of the impedance angle in Fig. 4.86. Magnitude and phase-angle jump have been calculated by using (4.83) and (4.86). During a three-phase fault all three phases will experience the same change in magnitude and phase-angle. The relation shown in Fig. 4.86 thus also holds for single-phase equipment. When testing equipment for sags due to three-phase faults one should consider that magnitude and phase-angle jump can reach the whole range of combinations in Fig. 4.86.

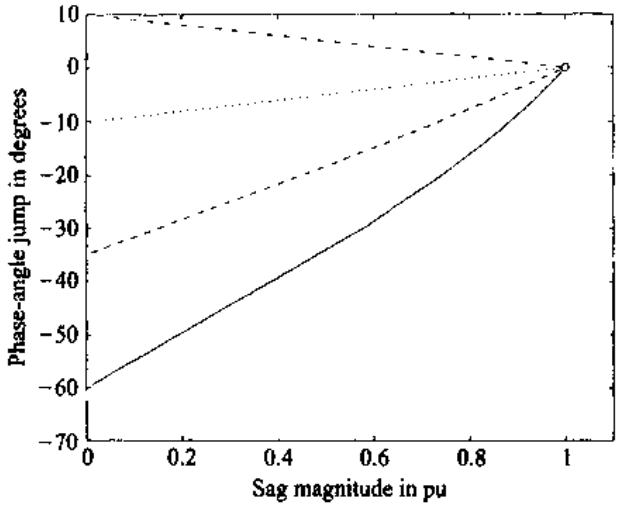

Figure 4.86 Relation between magnitude and phase-angle jump for three-phase faults: impedance angles: −60° (solid curve); −35° (dashed); −10° (dotted); +10° (dash-dot).

EXAMPLE Magnitude and phase-angle jump have been calculated for sags due to three-phase faults at the various voltage levels in the example supply shown in Fig. 4.21. Using the data in Tables 4.3 and 4.4 we can calculate the complex voltage at the pcc for any fault in the system. The absolute value and argument of this complex voltage are shown in Fig. 4.87. The complex voltage has been calculated for distances to the fault less than the maximum feeder length indicated in the last column of Table 4.4. As the maximum feeder length at 132 kV is only 2 km, the sag magnitude due to 132 kV faults does not exceed 20%. We see that distribution system faults give phase-angle jumps up to 20^0, with the largest ones due to 33 kV faults. Transmission system faults only cause very mild phase-angle jumps. These magnitudes and phase-angle jumps hold for single-phase as well as three-phase equipment, connected to any voltage level and irrespective of the load being connected in star or in delta.

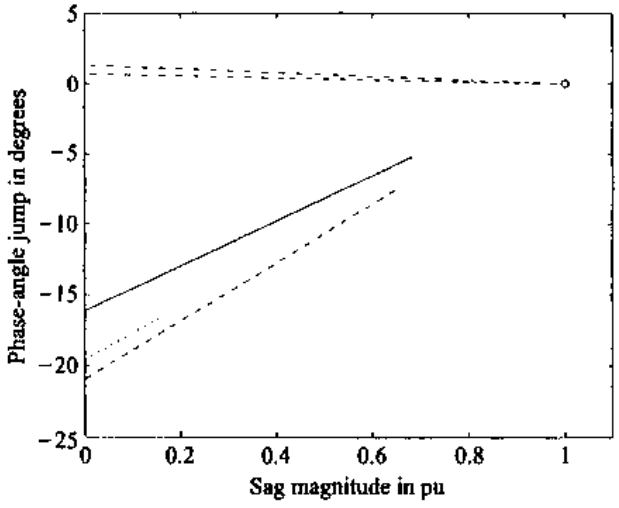

Figure 4.87 Magnitude and phase-angle jump for three-phase sags in the example supply in Fig. 4.21—solid line: 11 kV; dashed line: 33 kV; dotted line: 132 kV; dash-dot line: 400 kV.

4.6 MAGNITUDE AND PHASE-ANGLE JUMPS FOR THREE-PHASE UNBALANCED SAGS

4.6.1 Definition of Magnitude and Phase-Angle Jump

4.6.1.1 Three Different Magnitudes and Phase-Angle Jumps. The magnitude of a voltage sag was defined in Section 4.2 as the rms value of the voltage during the fault. As long as the voltage in only one phase is considered this is an implementable

definition, despite the problems with actually obtaining the rms value. For three-phase unbalanced sags the problem becomes more complicated as there are now three rms values to choose from. The most commonly used definition is: *The magnitude of a three-phase unbalanced sag is the rms value of the lowest of the three voltages.* Alternatives suggested earlier are to use the average of the three rms values, or the lowest value but one [205]. Here we will propose a magnitude definition based on the analysis of three-phase unbalanced sags.

First we need to distinguish between three different kinds of magnitude and phase-angle jump. In all cases magnitude and phase-angle jump are absolute value and argument, respectively, of a complex voltage.

- The *initial complex voltage* is the voltage at the point-of-common coupling at the faulted voltage level. For a single-phase-to-ground fault the initial complex voltage is the voltage between the faulted phase and ground at the pcc. For a phase-to-phase fault the initial complex voltage is the voltage between the two faulted phases. For a two-phase-to-ground or a three-phase fault it can be either the voltage in one of the faulted phases or between two faulted phases (as long as pu values are used). The initial sag magnitude is the absolute value of the complex initial voltage; the initial phase-angle jump is the argument of the complex initial voltage.
- The *characteristic complex voltage* of a three-phase unbalanced sag is defined as the value of V in Tables 4.9 and 4.12. We will give an easy interpretation of the characteristic complex voltage later on. The characteristic sag magnitude is the absolute value of the characteristic complex voltage. The characteristic phase-angle jump is the argument of the characteristic complex voltage. These can be viewed as generalized definitions of magnitude and phase-angle jumps for three-phase unbalanced sags.
- The *complex voltages at the equipment terminals* are the values of V_a, V_b, and V_c in Tables 4.9 and 4.12 and in several of the equations around these tables. The sag magnitude and phase-angle jump at the equipment terminals are absolute value and argument, respectively, of the complex voltages at the equipment terminals. For single-phase equipment these are simply sag magnitude and phase-angle jump as previously defined for single-phase voltage sags.

4.6.1.2 Obtaining the Characteristic Magnitude. In Section 4.4 we have introduced seven types of sags together with their characteristic complex voltage V. For type D and type F the magnitude is the rms value of the lowest of the three voltages. For type C and type G it is the rms value of the difference between the two lowest voltages (in pu). From this we obtain the following method of determining the characteristic magnitude of a three-phase sag from the voltages measured at the equipment terminals:

- Determine the rms values of the three voltages.
- Determine the rms values of the three voltage differences.
- The magnitude of the three-phase sag is the lowest of these six values.

It is easy to see from the expressions given earlier, that this will give the value of $|V|$ as used for the definition of the three-phase unbalanced sags. An exception are sags of type B and type E. For sags conforming to (4.54) and (4.67) the method would still give the

exact value for the magnitude. But the difference between zero-sequence and positive-sequence source impedance makes that the actual sags can deviate significantly. In that case the method is likely to give a completely wrong picture. Another problem is that for these sags the magnitude changes when they propagate to a lower voltage level. This makes measurements at a medium voltage level not suitable for predicting the sag magnitude at the equipment terminals. This problem can be solved by removing the zero-sequence component from the voltage and applying the method to the remaining voltages. The complete procedure proceeds as follows:

- obtain the three voltages as a function of time: $V_a(t)$, $V_b(t)$, and $V_c(t)$.
- determine the zero-sequence voltage:

$$V_0(t) = \frac{V_a(t) + V_b(t) + V_c(t)}{3} \tag{4.88}$$

- determine the remaining voltages after subtracting the zero-sequence voltage:

$$\begin{aligned} V'_a(t) &= V_a(t) - V_0(t) \\ V'_b(t) &= V_b(t) - V_0(t) \\ V'_c(t) &= V_c(t) - V_0(t) \end{aligned} \tag{4.89}$$

- determine the rms values of the voltages V'_a, V'_b, and V'_c.
- determine the three voltage differences:

$$\begin{aligned} V_{ab}(t) &= \frac{V_a(t) - V_b(t)}{\sqrt{3}} \\ V_{bc}(t) &= \frac{V_b(t) - V_c(t)}{\sqrt{3}} \\ V_{ca}(t) &= \frac{V_c(t) - V_a(t)}{\sqrt{3}} \end{aligned} \tag{4.90}$$

- determine the rms values of the voltages V_{ab}, V_{bc}, and V_{ca}.
- the magnitude of the three-phase sag is the lowest of the six rms values.

In case also phase-angle jump and sag type are needed, it is better to use a more mathematically correct method. A method based on symmetrical components has recently been proposed by Zhang [203], [204].

EXAMPLE This procedure has been applied to the voltage sag shown in Fig. 4.1. At first the rms values have been determined for the three measured phase-to-ground voltages, resulting in Fig. 4.88. The rms value has been determined each half-cycle over the preceeding 128 samples (one half-cycle). We see the behavior typical for a single-phase fault on an overhead feeder: a drop in voltage in one phase and a rise in voltage in the two remaining phases.

After subtraction of the zero-sequence component, all three voltages show a drop in magnitude (see Fig. 4.89). The phase-to-ground voltages minus the zero-sequence are indicated through solid lines, the phase-to-phase voltages through dashed lines. The lowest rms value is reached for a phase-to-ground voltage, which indicates a sag of type D. This is not surprising as the original sag was of type B (albeit with a larger than normal zero-sequence component). After removal of the zero-sequence voltage a sag of type D remains. The characteristic magnitude of this three-phase unbalanced sag is 63%.

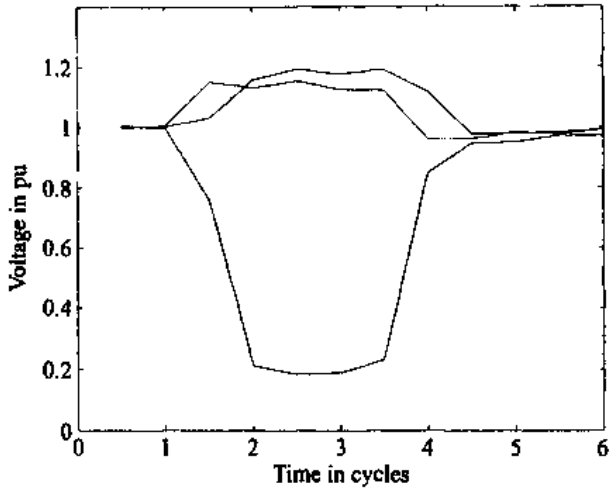

Figure 4.88 The rms values of the phase-to-ground voltages for the sag shown in Fig. 4.1.

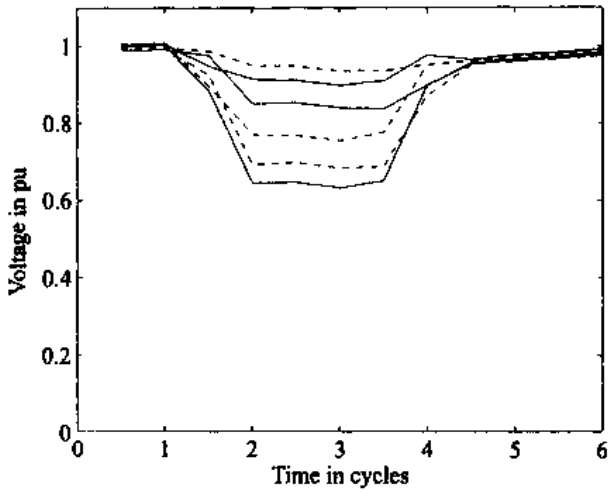

Figure 4.89 The rms values of phase-to-phase (dashed lines) and phase-to-ground voltages after removal of the zero-sequence component (solid lines) for the sag shown in Fig. 4.1.

4.6.2 Phase-to-Phase Faults

The impact of phase-to-phase faults depends on the transformer winding connections between the fault and the equipment. As shown in Section 4.4, the result is a sag either of type C or of type D. It was shown in Section 4.4.2 that the voltage between the faulted phases can be obtained by using the same voltage divider model as for the three-phase sag. The latter has been used to obtain expressions (4.83) and (4.86) for phase-angle jump and magnitude versus distance. These expressions can thus also be used to calculate initial magnitude and initial phase-angle jump: absolute value and argument of the voltage between the faulted phases at the pcc. The three-phase unbalanced sags in Section 4.4 were all derived under the assumption that the initial voltage drops in magnitude without change in phase angle. In case of a phase-angle jump in the initial voltage, the characteristic voltage of the three-phase unbalanced sag at the pcc also becomes complex. The expressions in Tables 4.9 and 4.12 still hold with the exception that the characteristic voltage V has become a complex number. The characteristic

voltage for sag types C and D does not change when they are transformed down to lower voltage levels, so that the characteristic complex voltage remains equal to the initial complex voltage.

4.6.2.1 Sags of Type C. The phasor diagram for a sag of type C is shown in Fig. 4.90, where ϕ is the characteristic phase-angle jump and V the characteristic magnitude. Depending on the phase to which it is connected, single-phase equipment will experience a sag with magnitude V_b and phase-angle jump ϕ_b, a sag with magnitude V_c and phase-angle jump ϕ_c, or no sag at all. Due to the initial phase-angle jump ϕ the voltage magnitudes in the two faulted phases are no longer equal. Note that in Fig. 4.90 $\phi < 0$, $\phi_b < 0$, and $\phi_c > 0$.

From Fig. 4.90 expressions can be derived for magnitude and phase-angle jump at the equipment terminals. As a first step the sine rule and the cosine rule are applied to the two triangles indicated in Fig. 4.90 resulting in

$$V_b^2 = \frac{1}{4} + \frac{3}{4}V^2 - 2 \cdot \frac{1}{2} \cdot \frac{1}{2} V\sqrt{3}\cos(90° - \phi) \tag{4.91}$$

$$\frac{\sin(60° + \phi_b)}{\frac{1}{2}V\sqrt{3}} = \frac{\sin(90° - \phi)}{V_b} \tag{4.92}$$

$$V_c^2 = \frac{1}{4} + \frac{3}{4}V^2 - 2 \cdot \frac{1}{2} \cdot \frac{1}{2} V\sqrt{3}\cos(90° + \phi) \tag{4.93}$$

$$\frac{\sin(60° - \phi_c)}{\frac{1}{2}V\sqrt{3}} = \frac{\sin(90° + \phi)}{V_c} \tag{4.94}$$

from which the following desired expressions are obtained:

$$\begin{aligned} V_a &= 1 \\ V_b &= \sqrt{\frac{1}{4} + \frac{3}{4}V^2 - \frac{1}{2}V\sqrt{3}\sin(\phi)} \\ V_c &= \sqrt{\frac{1}{4} + \frac{3}{4}V^2 + \frac{1}{2}V\sqrt{3}\sin(\phi)} \end{aligned} \tag{4.95}$$

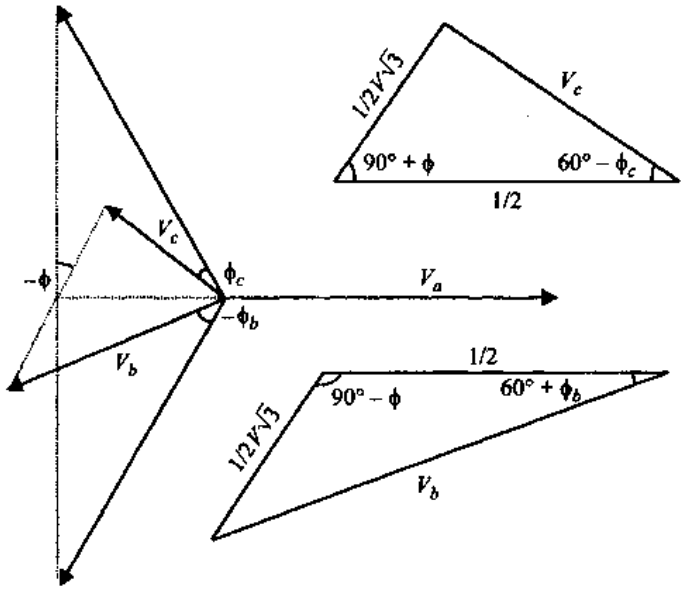

Figure 4.90 Phasor diagram for a sag of type C with characteristic magnitude V and characteristic phase-angle jump ϕ.

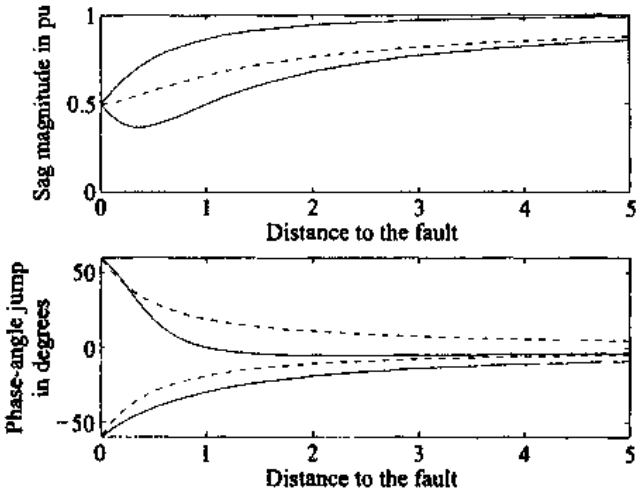

Figure 4.91 Magnitude (top) and phase-angle jump (bottom) for sags of type C due to phase-to-phase faults. Dashed line: zero impedance angle (no characteristic phase-angle jump). Solid line: −60° impedance angle (large characteristic phase-angle jump).

$$\begin{aligned}\phi_a &= 0\\ \phi_b &= -60^\circ + \arcsin\left(\frac{1}{2}\sqrt{3}\frac{V}{V_b}\cos(\phi)\right)\\ \phi_c &= 60^\circ - \arcsin\left(\frac{1}{2}\sqrt{3}\frac{V}{V_c}\cos(\phi)\right)\end{aligned} \tag{4.96}$$

Combining (4.95) and (4.96) with (4.83) and (4.86) gives the magnitude and phase-angle jump in the three phases as a function of the distance to the fault. This is done in Fig. 4.91 for impedance angles equal to 0 and −60°. The horizontal scale corresponds to $\lambda = \frac{zl}{Z_s}$ as in (4.83). We see that the severity of sags decreases with increasing distance when there is no characteristic phase-angle jump. The introduction of a characteristic phase-angle jump creates asymmetry between the faulted phases. We see, e.g., that the voltage in one of the phases initially decreases with increasing distance to the fault. For one of the phases the phase-angle jump drops to zero rather quickly, whereas for the other phase the phase-angle jump remains high much longer.

Figure 4.92 plots magnitude versus phase-angle jump for four values of the impedance angle. We can see that the characteristic phase-angle jump significantly disturbs the symmetry between the two faulted phases. Also the voltage can drop well below 50%, which is not possible without characteristic phase-angle jump.

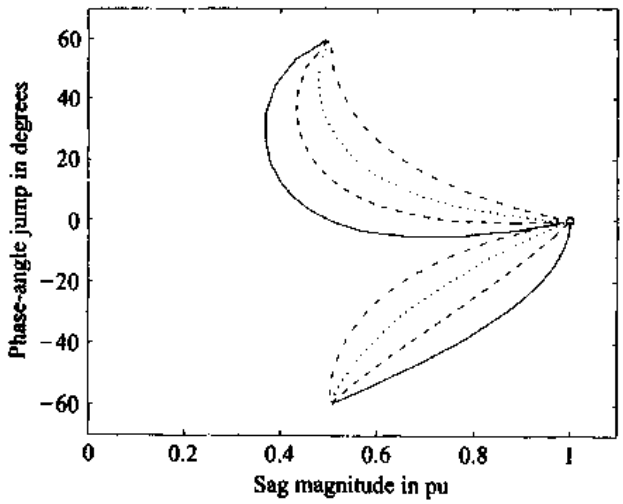

Figure 4.92 Magnitude versus phase-angle jump for sag type C due to phase-to-phase faults for impedance angle −60° (solid line), −40° (dashed), −20° (dotted), 0 (dash-dot).

4.6.2.2 Sags of Type D. The phasor diagram for a type D sag is shown in Fig. 4.93, where ϕ is again the characteristic phase-angle jump. One phase will go down significantly with a phase-angle jump equal to the characteristic value. Equipment connected to one of the two other phases will see a small drop in voltage and a phase-angle jump of up to 30°. Severe characteristic phase-angle jumps can even lead to voltage swells. The two phases with the small voltage drop can experience positive as well as negative phase-angle jumps. The phase with the large voltage drop always experiences a negative phase-angle jump.

From Fig. 4.93 magnitude and phase-angle jump in the three phases can be calculated for a sag of type D. Applying the sine rule and the cosine rule to the two triangles indicated in Fig. 4.93 gives the following expressions:

$$V_b^2 = \frac{1}{4}V^2 + \frac{3}{4} - 2 \cdot \frac{1}{2}V \cdot \frac{1}{2}\sqrt{3}\cos(90° + \phi) \tag{4.97}$$

$$\frac{\sin(30° - \phi_b)}{\frac{1}{2}V} = \frac{\sin(90° + \phi)}{V_b} \tag{4.98}$$

$$V_c^2 = \frac{1}{4}V^2 + \frac{3}{4} - 2 \cdot \frac{1}{2}V \cdot \frac{1}{2}\sqrt{3}\cos(90° - \phi) \tag{4.99}$$

$$\frac{\sin(30° + \phi_c)}{\frac{1}{2}V} = \frac{\sin(90° - \phi)}{V_c} \tag{4.100}$$

Rewriting these expressions results in

$$\begin{aligned} V_a &= V \\ V_b &= \sqrt{\frac{3}{4} + \frac{1}{4}V^2 + \frac{1}{2}V\sqrt{3}\sin(\phi)} \\ V_c &= \sqrt{\frac{3}{4} + \frac{1}{4}V^2 - \frac{1}{2}V\sqrt{3}\sin(\phi)} \end{aligned} \tag{4.101}$$

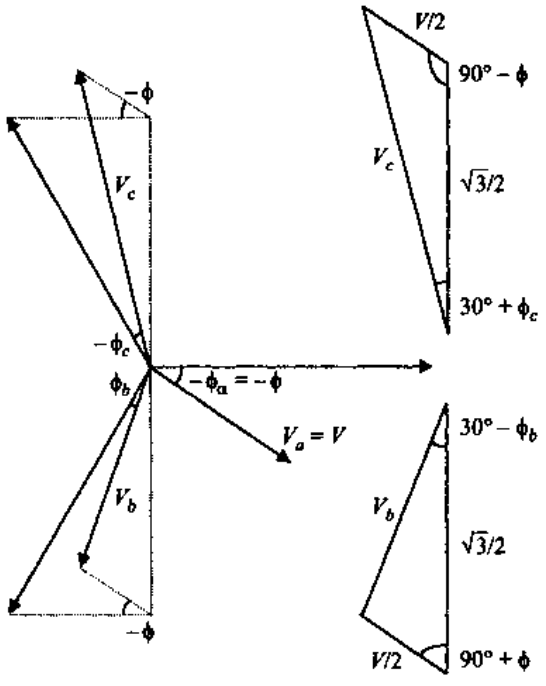

Figure 4.93 Phasor diagram for a sag of type D, with characteristic magnitude V and phase-angle jump ϕ.

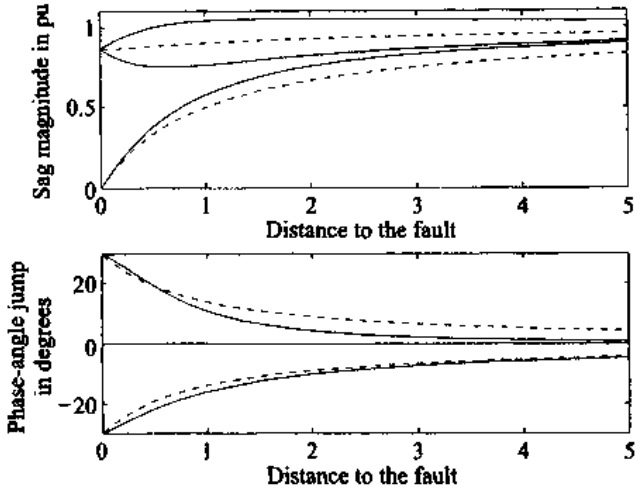

Figure 4.94 Magnitude (top) and phase-angle jump (bottom) for sags of type D due to phase-to-phase faults. Dashed line: zero impedance angle. Solid line: impedance angle of −60°.

$$\begin{aligned}\phi_a &= \phi \\ \phi_b &= 30^\circ - \arcsin\left(\frac{V}{2V_b}\cos(\phi)\right) \\ \phi_c &= -30^\circ + \arcsin\left(\frac{V}{2V_c}\cos(\phi)\right)\end{aligned} \tag{4.102}$$

Again we can plot magnitude and phase-angle jump versus distance and magnitude versus phase-angle jump. Figure 4.94 gives magnitude and phase-angle jump as a function of distance for impedance angles equal to zero and −60°. Here we see that the voltage drop in the non-faulted phases is rather small; the voltage drops to about 75%. The characteristic phase-angle jump causes an additional drop in voltage at the equipment terminals. Magnitude versus phase-angle jump is plotted in Fig. 4.95 for four values of the impedance angle.

4.6.2.3 Range of Magnitude and Phase-Angle Jump. As mentioned before, phase-to-phase faults lead to sags of type C or of type D. Combining the range of magnitude and phase-angle jump due to type C sags (Fig. 4.92) with the range due

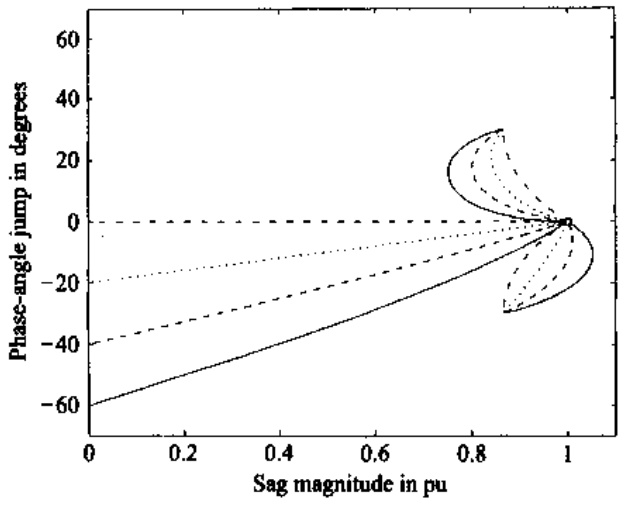

Figure 4.95 Magnitude versus phase-angle jump for sag type D due to phase-to-phase faults: impedance angle −60° (solid line), −40° (dashed), −20° (dotted), 0 (dash-dot).

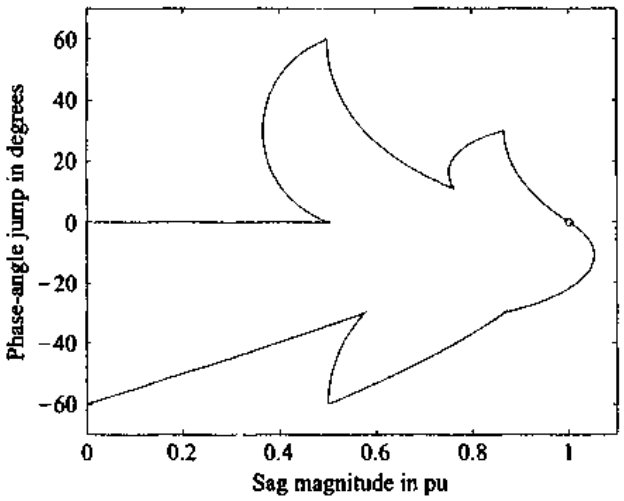

Figure 4.96 Range of sags due to phase-to-phase faults, as experienced by single-phase equipment.

to type D sags (Fig. 4.95) gives the whole range of sags experienced by single-phase equipment during phase-to-phase faults. The merger of the two mentioned figures is shown in Fig. 4.96, where only the outer contour of the area is indicated.

Sags due to three-phase faults are automatically included in Fig. 4.96. A three-phase fault gives a sag with the initial magnitude and the initial phase-angle jump, in all the three phases. Such a sag also appears in one of the phases for a type D sag due to a phase-to-phase fault. This is the large triangular area in Fig. 4.96. Sags due to single-phase and two-phase-to-ground faults have not yet been included. These will be treated below.

EXAMPLE: PHASE-TO-PHASE FAULTS, THREE-PHASE LOAD The magnitude and phase-angle jump due to phase-to-phase faults have been calculated for faults in the example supply in Fig. 4.21. The calculations have been performed for two different types of load:

- three-phase load connected in delta at 660 V.
- single-phase load connected in star (phase-to-neutral) at 420 V.

For a three-phase load, we can use the classification introduced in Section 4.4 to characterize the sag. The magnitude and phase-angle jump of these three-phase unbalanced sags are the same as those of sags due to three-phase faults. The only difference is the type of sag. A phase-to-phase fault at 11 kV will, for delta-connected load at 11 kV, lead to a sag of type D. The Dy transformer between the fault (at 11 kV) and the load (at 660 V) will change this into a type C sag. Thus, the delta-connected load at 660 V will, due to a phase-to-phase fault at 11 kV, experience a sag of type C. The characteristic magnitude and phase-angle jump of this three-phase unbalanced sag will be equal to the magnitude and phase-angle jump of the voltage (in any phase) due to a three-phase fault at the same position as the phase-to-phase fault. Using the same reasoning we find that phase-to-phase faults at 33 kV lead to type D sags and faults at 132 kV and 400 kV to sags of type C. The results of the calculations are shown in Fig. 4.97: characteristic magnitude and phase-angle jump of three-phase unbalanced sags due to phase-to-phase faults. Note the similarity with Fig. 4.87. The curves are at exactly the same position; the only difference is that the ones due to 33 kV faults are of type D and the others are of type C. Three-phase faults at any voltage level will lead to a sag of type A.

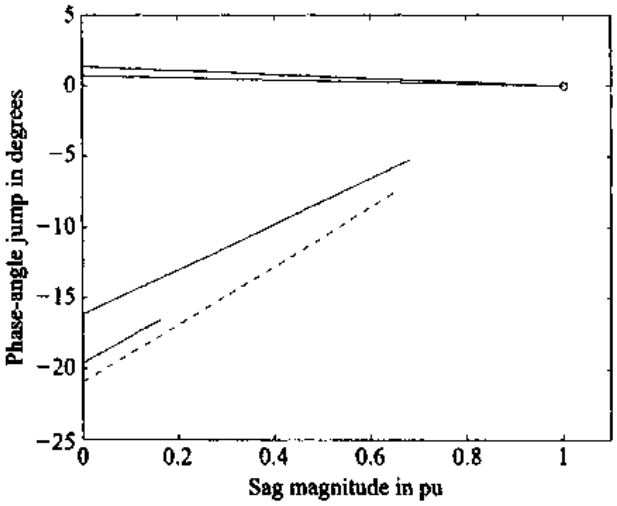

Figure 4.97 Characteristic magnitude and phase-angle jump for sags due to phase-to-phase faults in the example supply in Fig. 4.21—solid line: type C sags, dashed line: type D sags.

EXAMPLE: PHASE-TO-PHASE FAULTS, SINGLE-PHASE LOAD Magnitude and phase-angle jump at the equipment terminals due to phase-to-phase faults have been calculated for a single-phase load connected phase-to-neutral at 420 V. The classification of three-phase sags no longer fully describes the voltage at the equipment terminals. The additional information needed is the phases between which the fault takes place. One can calculate the voltage sag in one phase for three different faults; but it is easier to calculate the voltages in the three phases for one fault. These three voltages are the voltages in one phase for the three different faults. We saw before that we do not need to calculate the whole transfer of the sag from the faulted voltage level to the load terminals. All we need to do is determine whether the equipment terminal voltage corresponds to phase-to-phase or phase-to-neutral voltage at the faulted voltage level. In this example, the equipment terminal voltage corresponds to phase-to-phase voltages at 11 kV, 132 kV, and 400 kV and to phase-to-neutral voltages at 33 kV.

The resulting magnitude and phase-angle jump are plotted in Fig. 4.98. Faults at 11 kV, 132 kV, and 400 kV cause a three-phase unbalanced sag of type D for star-connected equipment. For a type D sag one voltage drops to a low value, and the two remaining voltages show a small drop with a phase-angle jump up to 30°. Note the symmetry in the sags originating at 400 kV, which is not present in the sags originating at 11 kV and 132 kV. This is due to the large initial

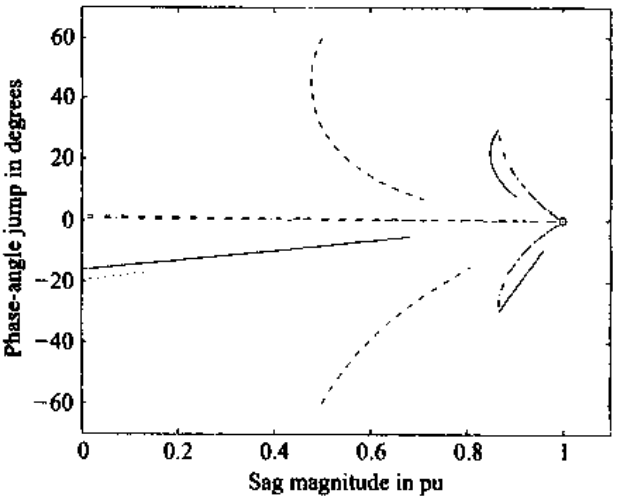

Figure 4.98 Magnitude and phase-angle jump at the equipment terminals due to phase-to-phase faults in the supply in Fig. 4.21, experienced by single-phase load connected phase-to-ground at 420 V—solid line: 11 kV, dashed line: 33 kV, dotted line: 132 kV, dash-dot line: 400 kV.

phase-angle jump for the latter two. Faults at 33 kV cause a sag of type C, with two voltages down to about 50% and phase-angle jumps up to ±60°.

4.6.3 Single-Phase Faults

For single-phase faults the situation becomes slightly more complicated. Expressions (4.83) and (4.86) can still be used to calculate magnitude and phase-angle jump of the voltage in the faulted phase at the pcc (i.e., the initial magnitude and phase-angle jump). Star-connected equipment at the same voltage level as the fault would experience a sag of type B. But as we have seen before, this is a rather rare situation. In almost all cases a sag due to a single-phase fault is of type C or type D. The characteristic magnitude of these three-phase unbalanced sags is no longer equal to the initial magnitude. The same holds for the phase-angle jump.

4.6.3.1 Initial and Characteristic Magnitude. To obtain an expression for the characteristic magnitude and phase-angle jump, we need to go back to the type B sag. The voltages for a type B sag are

$$\begin{aligned} V_a &= V\cos\phi + jV\sin\phi \\ V_b &= -\frac{1}{2} - \frac{1}{2}j\sqrt{3} \\ V_c &= -\frac{1}{2} + \frac{1}{2}j\sqrt{3} \end{aligned} \tag{4.103}$$

with V the initial magnitude and ϕ the initial phase-angle jump. When this three-phase unbalanced sag propagates to lower voltage levels, the zero-sequence voltage is lost. The zero-sequence component for (4.103) is

$$V_0 = \frac{1}{3}(V_a + V_b + V_c) = \frac{1}{3}(V\cos\phi + jV\sin\phi - 1) \tag{4.104}$$

Subtracting the zero-sequence voltage from (4.103) gives a three-phase unbalanced sag of type D. Characteristic magnitude and phase-angle jump for a sag of type D are equal to the absolute value and the argument of the complex voltage in the worst-effected phase, V_a in this case.

$$V_a = \frac{1}{3} + \frac{2}{3}(V\cos\phi + jV\sin\phi) \tag{4.105}$$

Note that this expression can also be obtained by substituting $V = V\cos\phi + jV\sin\phi$ in (4.62). For three-phase unbalanced sags due to single-phase faults the characteristic magnitude becomes

$$V_{char} = |V_a| = \frac{2}{3}\sqrt{V^2 + V\cos\phi + \frac{1}{4}} \tag{4.106}$$

with V and ϕ the initial magnitude and phase-angle jump, and V_a according to (4.105). The characteristic phase-angle jump is

$$\phi_{char} = \arg(V_a) = \arctan\left(\frac{2V\sin\phi}{1 + 2V\cos\phi}\right) \tag{4.107}$$

For small values of ϕ these expressions can be approximated by using

$$\sin\phi \approx \phi$$
$$\cos\phi \approx 1$$
$$\arctan(x\phi) \approx x\phi, \quad x < 1$$

resulting in

$$V'_{char} = \frac{1}{3} + \frac{2}{3}V \tag{4.108}$$

$$\phi'_{char} = \frac{2V\phi}{1+2V} \tag{4.109}$$

Figures 4.99 and 4.100 show the error made by using the approximated expressions (4.108) and (4.109). The error has been defined as $1 - \frac{V_{char}}{V'_{char}}$. The calculations have been performed for impedance angles equal to $-60°$, $-40°$, and $-20°$. Even for a system with large phase-angle jumps, an impedance angle of $-60°$, the errors are not very big. Only for calculating the characteristic phase-angle jump with deep sags might it be needed to use the exact expression. One should realize, however, that the

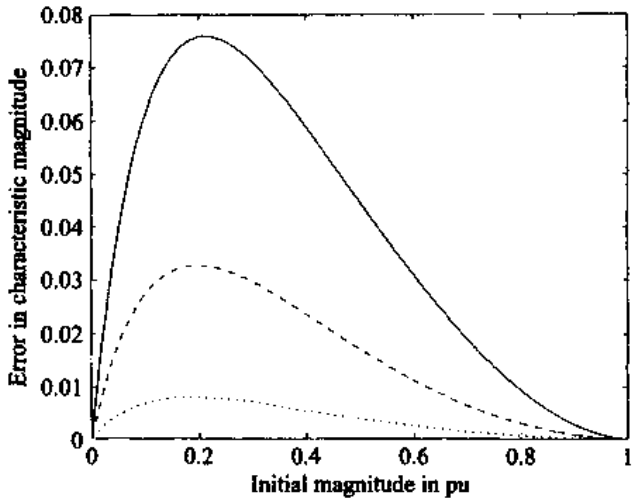

Figure 4.99 Transformation of sags due to single-phase faults—error in approximate expressions for characteristic magnitude. Impedance angle: $-60°$ (solid line); $-40°$ (dashed); $-20°$ (dotted).

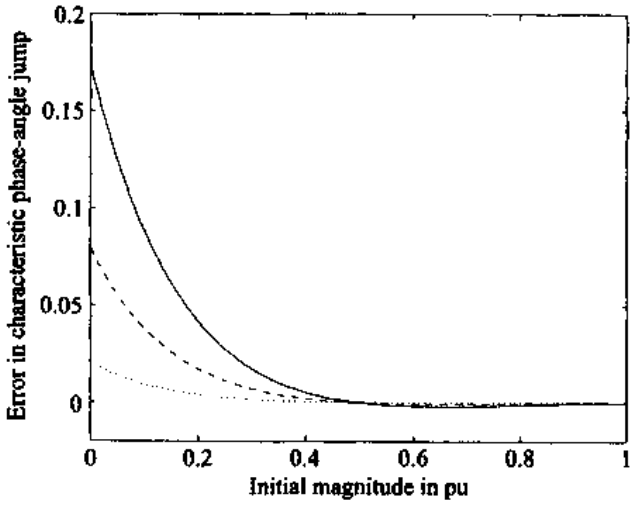

Figure 4.100 Transformation of sags due to single-phase faults—error in approximate expressions for characteristic phase-angle jump. Impedance angle: $-60°$ (solid line); $-40°$ (dashed); $-20°$ (dotted).

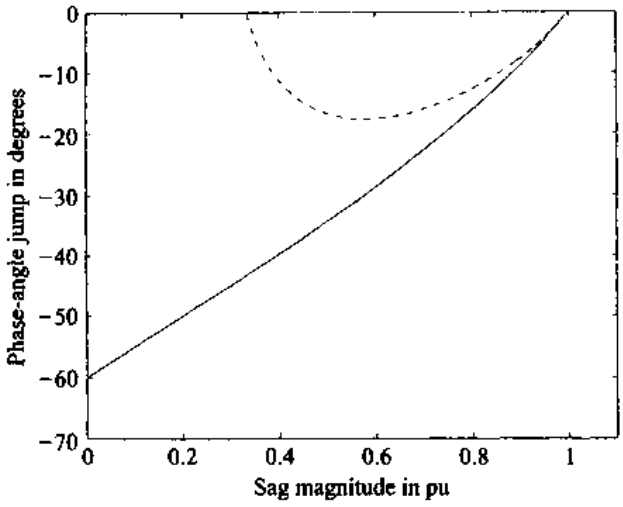

Figure 4.101 Relation between phase-angle jump and magnitude of sags due to single-phase faults: characteristic values (dashed curve) and initial values (solid curve).

characteristic phase-angle jump is close to zero for single-phase faults with a small initial magnitude, as can be seen from (4.107). The absolute error is even for an impedance angle of −60° less than 1°.

Figure 4.101 compares initial magnitude and phase-angle jump with the characteristic values. An impedance angle of −60° has been used. The bottom (solid) curve also gives the relation between characteristic magnitude and phase-angle jump due to phase-to-phase and three-phase faults. Sags due to single-phase faults are clearly less severe: in magnitude as well as in phase-angle jump.

4.6.3.2 Sags of Type C and Type D. Knowing characteristic magnitude and phase-angle jump for the type C or type D sag it is again possible to calculate magnitude and phase-angle jump at the equipment terminals. This results in similar curves as for sags due to phase-to-phase faults. The main difference is that voltage sags due to single-phase faults are less severe than due to phase-to-phase faults. Figure 4.102 plots magnitude versus phase-angle jump for sag type C, for four values of the impedance angle. The lowest sag magnitude at the equipment terminals is about 58%, the largest phase-angle jump is 30°.

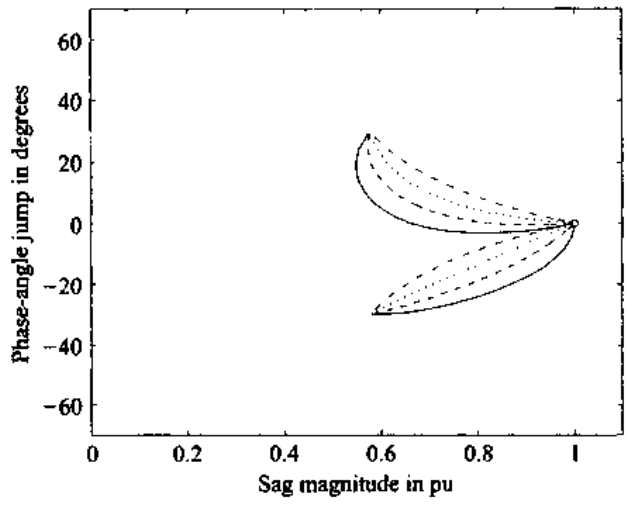

Figure 4.102 Range of sags experienced by single-phase equipment for sag type C and single-phase fault, impedance angle: −60° (solid line), −40° (dashed), −20° (dotted), 0 (dash-dot).

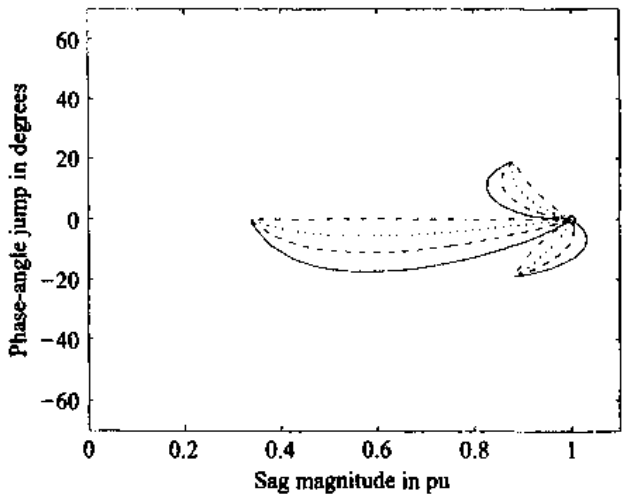

Figure 4.103 Range of sags experienced by single-phase equipment for sag type D and single-phase fault, impedance angle: −60° (solid line), −40° (dashed), −20° (dotted), 0 (dash-dot).

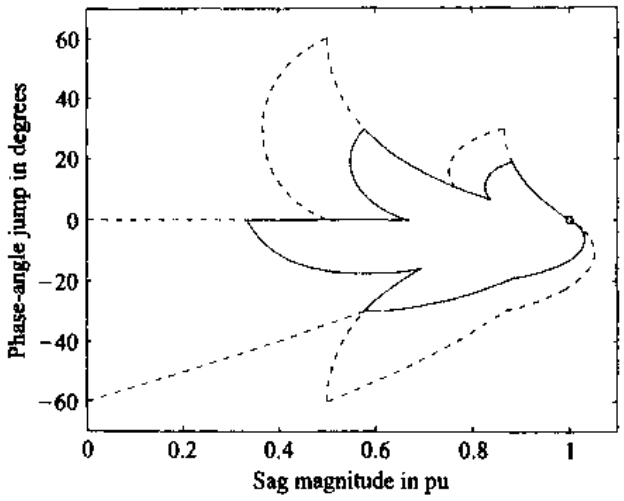

Figure 4.104 Range of sags due to single-phase faults (solid curve) and due to phase-to-phase faults (dashed curve).

Figure 4.103 repeats this for type D sags due to single-phase faults. The lowest sag magnitude is 33% with a maximum phase-angle jump of 19°. Sags due to type C and type D are merged into one plot in Fig. 4.104 which gives the whole range of sags experienced by single-phase equipment due to single-phase faults. This range is smaller than the range due to phase-to-phase faults, indicated by a dashed line in Fig. 4.104.

EXAMPLE: SINGLE-PHASE FAULTS, THREE-PHASE LOAD The calculations for phase-to-phase faults shown in the previous section have been repeated for single-phase faults. For single-phase faults at the various voltage levels in Fig. 4.21, the sag magnitude, phase-angle jump, and type have been calculated for delta-connected (three-phase) load at 660 V. Equations (4.108) and (4.109) have been derived for a system with equal positive, negative and zero-sequence impedance. This is a good approximation for the (solidly grounded) 132 kV system but not for the (resistance-grounded) 11 kV and 33 kV systems. At 400 kV the source impedance is mainly determined by overhead lines, so that the zero-sequence source impedance is larger than the positive-sequence value. To calculate the characteristic magnitude of three-phase unbalanced sags due to single-phase faults, we can first calculate the phase-to-neutral voltage in the faulted phase according to (4.40). Characteristic values are obtained from this by applying (4.108) and (4.109). Alternatively we can calculate the complex phase-to-

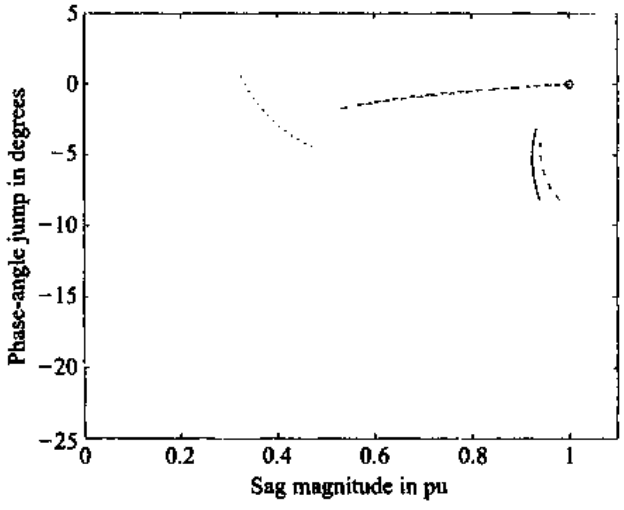

Figure 4.105 Characteristic magnitude and phase-angle jump for sags due to single-phase faults in the example supply in Fig. 4.21, experienced by three-phase load-connected phase-to-phase at 660 V—solid line: 11 kV, dashed line: 33 kV, dotted line: 132 kV, dash-dot line: 400 kV.

ground voltages at the pcc, and apply a type 2 transformer to these. A type 2 transformer removes the zero-sequence voltage and results in a three-phase unbalanced sag of type D. Magnitude and phase-angle jump of the worst-affected phase are equal to the characteristic values. In other words, the characteristic complex voltage can be obtained by subtracting the zero-sequence voltage from the voltage in the faulted phase at the pcc.

The results are shown in Fig. 4.105. We see that single-phase faults at 11 kV and 33 kV cause only a small drop in voltage, but a moderate phase-angle jump. This is due to the resistance grounding applied at these voltage levels. Sags originating in the 132 kV and 400 kV networks show a much larger drop in voltage magnitude but a smaller phase-angle jump. Note that the curves for sags due to 400 kV faults do not start at 33% voltage as expected for solidly-grounded systems. The reason is that the source impedance in PAD-400 mainly consists of overhead lines. Therefore the zero-sequence impedance is larger than the positive-sequence impedance. For faults in the direction of PEN, the source impedances are $Z_{S1} = 0.084 + j1.061$, $Z_{S0} = 0.319 + j2.273$, which gives for the initial phase-to-neutral voltage during a terminal fault:

$$V_{an} = 1 - \frac{3Z_{S1}}{2Z_{S1} + Z_{S0}} = 0.2185 + j0.0243 \tag{4.110}$$

The characteristic magnitude at a lower voltage level is found from

$$V_{char} = \left| \frac{1}{3} + \frac{2}{3} V_{an} \right| = 0.519 \tag{4.111}$$

For single-phase faults in the direction of EGG we find: $V_{an} = 0.3535 - j0.0026$ and $V_{char} = 0.571$. This is a moderate version of the effect which leads to very shallow sags in resistance-grounded systems. Note that we still assume the system to be radial, which gives an erroneous result for single-phase faults at 400 kV. This explains the difference in resulting voltage sags for a terminal fault in the two directions. The actual value is somewhere between 0.519 and 0.571. The difference is small enough to be neglected here.

Figure 4.105 does not plot the sag type: faults at 33 kV lead to a type C sag; faults at 11 kV, 132 kV, and 400 kV cause a sag of type D at the equipment terminals for delta-connected load. At the equipment terminals it is not possible to distinguish between a sag due to a single-phase fault and a sag due to a phase-to-phase fault: they both cause sags of type C or type D. Therefore, we have merged Figs. 4.97 and 4.105 into one figure. The result is displayed in Fig. 4.106, showing characteristic magnitude and phase-angle jump of all three-phase unbalanced sags due to single-phase and phase-to-phase faults, as experienced by a delta-connected three-phase load at 660 V. We see that the equipment experiences the whole range of magnitudes and phase-angle jumps. These have to be considered when specifying the voltage-tolerance requirements of equipment. To

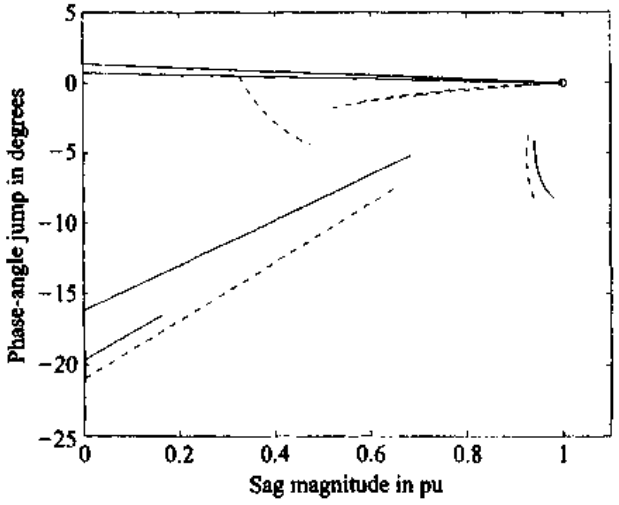

Figure 4.106 Characteristic magnitude and phase-angle jump for three-phase unbalanced sags in Fig. 4.21, experienced by three-phase delta-connected load—solid line: type C, dashed line: type D.

be able to fully interpret these results, two more dimensions are needed. At first, one has to realize that not all sags are of equal duration. Typically sags due to 11 kV and 33 kV faults are of longer duration than those due to 132 kV and 400 kV faults. What is also different for different sags is its likelihood. Roughly speaking one can say that deeper sags are less likely than shallower sags. We will come back to probabilities in detail in Chapter 6. To include magnitude, phase-angle jump, duration, and probability in one, two-dimensional, figure is very difficult if not impossible.

EXAMPLE: SINGLE-PHASE FAULTS, SINGLE-PHASE LOAD The magnitude and phase-angle jump have been calculated for voltage sags due to single-phase faults, experienced by single-phase star-connected load. For this we have calculated either the phase-to-phase voltage, or the phase-to-ground voltage minus the zero-sequence voltage, at the faulted voltage level. For a single-phase fault at 11 kV, star-connected load at 420 V experiences a sag of type C. The complex voltages at the equipment terminals are equal to the phase-to-phase voltages at the pcc. The same calculation method can be used for single-phase faults at 132 kV and at 400 kV. Single-phase faults at 33 kV lead to sags of type D. The complex voltages at the equipment terminals can be calculated as the phase-to-ground voltages at the pcc minus the zero-sequence component. The results of these calculations are shown in Fig. 4.107. We see that the voltage never drops below 50%, and that the phase-angle jumps are between $-30°$ and $+30°$. Faults at 11 kV and 33 kV again only cause shallow sags due to the system being resistance-grounded. Due to a 33 kV fault, the load can even experience a small voltage swell. Faults at 400 kV are also somewhat damped because the zero-sequence source impedance is about twice the positive-sequence value. Therefore, sags due to single-phase faults are milder than expected for a solidly-grounded system. In the 132 kV system, the zero-sequence source impedance is even a bit smaller than the positive sequence value, thus leading to deep sags. But at 420 V they appear as a type C in which the drop in phase voltages is not below 50%. For this specific system, single-phase faults do not cause very deep sags for star-connected load. Note that this is not a general conclusion. Had the 11 kV/420 V transformer been of type Dd, the equipment would have experienced voltage drops down to 30% (see Fig. 4.105).

To get a complete picture of all sags experienced by the single-phase load, we have merged Fig. 4.87 (three-phase faults), Fig. 4.98 (phase-to-phase faults), and Fig. 4.107 (single-phase faults), resulting in Fig. 4.108. Here we see the whole range of values both in magnitude and in phase-angle jump.

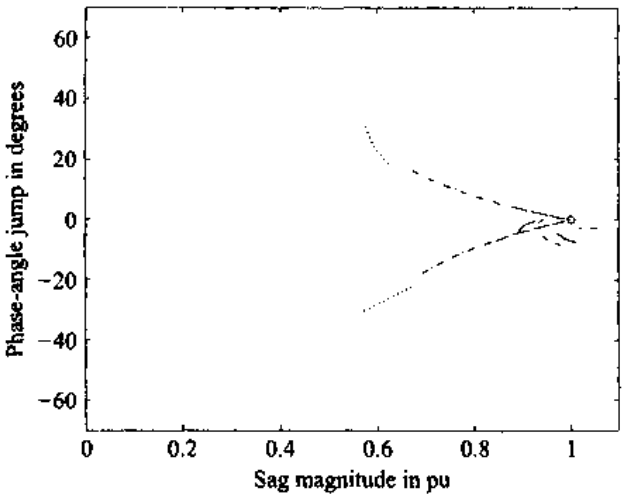

Figure 4.107 Magnitude and phase-angle jump for sags due to single-phase faults in the example supply in Fig. 4.21, experienced by single-phase load-connected phase-to-ground at 420 V—solid line: 11 kV, dashed line: 33 kV, dotted line: 132 kV, dash-dot line: 400 kV.

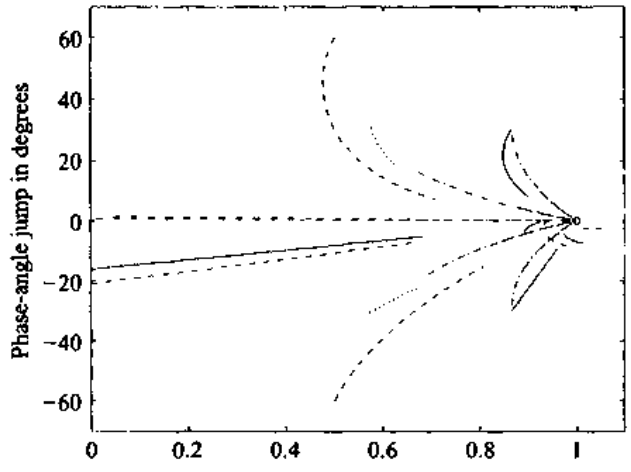

Figure 4.108 Magnitude and phase-angle jump for all sags in the example supply in Fig. 4.21, experienced by single-phase load-connected phase-to-ground at 420 V—solid line: 11 kV, dashed line: 33 kV, dotted line: 132 kV, dash-dot line: 400 kV.

4.6.4 Two-Phase-to-Ground Faults

The analysis of two-phase-to-ground faults does not differ from the treatment of phase-to-phase faults. We saw in Section 4.4.4 that two-phase-to-ground faults lead to three-phase unbalanced sags of type E, type F, or type G. Type E is a rare type which we will not discuss here. Like type B for the single-phase-to-ground fault, the type E contains a zero-sequence component which is normally not transferred to the utility voltage, and never seen by delta-connected equipment.

For type F and type G we can again plot characteristic magnitude against phase-angle jump. The relation between the characteristic magnitude and phase-angle jump of the unbalanced three-phase sag is identical to the relation between the initial magnitude and phase-angle jump, i.e. magnitude and phase-angle jump of the voltage in the faulted phases at the pcc. This relation is described by (4.83) and (4.86) and is shown in Fig. 4.86.

4.6.4.1 Sags of Type F. A detailed phasor diagram of a sag of type F is shown in Fig. 4.109. Like with a type D sag, one phase drops significantly in magnitude, and the other two phases less. The difference with the type D sag is in the latter two

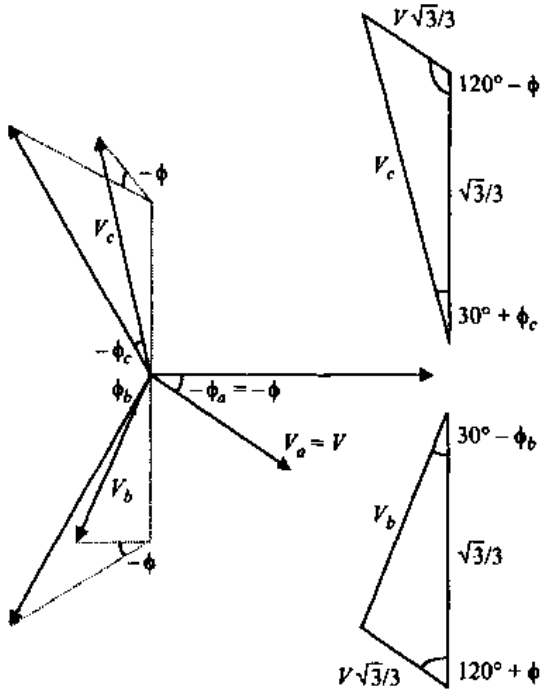

Figure 4.109 Phasor diagram for three-phase unbalanced sag of type F with characteristic magnitude V and characteristic phase-angle jump ϕ.

phases. With a type D sag they drop from $-\frac{1}{2} \pm \frac{1}{2}j\sqrt{3}$ to $\pm\frac{1}{2}j\sqrt{3}$, but with a type F sag they drop significantly more: to $\pm\frac{1}{3}j\sqrt{3}$. The lowest magnitude for a type D sag is 86.6%, whereas it is 57.7% for a type F sag.

In the upper triangle indicated in Fig. 4.109 we can again apply the cosine and sine rule to obtain magnitude and phase-angle jump at the equipment terminals. Note that in Fig. 4.109, $\phi < 0$, $\phi_b > 0$, and $\phi_c < 0$. The cosine rule gives

$$V_c^2 = \left(\frac{1}{3}\sqrt{3}\right)^2 + \left(\frac{1}{3}V\sqrt{3}\right)^2 - 2 \times \frac{1}{3}\sqrt{3} \times \frac{1}{3}V\sqrt{3} \times \cos(120° - \phi) \tag{4.112}$$

which results in an expression for the voltage magnitude V_c:

$$V_c = \sqrt{\frac{1}{3} + \frac{1}{3}V^2 - \frac{2}{3}V\cos(120° - \phi)} \tag{4.113}$$

The sine rule in the same triangle gives

$$\frac{\sin(30° + \phi_c)}{\frac{1}{3}V\sqrt{3}} = \frac{\sin(120° - \phi)}{V_c} \tag{4.114}$$

The phase-angle jump ϕ_c follows as

$$\phi_c = -30° + \arcsin\left\{\frac{V}{V_c\sqrt{3}}\sin(120° - \phi)\right\} \tag{4.115}$$

The same rules can be applied to the lower triangle, which leads to the following expressions for magnitude V_b and phase-angle jump ϕ_b:

$$V_b = \sqrt{\frac{1}{3} + \frac{1}{3}V^2 - \frac{2}{3}V\cos(120° + \phi)} \tag{4.116}$$

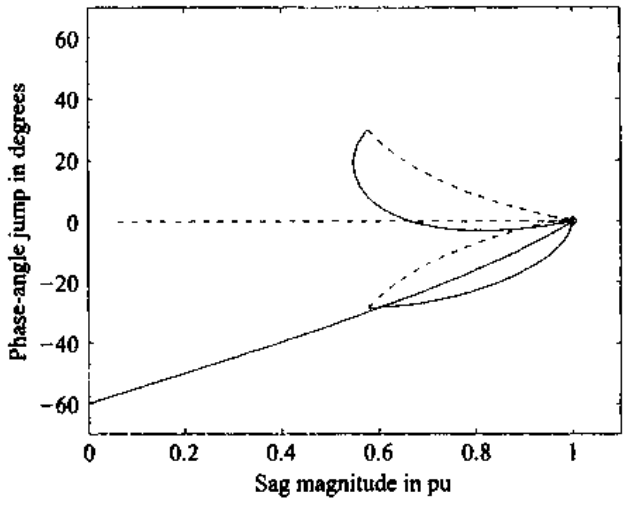

Figure 4.110 Magnitude and phase-angle jump at the equipment terminals for a type F sag, due to a two-phase-to-ground fault. The curves are given for an impedance angle of 0 (dashed line) and −60° (solid line).

$$\phi_b = 30° - \arcsin\left\{\frac{V}{V_b\sqrt{3}}\sin(120° + \phi)\right\} \tag{4.117}$$

From these equations we can again calculate magnitude and phase-angle jump at the equipment terminals, e.g., as a function of the distance to the fault. Figure 4.110 plots magnitude versus phase-angle jump for a type F sag due to a two-phase-to-ground fault. We see that one phase behaves again like the sag due to a three-phase fault. The other two phase are somewhat like the two phases with a shallow sag in the type D sag shown in Fig. 4.95. The difference is that for a type F sag the voltages show a significantly larger drop. The maximum phase-angle jump for these two phases is again 30°.

4.6.4.2 Sags of Type G. A detailed phasor diagram for a type G sag is shown in Fig. 4.111. The complex voltage in phase a drops to a value of $\frac{2}{3}$ (no drop for a sag of type C); the complex voltages in phase b and c drop to a value of $-\frac{1}{3}$ ($-\frac{1}{2}$ for type C).

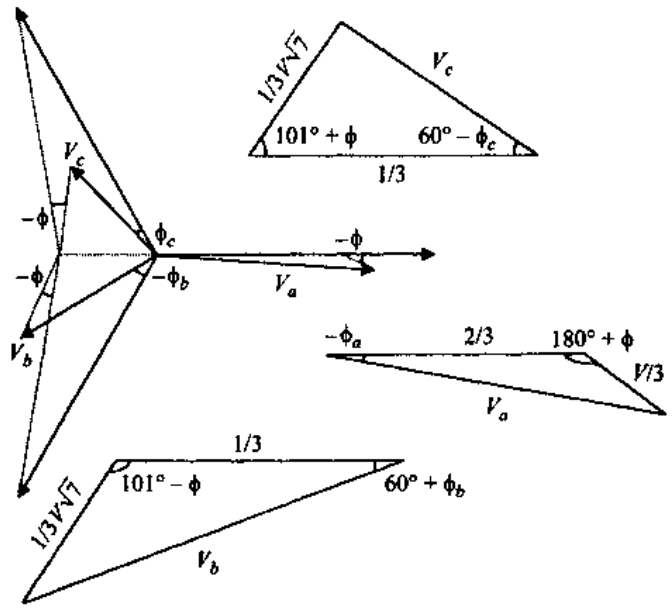

Figure 4.111 Detailed phasor diagram for three-phase unbalanced sag of type G with characteristic magnitude V and characteristic phase-angle jump ϕ.

The cosine rule and the sine rule applied to the triangle on the right give the following expressions:

$$V_a^2 = \frac{4}{9} + \frac{1}{9}V^2 - 2 \times \frac{2}{3} \times \frac{V}{3}\cos(180° + \phi) \tag{4.118}$$

$$\frac{\sin(180° + \phi)}{V_a} = \frac{\sin(-\phi_a)}{\frac{1}{3}V} \tag{4.119}$$

This leads again to expressions for magnitude and phase-angle jump at the equipment terminals.

$$V_a = \sqrt{\frac{4}{9} + \frac{1}{9}V^2 + \frac{4}{9}V\cos\phi} \tag{4.120}$$

$$\phi_a = \arcsin\left(\frac{V}{3V_a}\sin\phi\right) \tag{4.121}$$

Repeating the calculations for the other triangles gives expressions for magnitude and phase-angle jump in the other two phases. Note the angle 101° and the factor $\frac{1}{3}\sqrt{7}$. These originate from the triangle formed by the complex numbers 0, $-\frac{1}{3}$, and $-\frac{1}{2} \pm \frac{1}{2}j\sqrt{3}$.

$$V_b = \frac{1}{3}\sqrt{1 + 7V^2 - 2V\sqrt{7}\cos(101° - \phi)} \tag{4.122}$$

$$\phi_b = -60° + \arcsin\left(\frac{1}{3}\sqrt{7}\frac{V}{V_b}\sin(101° - \phi)\right) \tag{4.123}$$

$$V_c = \frac{1}{3}\sqrt{1 + 7V^2 - 2V\sqrt{7}\cos(101° + \phi)} \tag{4.124}$$

$$\phi_c = 60° - \arcsin\left(\frac{1}{3}\sqrt{7}\frac{V}{V_c}\sin(101° + \phi)\right) \tag{4.125}$$

The results for type G sags are shown in Fig. 4.112. We see that the type G sag is somewhat similar to the type C sag, as shown in Fig. 4.92. Unlike the phase-to-phase

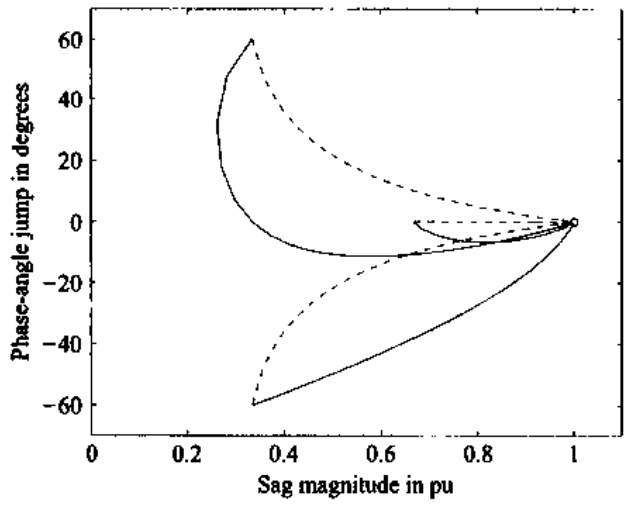

Figure 4.112 Magnitude and phase-angle jump at the equipment terminals for a type G sag, due to a two-phase-to-ground fault. The curves are given for an impedance angle of 0 (dashed line) and −60° (solid line).

fault, two-phase-to-ground faults cause two voltages to drop to 33% instead of 50%. For faults some distance away from the pcc the voltage magnitude can even become a bit less than 33% due to the initial phase-angle jump. Another difference with the phase-to-phase fault is that all three phases drop in magnitude. The third phase, which is not influenced at all by a phase-to-phase fault, may drop to 67% during a two-phase-to-ground fault.

4.6.4.3 Range of Magnitude and Phase-Angle Jump. Merging Fig. 4.110 and Fig. 4.112 gives the whole range of magnitudes and phase-angle jumps experienced by a single-phase load due to two-phase-to-ground faults. In Fig. 4.113 the area due to two-phase-to-ground faults (solid curve) is compared with the area due to phase-to-phase faults (dashed curve). We see that there are certain combinations of magnitude and phase-angle jump which can occur due to phase-to-phase faults but not due to two-phase-to-ground faults, but also the other way around. These curves have been obtained under the assumption that zero-sequence and positive-sequence impedances are equal. For a zero-sequence impedance larger than the positive-sequence source impedance, the resulting sags due to two-phase-to-ground faults are closer toward sags due to phase-to-phase faults. The results are that even a larger range of magnitude and phase-angle jumps can be expected. An increasing zero-sequence impedance will mean that the area enclosed by the solid curve in Fig. 4.113 will shift toward the area enclosed by the dashed curve. The latter is reached for an infinite zero-sequence impedance value.

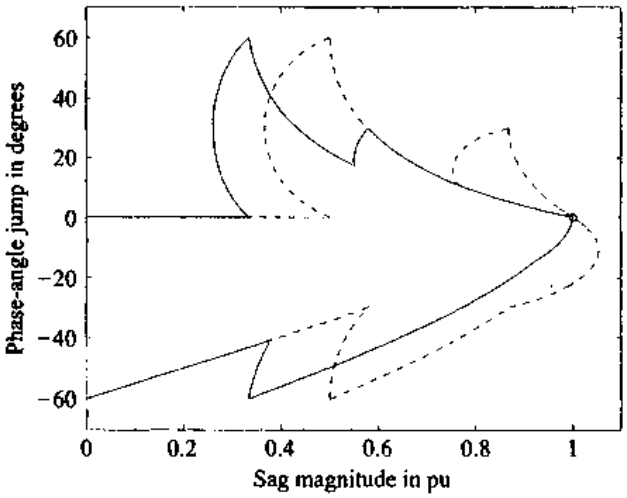

Figure 4.113 Range of magnitude and phase-angle jump at the equipment terminals due to phase-to-phase (dashed curve) and two-phase-to-ground faults (solid curve).

EXAMPLE: TWO-PHASE-TO-GROUND FAULTS, SINGLE-PHASE LOAD

For the same example system as used before (Fig. 4.21) the complex voltages at the equipment terminals due to two-phase-to-ground faults have been calculated. Characteristic magnitude and phase-angle jump due to a two-phase-to-ground fault are the same as due to a phase-to-phase fault. For three-phase delta-connected equipment we can directly use the results obtained for phase-to-phase faults in Fig. 4.97. For two-phase-to-ground faults, the solid lines refer to sags of type G, the dashed lines to sags of type F. A two-phase-to-ground fault at 11 kV leads to a sag of type F for delta-connected load, according to Table 4.13. The Dy 11 kV/660 V transformer changes this into a sag of type G, according to Table 4.14. Two-phase-to-ground faults at 33 kV lead to sags of type F, and faults at 132 kV and 400 kV to type G.

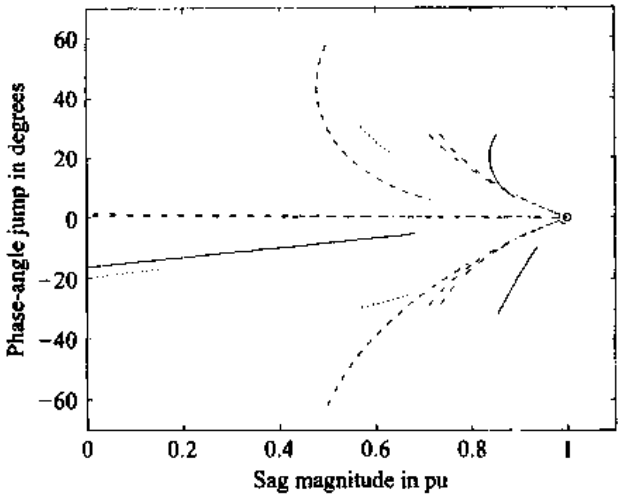

Figure 4.114 Magnitude and phase-angle jump at the equipment terminals due to two-phase-to-ground faults in Fig. 4.21, experienced by single-phase load-connected phase-to-ground at 420 V — solid line: 11 kV, dashed line: 33 kV, dotted line: 132 kV, dash-dot line: 400 kV.

For star-connected single-phase load, the situation is completely different. The zero-sequence source and feeder impedances influence the voltages during a two-phase-to-ground fault, but not during a phase-to-phase fault. The voltage sags experienced by single-phase equipment are shown in Fig. 4.114. Faults at 11 kV, 132 kV, and 400 kV cause sags of type G, in which one phase shows a deep sag and the two other phases a shallow sag. At 11 kV the zero-sequence source impedance is much larger than the positive-sequence one, due to the resistance grounding of this voltage level. The resulting sag is very close to the type D sags due to a phase-to-phase fault. The large zero-sequence impedance makes that the ground connection of a two-phase-to-ground fault does not carry much current. The voltage magnitude in the two phases with shallow sags is thus only down to about 90%. For faults at 132 kV, which is solidly grounded, these voltages are down to about 55%. The 400 kV system is also solidly grounded, but the line impedance dominates the source impedance, making that the zero-sequence impedance is more than twice as large as the positive-sequence impedance. In the phase with the largest voltage drop, the voltage magnitude is about the same for the three voltage levels. Faults at 33 kV will cause a type G sag. As the system is resistance grounded this sag is very close to a type C sag due to a phase-to-phase fault.

4.6.5 High-Impedance Faults

In all the previous calculations in this chapter, we have assumed the fault impedance to be zero. The argumentation for this was that the fault impedance could be incorporated in the feeder impedance, Z_F in (4.9). This argument still holds as long as the magnitude of the sag is concerned, but the phase-angle jump can be significantly affected. We will first address three-phase faults and after that single-phase faults. High-impedance faults are more likely for single-phase-to-ground faults than for three-phase faults.

4.6.5.1 Three-Phase Faults. Consider again the basic voltage divider expression (4.9), but this time with the fault resistance R_{flt} explicitly included:

$$V_{sag} = \frac{\overline{Z}_F + R_{flt}}{\overline{Z}_S + \overline{Z}_F + R_{flt}} \tag{4.126}$$

In many cases the source impedance and the feeder impedance are largely reactive, whereas the fault impedance is mainly resistive. The angle between source impedance

and feeder plus fault impedance gets close to 90°, which can lead to very large phase-angle jumps.

The fault resistance only noticeably affects the voltage if $|\overline{Z}_F| \ll R_{flt}$, thus for faults close to the point-of-common coupling with the load. For zero distance to the fault we get for the complex voltage (with $\overline{Z}_S = jX_s$):

$$V_{sag} = \frac{R_{flt}}{jX_S + R_{flt}} \tag{4.127}$$

The fault resistance is normally not more than a fraction of the source reactance, in which case the sag magnitude is the ratio of the fault and the source impedances with a phase-angle jump equal to almost 90°.

To quantify the influence of the fault resistance, the complex voltage during the sag was calculated as a function of the distance to the fault for three-phase faults at 11 kV in Fig. 4.21. The calculations have been performed for a zero fault resistance and for fault resistances equal to 10%, 20%, and 30% of the (absolute value of the) source impedance. The sag magnitude (the absolute value of the complex voltage) is plotted in Fig. 4.115 as a function of the distance to the fault. As expected the influence on the sag magnitude is limited to small distances to the fault. The fault resistance increases the impedance between the pcc and the fault, and thus reduces the voltage drop at the pcc.

The phase-angle jump is much more influenced, as shown in Fig. 4.116. The phase-angle jump reaches values up to 80°. For increasing fault resistance the maximum phase-angle jump does not reduce much.

4.6.5.2 Single-Phase Faults. To assess the effect of high-impedance single-phase faults on the voltage at the equipment terminals, we use the classification of three-phase unbalanced sags again. At first we consider a solidly-grounded system, for which we can assume that the two non-faulted phase voltages remain at their pre-fault values. In other words, we have a clean type B sag. The voltage in the faulted phase is influenced by the fault resistance as shown in Figs. 4.115 and 4.116. At the equipment terminals the sag will be of type C or D. Magnitude and phase-angle jump at the equipment terminals are shown in Fig. 4.117 for a type C sag and in Fig. 4.118 for a type D sag. In Fig. 4.117 we see how an increasing fault resistance increases the unbalance between the two affected phases. Although the characteristic

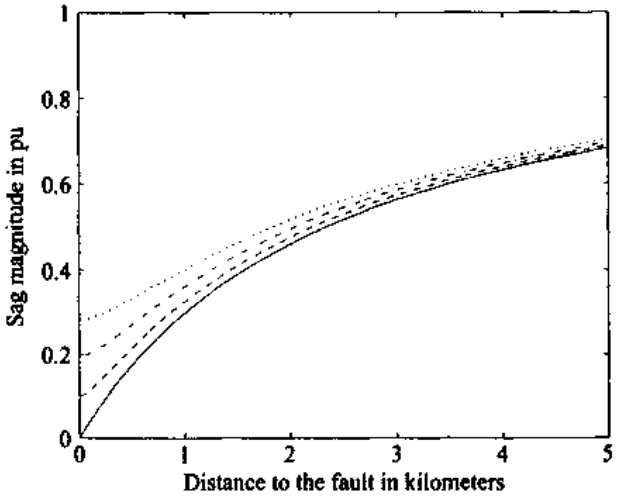

Figure 4.115 Sag magnitude versus distance for three-phase faults with fault resistances equal to zero (solid line), 10% (dashed line), 20% (dash-dot line), and 30% (dotted line) of the source impedance.

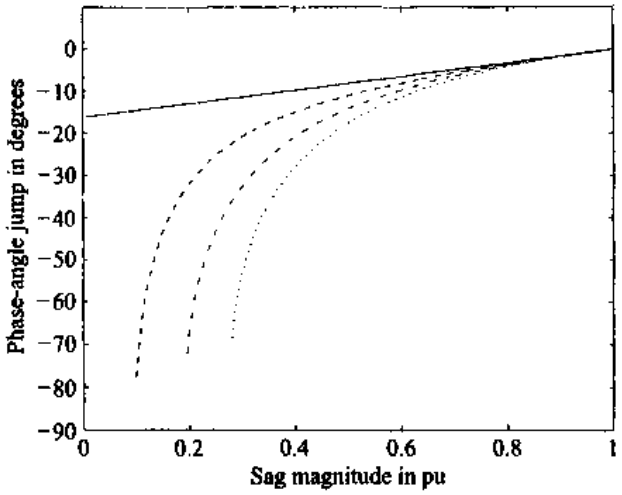

Figure 4.116 Sag magnitude versus phase-angle jump for three-phase faults with fault resistances equal to zero (solid line), 10% (dashed line), 20% (dash-dot line), and 30% (dotted line) of the source impedance.

magnitude increases due to the fault resistance, one of the phases actually drops in voltage. The characteristic magnitude is the difference between the two affected phases in the figure. We also see that the phase-angle jump at the equipment terminals only slightly exceeds 30°, despite the very large initial phase-angle jump. The largest phase-angle jump occurs for a 30% fault resistance at zero distance: −31.9°. In Fig. 4.118 we see that for a type D sag, the fault resistance increases the phase-angle jump in the phase with the large voltage drop, and that it raises one of the other two voltages and reduces the other. Fault resistances above 30% cause a small swell in one of the phases.

For Figs. 4.117 and 4.118, the 11 kV system was assumed to be solidly grounded. Therefore, the zero-sequence source impedance was made equal to the positive-sequence value. In reality this system is resistive grounded: positive- and zero-sequence source impedance are significantly different. The phase-to-neutral voltage is much lower in this case. To calculate the phase-to-neutral voltage a slightly revised version of (4.38) has been used:

$$V_{an} = 1 - \frac{3Z_{S1}}{2Z_{F1} + Z_{F0} + 2Z_{S1} + Z_{S0} + 3R_{flt}} \tag{4.128}$$

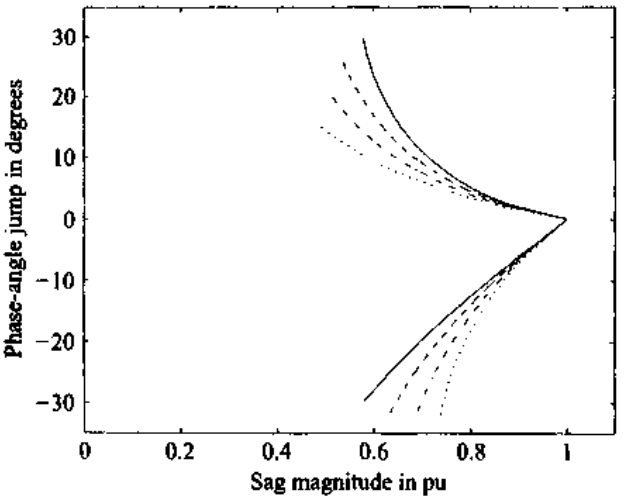

Figure 4.117 Magnitude versus phase-angle jump at the equipment terminals for single-phase faults in a solidly grounded system, sag type C; fault resistances equal to zero (solid line), 10% (dashed line), 20% (dash-dot line), and 30% (dotted line) of the source impedance.

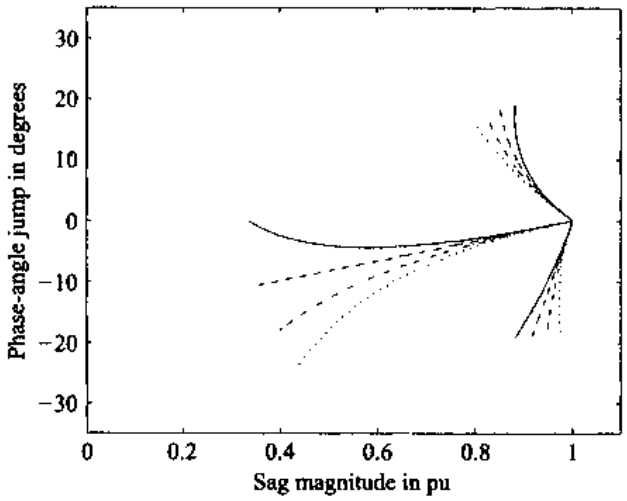

Figure 4.118 Magnitude versus phase-angle jump at the equipment terminals for single-phase faults in a solidly grounded system, sag type D, fault resistances equal to zero (solid line), 10% (dashed line), 20% (dash-dot line), and 30% (dotted line) of the source impedance.

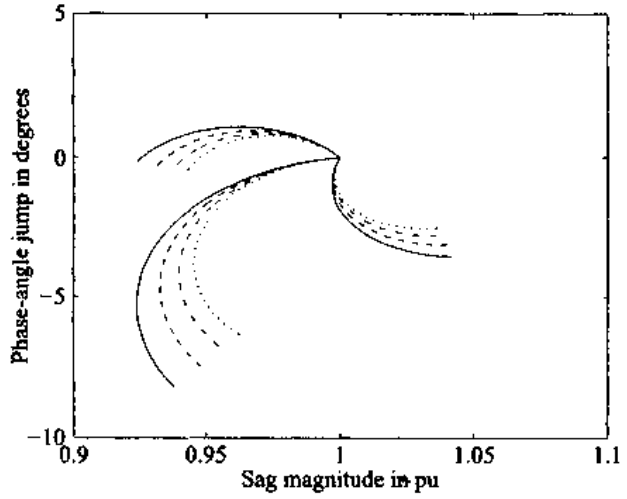

Figure 4.119 Magnitude versus phase-angle jumps at the equipment terminals for single-phase faults in a resistance-grounded system, sag type D; fault resistances equal to zero (solid line), 50% (dashed line), 100% (dash-dot line), and 150% (dotted line) of the source impedance.

The influence of the fault resistance is small in this case, as can be seen in Fig. 4.119. The magnitude and phase-angle jump at the equipment terminals are plotted for a type D sag. Due to the small fault currents arc resistances can reach much higher values in a resistance-grounded system than in a solidly-grounded system. In the calculations leading to Fig. 4.119 fault resistances equal to 50%, 100%, and 150% of the positive-sequence source impedance were used. The main effect of large fault resistances is that the sag becomes less severe in magnitude and in phase-angle jump.

4.6.6 Meshed Systems

All calculations in Sections 4.4 and 4.5 were based on the assumption that the system is radial; thus that we can uniquely identify a point-of-common coupling (pcc), a source impedance Z_S, and a feeder impedance Z_F, as were shown in Fig. 4.14. From Fig. 4.14 we obtained the basic voltage divider equation for the complex sag voltage:

$$V_{sag} = 1 - \frac{Z_S}{Z_S + Z_F} \tag{4.129}$$

In case the system is loaded, we can use Thevenin's superposition theorem which states that the voltage during the fault equals the voltage before the fault plus the change in voltage due to the fault:

$$V_{sag} = V_{pcc}^{(0)} - \frac{Z_S}{Z_S + Z_F} V_f^{(0)} \tag{4.130}$$

with $V_{pcc}^{(0)}$ the pre-fault voltage at the pcc and $V_f^{(0)}$ the pre-fault voltage at the fault position. Note that the source impedance Z_S includes the effect of loads elsewhere in the system.

For a meshed system we need matrix methods to calculate voltage during the fault, as introduced in Section 4.2.5. We obtained the following expression (4.24) for the voltage V_k at node k due to a fault at node f:

$$V_k = V_k^{(0)} - \frac{Z_{kf}}{Z_{ff}} V_f^{(0)} \tag{4.131}$$

with $V_k^{(0)}$ the voltage at node k before the fault and $V_f^{(0)}$ the voltage at the fault position before the fault, and Z_{ij} element ij of the node impedance matrix. Comparing this equation with (4.129) we see that they have the same structure. The voltage divider model can be used for meshed systems, when the following source and feeder impedances are used:

$$Z_S = Z_{kf} \tag{4.132}$$

$$Z_F = Z_{ff} - Z_{kf} \tag{4.133}$$

The main difference is that both Z_S and Z_F are dependent on the fault location. Equivalent source and feeder impedances can be obtained for positive-, negative-, and zero-sequence networks, and all the previously discussed analysis can still be applied.

4.7 OTHER CHARACTERISTICS OF VOLTAGE SAGS

4.7.1 Point-on-Wave Characteristics

The voltage sag characteristics discussed hitherto (magnitude, phase-angle jump, three-phase unbalance) are all related to the fundamental-frequency component of the voltage. They require the calculation of the rms value of the voltage or the complex voltage over a period of one half-cycle or longer. We saw earlier how this leads to an uncertainty in the calculation of sag duration. To obtain a more accurate value for the sag duration one needs to be able to determine "start" and "ending" of the sag with a higher precision. For this one needs to find the so-called "point-on-wave of sag initiation" and the "point-on-wave of voltage recovery" [38], [134]. Both require more advanced analysis techniques, which are still under development. We will see in the next chapter that the point-on-wave characteristics also affect the behavior of some equipment.

4.7.1.1 Point-on-Wave of Sag Initiation. The point-on-wave of sag initiation is the phase angle of the fundamental voltage wave at which the voltage sag starts. This angle corresponds to the angle at which the short-circuit fault occurs. As most faults are associated with a flashover, they are more likely to occur near voltage maximum than near voltage zero. In the sag shown in Fig. 4.1 the point-on-wave of sag initiation is close to voltage maximum. In Fig. 4.9 sag initiation takes place about 35°

after voltage maximum, at least in the phase with the largest voltage drop. In other phases the event starts at another angle compared to the fundamental voltage in that phase.

When quantifying the point-on-wave a reference point is needed. The upward zero crossing of the fundamental voltage is an obvious choice. One is likely to use the last upward zero crossing of the pre-event voltage as reference, as this closely resembles the fundamental voltage. The sag shown in Fig. 4.1 is partly repeated in Fig. 4.120: one cycle (1/60 of a second) starting at the last upward zero crossing before sag initiation. We see that the point-on-wave of sag initiation is about 275°. A closer look at the data learns that this point is between 276° and 280°. The slope at the beginning of the sag actually takes 4°, or about 185 μs. This is probably due to the low-pass character of the measurement circuit.

Figure 4.121 plots all three phases of the sag for which one phase was plotted in Fig. 4.120. For each phase, the zero point of the horizontal axis is the last upward zero crossing before the start of the event in that phase. We see that the point-on-wave is different in the three phases. This is obvious if one realizes that the event starts at the same moment in time in the three phases. As the voltage zero crossings are 120° shifted,

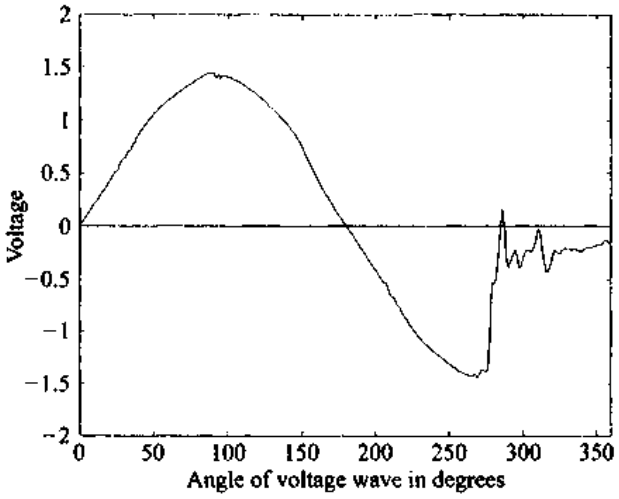

Figure 4.120 Enlargement of the sag shown in Fig. 4.1 indicating the point-on-wave of sag initiation.

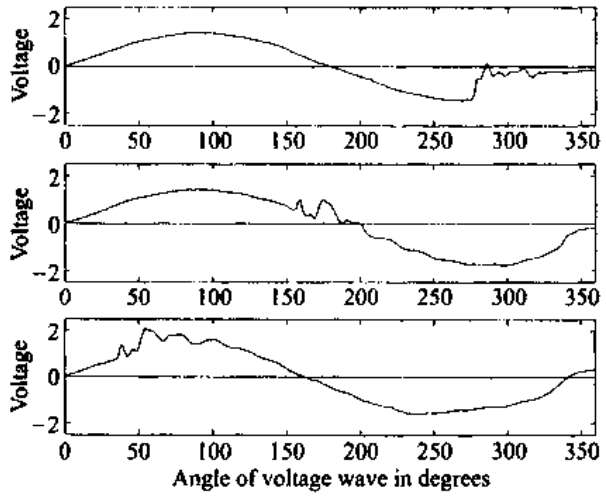

Figure 4.121 Event initiation in the three phases, compared to the last upward voltage zero crossing.

the point-on-wave values differ by 120°. In case phase-to-phase voltages are used, the resulting values are again different. When quantifying point-on-wave it is essential to clearly define the reference.

4.7.1.2 Point-on-Wave of Voltage Recovery. The point-on-wave of voltage recovery is the phase angle of the fundamental voltage wave at which the main recovery takes place. We saw before that most existing power quality monitors look for the point at which the voltage recovers to 90% or 95% of the nominal voltage. Note that there is in many cases no link between these two points. Consider as an example again the sag shown in Fig. 4.1. Voltage recovery in the meaning of this section takes place about 2.5 cycles after sag initiation, even though the voltage does not fully recover for at least another two cycles, as can be seen in Fig. 4.3.

Voltage recovery corresponds to fault clearing, which takes place at current zero crossing. Because the power system is mainly inductive, current zero crossing corresponds to voltage maximum. Thus we expect points-on-wave of voltage recovery to be around 90° and 270°. This assumes that we use the pre-event fundamental voltage as reference, not the during-event voltage. It is the pre-event voltage which drives the fault current and which is thus 90° shifted compared to the fault current. The recovery of the sag in Fig. 4.120 is shown in Fig. 4.122. The recovery is, at least in this case, slower than the sag initiation. The shape of the voltage recovery corresponds to the so-called "transient recovery voltage" well-known in circuit-breaker testing. The smooth sinusoidal curve in Fig. 4.122 is the continuation of the pre-event fundamental voltage. Considering the start of the recovery, we find a point-on-wave of 52°. If we further assume this to be the moment of fault-clearing taking place at current zero, we see that the current lags the voltage by 52°, which gives an X/R ratio at the fault position equal to $\tan^{-1}(52°) = 1.3$.

For a two-phase-to-ground or three-phase fault, fault clearing does not take place in all three phases at the same time. This could make a determination of the point-on-wave of voltage recovery difficult. An unambiguous definition of the reference point and phase is needed to apply this concept to three-phase unbalanced sags.

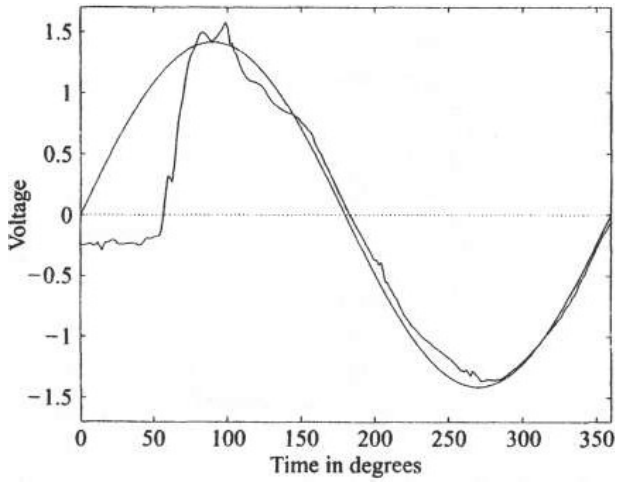

Figure 4.122 Enlargement of Fig. 4.1 showing the point-on-wave of voltage recovery. The smooth curve is the continuation of the pre-sag fundamental voltage.

4.7.2 The Missing Voltage

The missing voltage is another voltage sag characteristic which has been proposed recently [134]. The missing voltage is a way of describing the change in momentary voltage experienced by the equipment. The concept became important with the dimensioning of series-connected voltage-source converters to compensate for the voltage drop due to the fault. We will see in Chapter 7 that the voltage injected by the series compensator is equal to the missing voltage: the difference between the voltage as it would have been without the sag, and the actual voltage during the sag.

4.7.2.1 The Complex Missing Voltage. One can think of the missing voltage as a complex voltage (a phasor), being the difference in the complex plane between the pre-event voltage and the voltage during the sag. The absolute value of this complex missing voltage can be directly read from a plot like shown in Fig. 4.83. In Fig. 4.83 the missing voltage is the distance between the complex voltage during the sag (which is on one of the three curves) and the top-right corner of the diagram (the point 1+j0).

EXAMPLE Consider a sag on a 50 mm^2 underground cable, like in Fig. 4.83, with a sag magnitude of 60%. If the pre-event voltage was 100%, the drop in rms value of the voltage is 40%. Having no further information one would be tempted to say that a compensator should inject a voltage with an rms value equal to 40% of nominal.

Looking in the complex plane, we see that a magnitude of 60% corresponds to a complex voltage $\overline{V} = 0.45 - j0.39$. The missing voltage is the difference between the pre-fault voltage and the voltage during the sag, thus $1 - \overline{V} = 0.55 + j0.39$. The absolute value of the missing voltage is 67% in this example. Compare this with the 40% drop in rms voltage.

The complex missing voltage can also be calculated from the magnitude V and the phase-angle jump ϕ of the sag. The complex voltage during the sag is

$$\overline{V} = V\cos\phi + jV\sin\phi \tag{4.134}$$

The missing voltage is simply

$$1 - \overline{V} = 1 - V\cos\phi - jV\sin\phi \tag{4.135}$$

with as absolute value

$$V_{miss} = |1 - \overline{V}| = \sqrt{1 - V^2 - 2V\cos\phi} \tag{4.136}$$

When we neglect the phase-angle jump, thus assume that $\overline{V} = V$, the missing voltage is simply $\tilde{V}_{miss} = 1 - V$. We can assess the error made by writing $1 - V = \sqrt{1 + V^2 - 2V}$. Comparing this with (4.136) gives for the difference between the exact and the approximate expression for the missing voltage:

$$V_{miss}^2 - \tilde{V}_{miss}^2 = 2V(1 - \cos\phi) \tag{4.137}$$

4.7.2.2 The Missing Voltage in Time Domain. The concept of missing voltage can become much more useful by extending it to time domain. A very first step would be to look at the difference between the fundamental pre-event voltage and the fundamental during-event voltage. But that would not give any extra information compared to the complex missing voltage.

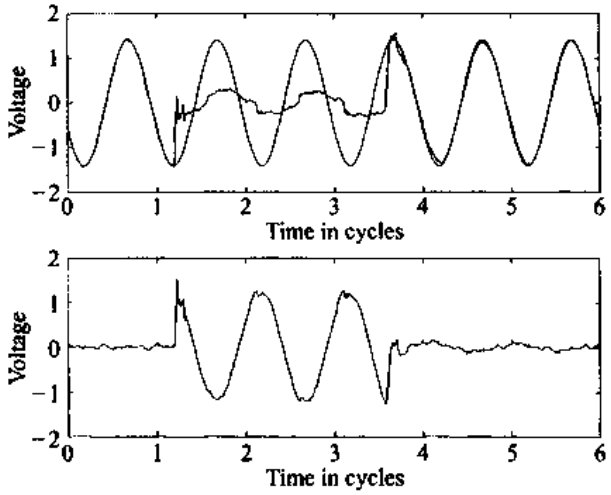

Figure 4.123 Time-domain voltage measurement together with pre-event fundamental voltage (top curve) and the time-domain missing voltage being the difference of those two (bottom curve).

In the top part of Fig. 4.123 the sag from Fig. 4.1 has been plotted again. Together with the actual time-domain voltage wave, the fundamental pre-event voltage has been plotted. The latter is obtained by applying a fast-Fourier-transform algorithm to the first cycle of the voltage wave form. From the complex coefficient for the fundamental term in the Fourier series C_1, the (time-domain) fundamental component of the voltage can be calculated:

$$V_{fund}(t) = \mathrm{Re}\{C_1 e^{-j\omega t}\} \tag{4.138}$$

This fundamental component of the pre-event voltage (pre-event fundamental voltage, for short) is the smooth sinusoidal curve in the top part of Fig. 4.123.

The missing voltage is calculated as the difference between the actual voltage and the pre-event fundamental voltage:

$$V_{miss}(t) = V(t) - V_{fund}(t) \tag{4.139}$$

This missing voltage is plotted in the bottom part of Fig. 4.123. Before the initiation of the sag there is obviously no fundamental component present; during the sag the fundamental component of the missing voltage is large; after the principal sag (after fault clearing) a small fundamental component remains. The reason for this becomes clear from the upper curve: the voltage does not immediately fully recover to its pre-event value.

Figure 4.124 repeats this for the voltage in one of the non-faulted phases, for the same event as in Fig. 4.123 and Fig. 4.1. In the top curve we see that the during-event voltage has a larger rms value than the pre-event voltage. In terms of rms voltages, we would call this an increase in voltage: a voltage swell. But looking at the missing voltage it is not possible to say whether the underlying event is a swell or a sag. This might be seen as a disadvantage of the missing voltage concept. But one should realize that this concept is not meant to replace the other ways of characterizing the sag; instead, it should give additional information.

Finally, Fig. 4.125 plots the missing voltage in all three phases. As expected for a single-phase-to-ground fault, the missing voltage in the two non-faulted phases is the same and in phase with the missing voltage in the faulted phase. After the fault the missing voltages in the three phases form a positive sequence set. This is probably due to the re-acceleration of induction motors fed from the supply.

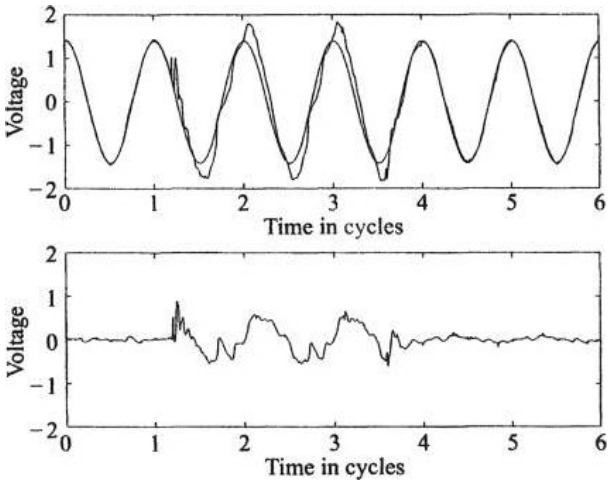

Figure 4.124 Measured voltage with pre-event fundamental voltage (top curve) and missing voltage (bottom curve) during a voltage swell event.

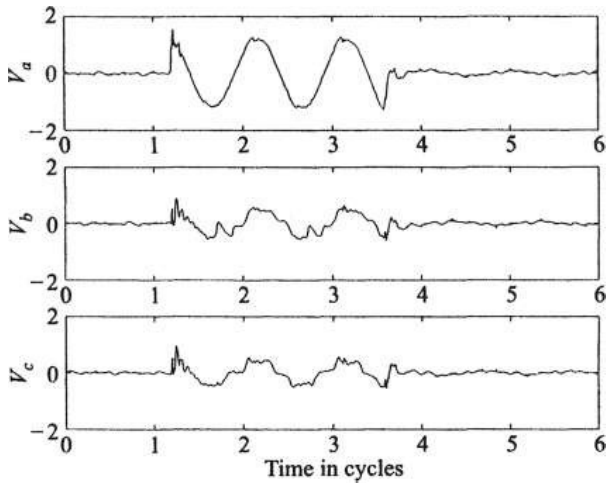

Figure 4.125 Missing voltage for the three phases of a sag due to a single-phase fault.

In Figs. 4.124 and 4.125 we used the fundamental pre-event voltage as a reference to obtain the missing voltage. The concept of missing voltage has been introduced to quantify the deviation of the voltage from its ideal value. In other words: we have used the fundamental pre-event voltage as the ideal voltage. This could become a point of discussion, as there are at least three alternatives:

- Use the full pre-event waveform, including the harmonic distortion, as a reference. One can either take the last cycle before the event or the average over a number of cycles. The latter option is limited in its application because there are normally not more than one or two pre-event cycles available.
- Use the fundamental component of the pre-event waveform as a reference. One can again choose between the fundamental obtained from the last cycle before the event (as was done in Fig. 4.124 and Fig. 4.125) or obtain the fundamental from a number of pre-event cycles.
- Use as a reference, a sinusoidal waveform with the same amplitude and rms value as the system nominal voltage and the same phase angle as the fundamental pre-event waveform. The difference between the last two alternatives is

the same as the discussion between defining the voltage drop with reference to the pre-event rms voltage or with reference to the nominal rms voltage. Both methods have their advantages and can thus be used. But it is important to always indicate which method is used.

4.7.2.3 Distribution of the Missing Voltage. An alternative and potentially very useful way of presenting the missing voltage is through the amount of time that the missing voltage, in absolute value, exceeds given values; in other words, the amount of time during which the deviation from the ideal voltage waveform is larger than a given value.

In the top curve of Fig. 4.126 the missing voltage from Fig. 4.123 is shown again. But this time the absolute value is plotted, instead of the actual waveform. We see, e.g., that this absolute value exceeds the value of 0.5, a total of six times during the event. The cumulative duration of these six periods is 1.75 cycles. The cumulative time during which the missing voltage in absolute value exceeds a given level can be determined for each level. The result of this calculation is shown in the bottom part of Fig. 4.126. This curve can be read as follows: the missing voltage is never larger than 1.53, is during 1 cycle larger than 0.98, during 1.75 cycle larger than 0.5, during two cycles larger than 0.32, etc. The long tail in Fig. 4.126 is due to the post-fault voltage sag as well as to the non-zero pre-event missing voltage. The latter contribution can be removed by either using the full pre-event waveshape as a reference to calculate the missing voltage, or by only considering the missing voltage samples from the instant of sag-initiation onward.

Through the same procedure, distributions of the missing voltage can be obtained for the other two phases, resulting in the curves shown in Fig. 4.127. The missing voltage in the faulted phase (solid curve) is naturally larger than in the non-faulted phases. But still, the missing voltage in the non-faulted phases is significant: during about 1 cycle it exceeds a value of 0.4. We also see a small difference in missing voltage between the two non-faulted phases: the value in phase b is somewhat higher than in phase c.

The missing voltage distribution curve can be used as a generalized way of defining the event duration. The larger the deviation from the ideal voltage one considers, the shorter the "cumulative duration" of the event. The cumulative duration of a

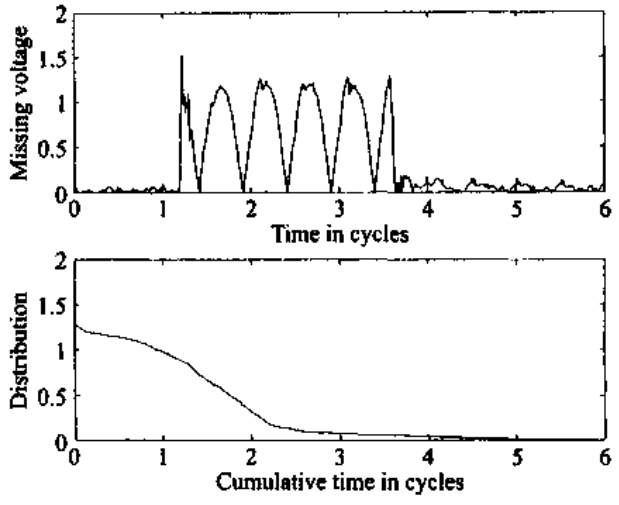

Figure 4.126 Absolute value of the missing voltage (top curve) and the distribution of the missing voltage (bottom curve) for the sag shown in Fig. 4.1.

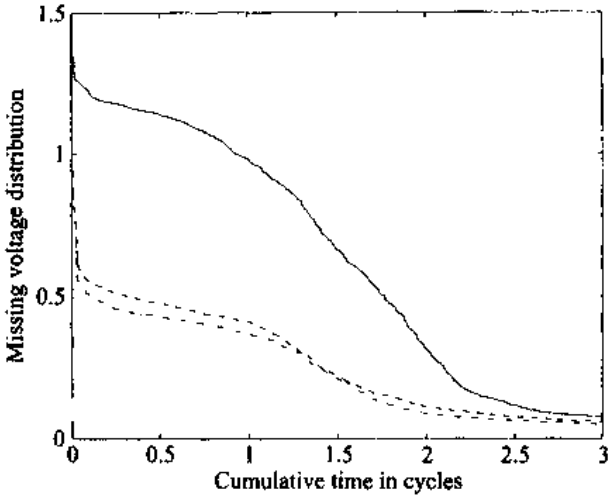

Figure 4.127 Missing voltage distribution for phase a (solid curve), phase b (dashed curve), and phase c (dash-dot curve).

voltage sag for a given deviation would be defined as the total amount of time during which the voltage deviates more than the given value from the ideal voltage waveshape.

4.8 LOAD INFLUENCE ON VOLTAGE SAGS

In the calculation of sag magnitude for various system configurations, in the classification of three-phase sags and in most of the examples, we have assumed that the load currents are zero. In this section we will discuss some situations in which the load currents can have a significant influence on the voltages during a fault. The main load having influence on the voltage during and after a sag is formed by induction and synchronous motors as they have the largest currents during and after a short-circuit fault. But we will also briefly discuss single-phase and three-phase rectifiers as they are a large fraction of the load at many locations.

4.8.1 Induction Motors and Three-Phase Faults

During a three-phase fault the voltages at the motor terminals drop in magnitude. The consequences of this drop are twofold:

- The magnetic flux in the air gap is no longer in balance with the stator voltage. The flux decays with a time constant of up to several cycles. During this decay the induction motor contributes to the fault and somewhat keeps up the voltage at the motor terminals.
- The decay in voltage causes a drop in electrical torque: the electrical torque is proportional to the square of the rms value of the voltage. The mechanical torque in the mean time remains largely unchanged. The result is that the motor slows down. While the motor slows down it will take a larger current with a smaller power factor. This could bring down the voltage even more. For small voltage drops, a new steady state could be reached at a lower speed, depending on the speed-torque behavior of the mechanical load. For deep sags the motor will continue to slow down until it reaches standstill, or until the voltage recovers, whichever comes first. The mechanical time constant of electrical motors is of the order of one second and more. Therefore the motor will normally not have reached zero speed yet upon voltage recovery.

The moment the voltage recovers the opposite phenomena occur. The flux in the air gap will build up again. This causes a large inrush current, which slows down the voltage recovery. After that, the motor will re-accelerate until it reaches its pre-event speed. During the re-acceleration the motor again takes a larger current with a smaller power factor, which causes a post-fault voltage sag sometimes lasting for several seconds.

The contribution of the induction motor load to the fault can be modeled as a voltage source behind reactance. The voltage source has a value of about 1 pu at fault initiation and decays with the subtransient time-constant (between 0.5 and 2 cycles). The reactance is the leakage reactance of the motor, which is between 10% and 20% on the motor base. Note that this is not the leakage reactance which determines the starting current, but the leakage reactance at nominal speed. For double-cage induction machines these two can be significantly different.

EXAMPLE Consider a bolted fault at primary side of a 33/11 kV transformer in the supply shown in Fig. 4.21. The total induction motor load connected to the 11 kV bus is 5% of the fault level. The induction motors have a leakage reactance of 10% on the motor base. We are interested in the voltage at secondary side of the transformer. Consider only the reactive part of the impedances.

The transformer impedance is the difference between the 33 kV and 11 kV fault levels: $Z_T = 47.6\%$ at a 100 MVA base. The fault level at 11 kV is 152 MVA, thus the total motor load is (5% of this): 7.6 MVA. The leakage reactance of the motors is 10% at a 7.6 MVA base, which is $Z_M = 132\%$ at a 100 MVA base. The voltage on secondary side of the transformer is found from the voltage divider equation:

$$V_{load} = \frac{Z_T}{Z_T + Z_M} = 27\% \tag{4.140}$$

To assess the increase in motor current after the fault, we use the common equivalent circuit for the induction motor, consisting of the series connection of the stator resistance R_S, the leakage reactance X_L and the slip-dependent rotor resistance $\frac{R_R}{s}$, with s the motor slip. The motor impedance is

$$Z_M = R_S + jX_L + \frac{R_R}{s} \tag{4.141}$$

The change of motor impedance with slip has been calculated for four induction motors of four different sizes. Motor parameters have been obtained from [135], [136], and the motor impedance has been calculated by using (4.141). The results are shown in Fig. 4.128. For each motor, the impedance at nominal slip is set at 1 pu, and the absolute value of the impedance is plotted between nominal slip and 25% slip. We see for each motor a decrease in motor impedance, and thus an increase in motor current, by a factor of about five. The decrease in impedance is much faster for large machines than for smaller ones.

If we assume the voltage to recover to 1 pu immediately upon fault clearing, the current taken by the motor is the inverse of the impedance (both equal to 1 pu in normal operation). The path of the current in the complex plane is shown in Fig. 4.129. The path is given for an increase in slip from its nominal value to 25%. The positive real axis is in the direction of the motor terminal voltage. For small motors we see predominantly an increase in resistive current, for large motors the main increase is in the inductive part of the current. When the slip increases further, even the resistive part

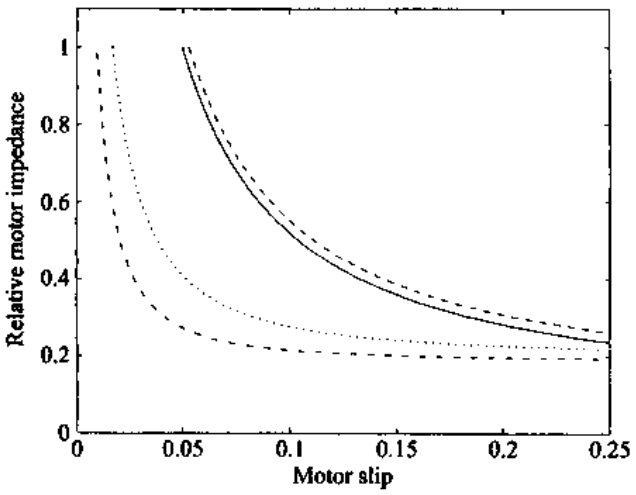

Figure 4.128 Induction motor impedance versus slip; the impedance at nominal slip is 1 pu; 3 hp 220 V (solid line), 50 hp 460 V (dashed line), 250 hp 2300 V (dotted line), 1500 hp 2300 V (dash-dot line).

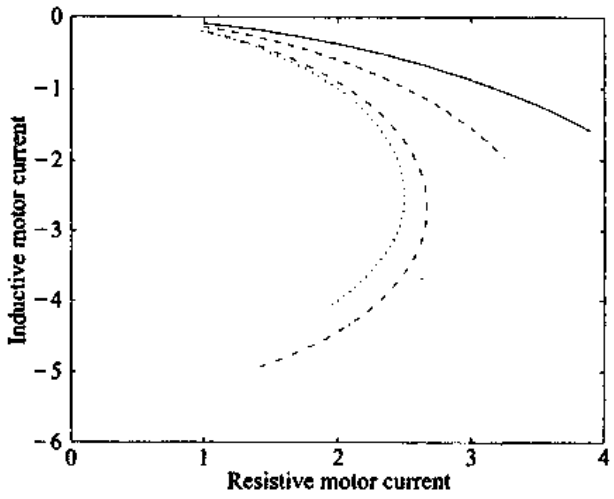

Figure 4.129 Change in induction motor current with increasing slip; the current at nominal slip is 1 pu; 3 hp 220 V (solid line), 50 hp 460 V (dashed line), 250 hp 2300 V (dotted line), 1500 hp 2300 V (dashed line).

of the current starts to decrease. The power factor of the current decreases significantly, especially for large motors.

The influence of large induction motors on voltage sags is described in detail by Yalçinkaya [136]. Fig. 4.130 shows the voltage sags (top curve) and the motor slip (bottom curve) due to a three-phase fault in an industrial system with a large induction motor load. Without induction motor load, the voltage would have been zero during the sag and 1 pu after the sag. The voltage plotted in Fig. 4.130 is the absolute value of a time-dependent phasor, used in a transient-stability program. The effect of the induction motor load is that the voltage during the fault is increased, and after the fault decreased. The slip of all motors increases fast during the sag, and even continues to increase a bit after fault clearing.

The voltage after fault clearing, the so-called post-fault sag, shows an additional decrease about 200 ms after fault clearing. This corresponds to the moment the motor starts to re-accelerate and draws larger currents. The low voltage immediately after fault clearing is due to the large current needed to rebuild the air gap flux.

During the fault the induction motors significantly keep up the voltage. Even toward the end of the sag the voltage at the motor busses is still above 10% of its pre-event value.

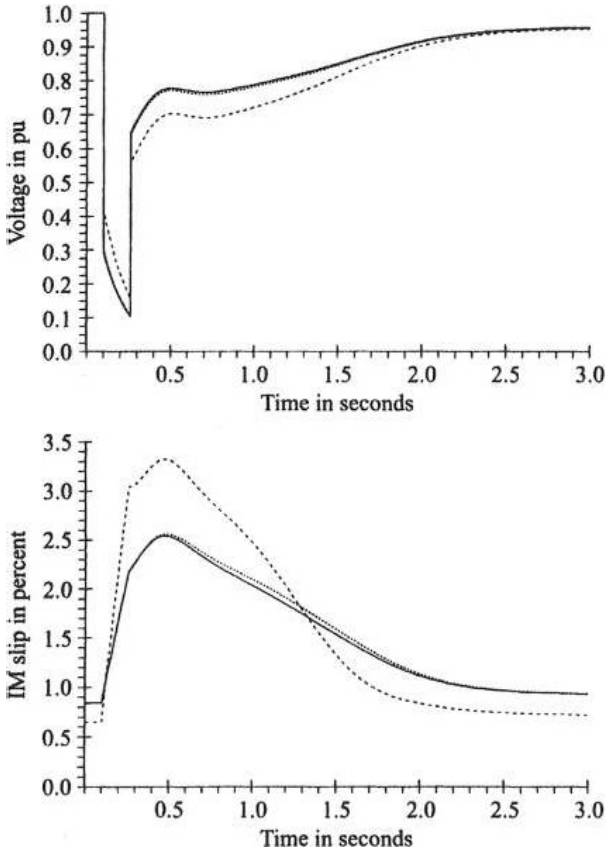

Figure 4.130 Voltage sag (top) and induction motor slip (bottom) for three busses in an industrial power system. (Reproduced from Yalçinkaya [136].)

One should realize that this is a somewhat exceptional case, as the motor load connected to the system is very large. Similar but less severe effects have been noticed in other systems. Another phenomenon which contributes to the post-fault voltage sag is that the fault occurs in one of two parallel transformers. The protection removes the faulted transformer, so that only one transformer is available for the supply after fault clearing. The post-fault fault level is thus significantly less than its pre-fault value. A similar effect occurs for a fault in one of two parallel feeders. The post-fault sag, described here for three-phase faults, has also been observed after single-phase faults.

4.8.2 Induction Motors and Unbalanced Faults

The behavior of an induction motor during an unbalanced fault is rather complicated. Only a network analysis program simulating a large part of the system can give an accurate picture of the quantitative effects. The following phenomena play a part in the interaction between system and induction motor during unbalanced faults.

- During the first one or two cycles after fault initiation the induction motor contributes to the fault. This causes an increase in positive-sequence voltage. Negative- and zero-sequence voltage are not influenced.
- The induction motor slows down, causing a decrease in positive-sequence impedance. This decrease in impedance causes an increase in current and thus a drop in positive-sequence voltage.

- The negative-sequence impedance of the motor is low, typically 10–20% of the nominal positive-sequence impedance. The negative-sequence voltage due to the fault will thus be significantly damped at the motor terminals. The negative-sequence impedance is independent of the slip. The negative-sequence voltage will thus remain constant during the event.
- The induction motor does not take any zero-sequence current. The zero-sequence voltage will thus not be influenced by the induction motor.

4.8.2.1 Simulation Example. Simulations of the influence of induction motor loads on unbalanced sags are shown in [136], [137]. Some of those results are reproduced here. The system studied was a radial one with large induction motor load connected to each of the low-voltage busses. Motor sizes and transformer impedances were chosen such that for each bus the fault level contribution from the source was 15 times the total motor load fed from the bus. Voltages and currents in the system were calculated by using the transient analysis package EMTP. All transformers in the system were connected star-star with both neutral points earthed. Although this is not a very common arrangement, it helped in understanding the phenomena. The voltages at the terminals of one of the motors are shown in Fig. 4.131. Without induction motor influence we would have seen a sag of type B of zero magnitude: zero voltage in phase a, and no change in the voltage in

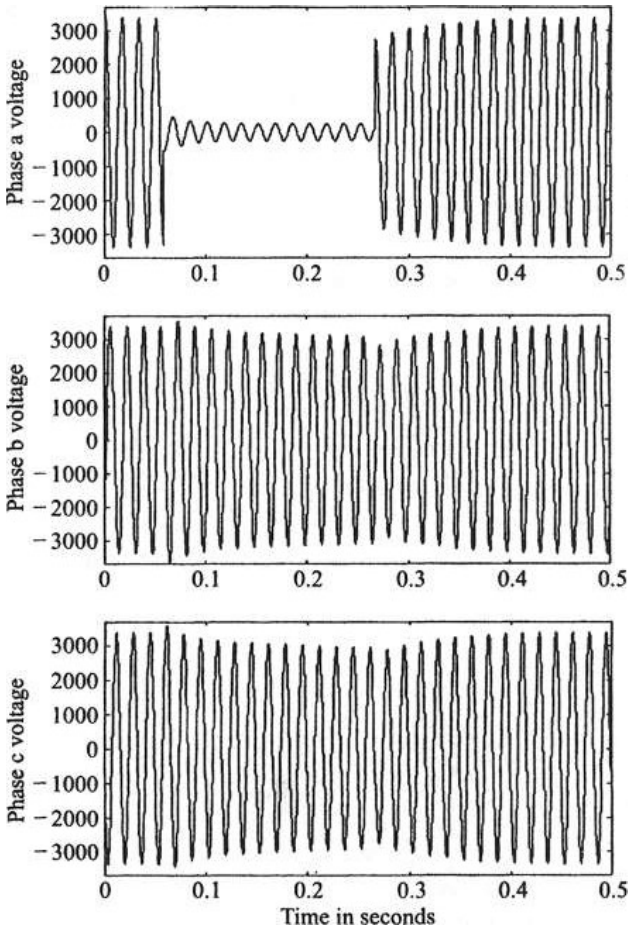

Figure 4.131 Voltages at the motor terminals, due to a single-phase-to-ground fault in the supply. (Reproduced from Yalçinkaya [136].)

phase b and phase c. Instead we see a small non-zero voltage in phase a and in the two non-faulted phases an initial increase followed by a slow decay. After fault clearing the system becomes balanced again, and the three phase voltages thus equal in amplitude. The motor re-acceleration causes a post-fault sag of about 100 ms duration.

The non-zero voltage in the faulted phase is due to the drop in negative-sequence voltage. We saw in (4.32) and (4.34) that the voltage in the faulted phase during a single-phase fault is given as

$$V_a = V_1 + V_2 + V_0 = |V_1| - |V_2| - |V_0| \tag{4.142}$$

The effect of the induction motor is that V_2 drops in absolute value, causing an increase in voltage in the faulted phase.

During the sag, the positive-sequence voltage also drops, which shows up as the slow but steady decrease in voltage in all phases.

The non-faulted phases show an initial increase in voltage. The explanation for this is as follows. The voltage in the non-faulted phases during a single-phase fault is made up of a positive-sequence, a negative-sequence, and a zero-sequence component. For phase c this summation in the complex plane is for the system without induction motor load.

$$V_c = V_{c1} + V_{c0} + V_{c2} = \frac{2}{3}a - \frac{1}{3} - \frac{1}{3}a^2 = a \tag{4.143}$$

Due to the induction motor load, the positive-sequence voltage will not immediately drop from 1 pu to 0.67 pu. The negative-sequence voltage will jump from zero to its new value immediately. The consequence is that the resulting voltage amplitude slightly exceeds its pre-fault value. After a few cycles the induction motor no longer keeps up the positive-sequence voltage. The voltage in the non-faulted phases drops below its pre-event value due to negative- and positive-sequence voltages being less than 33% and 67%, respectively.

The currents taken by the induction motors are shown in Figs. 4.132 and 4.133. Figure 4.132 shows the motor currents for a motor with a small decrease in speed. The slip of this motor increases from 2% to 6% during the sag. The motor shown in Fig. 4.133 experienced a much larger decrease in speed: its slip increased from 3% to 19%. This behavior is difficult to explain without considering symmetrical components. But generally we can observe that the current increases initially in the faulted phase, rises to a higher value in one of the non-faulted phases, and initially drops in the other non-faulted phase. The current in the second non-faulted phase rises again after a certain time, determined by the slowing down of the motor.

For the motor shown in Figs. 4.131 and 4.132 the component voltages and currents have been plotted in Figs. 4.134 and 4.135. From Fig. 4.134 we see that negative and zero-sequence voltage remain constant during the sag, but that the positive-sequence voltage shows a steady decay, due to the decrease in positive-sequence impedance when the motor slows down. Figure 4.135 clearly shows the increase in positive-sequence current when the motor slows down. The zero-sequence current is zero as the motor windings are connected in delta. From Figs. 4.134 and 4.135 the positive- and negative-sequence impedance of the motor load can be calculated, simply through dividing voltage by current. The results are shown in Fig. 4.136, where we see again that the negative-sequence impedance remains constant, whereas the positive-sequence impedance drops. When the motor reaches standstill, it is no longer a dynamic element, and positive- and negative-sequence impedance become equal.

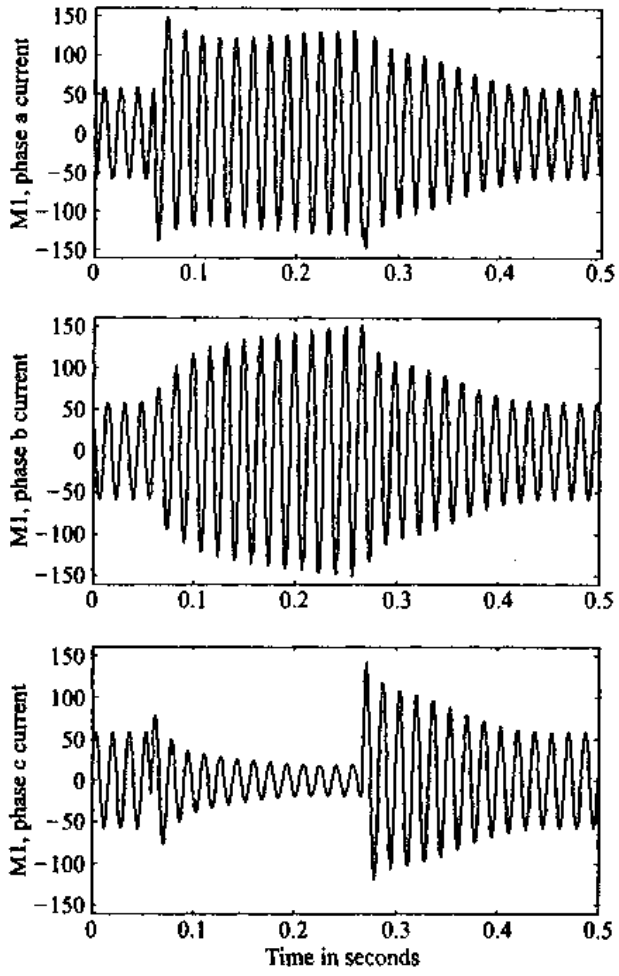

Figure 4.132 Induction motor currents during and after a single-line-to-ground fault in the supply. This motor showed only a small decrease in speed. (Reproduced from Yalçinkaya [136].)

4.8.2.2 Monitoring Example. An example of a three-phase unbalanced sag was shown in Fig. 4.48. The severe post-fault sag indicates the presence of induction motor load. For each of the three sampled waveforms, the complex voltage as a function of time was determined by using the method described in Section 4.5. From the three complex voltages, positive-, negative- and zero-sequence voltages have been calculated. Their absolute values are plotted in Fig. 4.137 as a function of time. The zero-sequence component is very small. The negative-sequence component is zero when the fault is not present and non-zero but constant during the fault. The positive-sequence voltage is 1 pu before the fault, shows a slow decay during the fault, and a slow increase after the fault. This is exactly in correspondence with the above-described theory and simulation results.

4.8.2.3 Simplified Analysis. From the simulation and monitoring results we can extract three stages in the voltage sag:

- The induction motor feeds into the fault, raising the positive-sequence voltage.
- The positive-sequence voltage is the same as it would have been without the induction motor load.
- The induction motor has slowed down, drawing additional positive-sequence current, thus causing the positive-sequence voltage to drop.

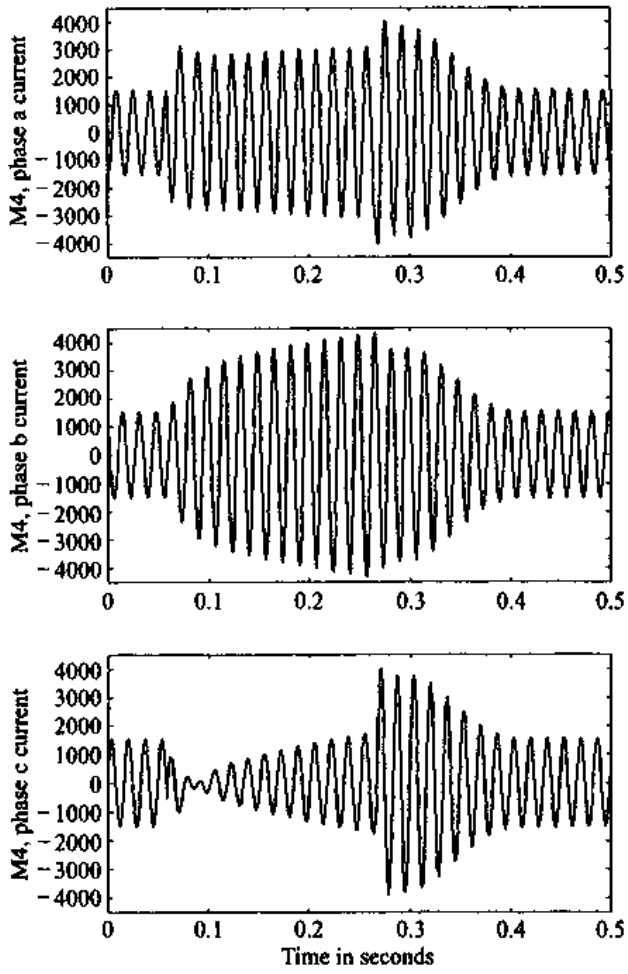

Figure 4.133 Induction motor currents during and after a single-line-to-ground fault in the supply. This motor showed a large decrease in speed. (Reproduced from Yalçinkaya [136].)

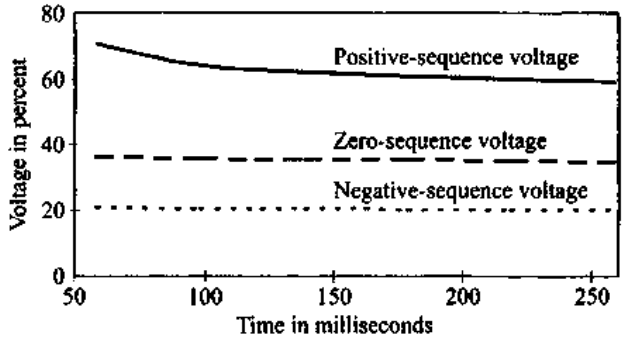

Figure 4.134 Symmetrical components for the voltages shown in Fig. 4.131. (Reproduced from Yalçinkaya [136].)

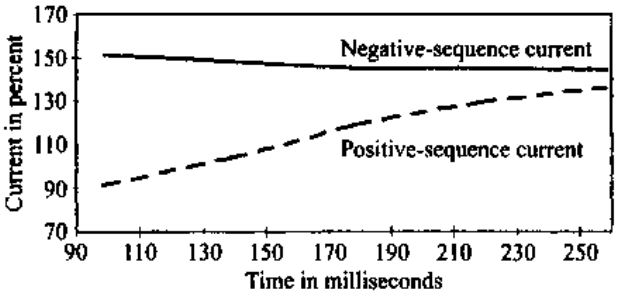

Figure 4.135 Symmetrical components for the currents shown in Fig. 4.132. (Reproduced from Yalçinkaya [136].)

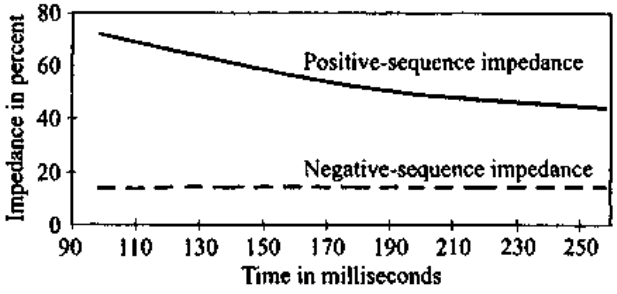

Figure 4.136 Positive- and negative-sequence impedance for an induction motor during a sag. (Reproduced from Yalçinkaya [136].)

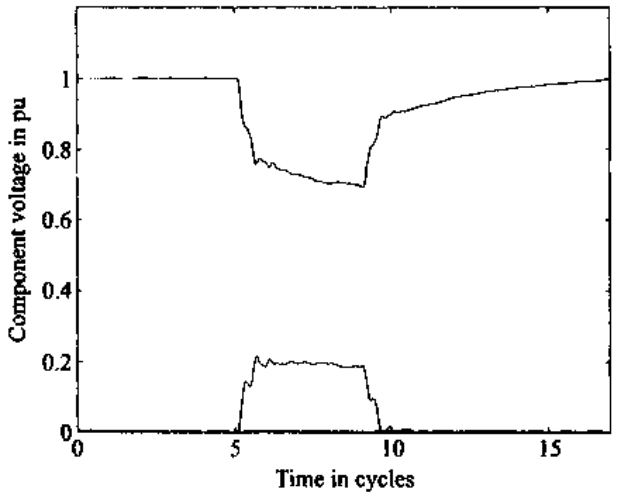

Figure 4.137 Positive-, negative- and zero-sequence voltages for the three-phase unbalanced sag shown in Fig. 4.47.

The negative-sequence voltage is constant during the fault, but lower than without induction motor load. To quantify the effect of induction motors, we use a two-step calculation procedure. At first we calculate positive- and negative-sequence voltage ($V_1^{(no)}, V_2^{(no)}$) for the no-load case. As we saw before this will lead to voltage sags of type C or type D with different characteristic magnitude. We assumed a zero characteristic phase-angle jump. As a second step the influence of the induction motor is incorporated. For this we model the supply as a source generating a type C or type D sag, with a finite source impedance. Note that this is a three-phase Thevenin source representation of the supply during the fault. The effect of the induction motor load is a difference between the source voltages and the voltages at the motor terminals, for positive as well as for negative-sequence components. The voltage at the motor terminals are denoted as $V_1^{(load)}$ and $V_2^{(load)}$. For the three above-mentioned "stages" these relations are assumed to be as follows:

1. The drop in positive-sequence voltage is reduced by 15%, the negative-sequence voltage drops by 30%.

$$V_1^{(load)} = 0.15 + 0.85V_1^{(no)}$$
$$V_2^{(load)} = 0.7V_2^{(no)}$$

2. The negative-sequence voltage drops by 30%.

$$V_1^{(load)} = V_1^{(no)}$$
$$V_2^{(load)} = 0.7V_2^{(no)}$$

3. The positive-sequence voltage drops by 10%, the negative-sequence voltage drops by 30%.

$$V_1^{(load)} = 0.9V_1^{(no)}$$
$$V_2^{(load)} = 0.7V_2^{(no)}$$

The voltages at the motor terminals are calculated from the positive- and negative-sequence voltages $V_1^{(load)}$ and $V_2^{(load)}$. The resulting phase voltages for the three stages are shown in Figs. 4.138 and 4.139. For sag type C the voltages are shown for one of the phases with a deep sag, and for the phase with a shallow sag. The more the motors slow down, the more the voltage in this phase drops. The voltage in the worst-affected phase is initially somewhat higher due to the induction motor influence, but drops when the motor slows down and the positive-sequence voltage drops in value as well. For type D we see that the voltage in the least-affected phases drops during all stages of the sag. The voltage in the worst-affected phase increases initially but decreases later.

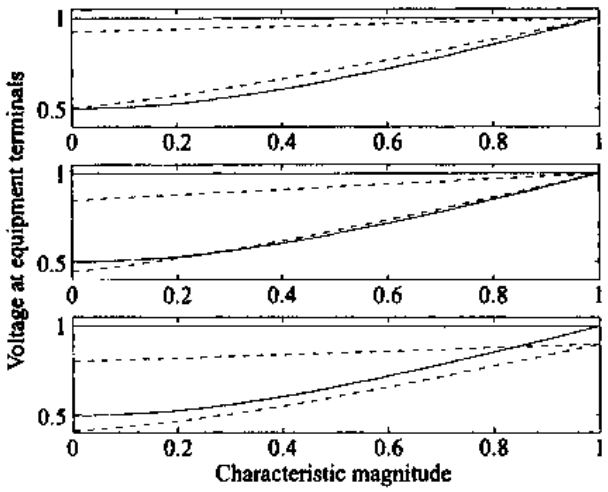

Figure 4.138 Voltages at the equipment terminals, for three stages of induction motor influence for type C sags. The solid lines are without induction motor influence, the dashed lines with.

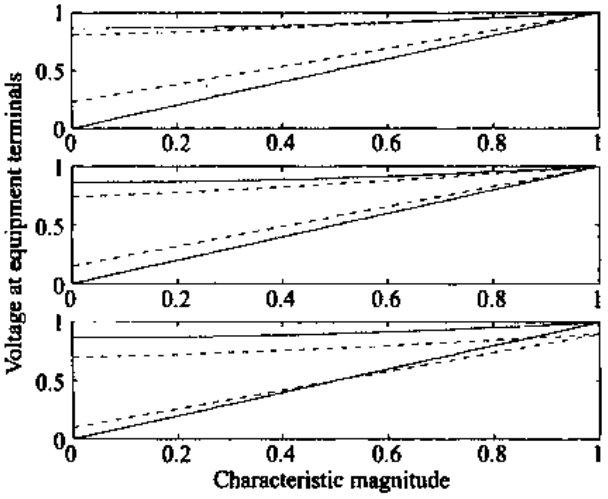

Figure 4.139 Voltages at the equipment terminals, for three stages of induction motor influence for type D sags. The solid lines are without induction motor influence, the dashed lines with.

From the curves in Figs. 4.138 and 4.139 we can see the following two patterns:

- The lowest voltage increases, the highest voltage decreases, thus the unbalance becomes less. This is understandable if we realize that the negative-sequence voltage drops significantly.
- For longer sags all voltages drop. This is due to the drop in positive-sequence voltage.

4.8.3 Power Electronics Load

In systems with a large fraction of the load formed by single-phase or three-phase rectifiers, these can also influence the voltage during and after the voltage sag. Below some qualitative aspects of the effect of rectifiers on the voltage will be discussed briefly. Different aspects will dominate in different systems. The behavior of power electronics equipment during voltage sags is discussed in detail in Chapter 5.

- Especially for longer and deeper sags, a large part of the electronics load will trip. This will reduce the load current and thus increase the voltage, during as well as after the sag.
- Equipment that does not trip will initially take a smaller current from the supply or even no current at all because the dc bus voltage is larger than the peak of the ac voltage. Within a few cycles the dc bus capacitor has discharged sufficiently for the rectifier to start conducting again. Normally the total power taken by the load remains constant so that the ac current will be higher. This current has a high harmonic contents so that the harmonic voltage distortion during the sag will increase.
- Upon voltage recovery, the dc bus capacitors will take a large current pulse from the supply. This can postpone the voltage recovery by up to one cycle.
- For three-phase rectifiers, under unbalanced sags, the largest current flows between the two phases with the largest voltage difference. The effect is that the voltage in these phases drops and increases in the other phase. The three-phase rectifier thus reduces the unbalance between the phases. In this sense they behave similar to induction motor load. For unbalanced sags the current to three-phase rectifiers contains so-called non-characteristic harmonics, noticeably a third harmonic current, so that the voltage during the sag contains a third harmonic component higher than normal.
- Three-phase controlled rectifiers will experience a longer commutation period because the source voltage is lower during the sag. This leads to more severe commutation transients (notches) during the sag. Again this assumes that the equipment will not trip.

4.9 SAGS DUE TO STARTING OF INDUCTION MOTORS

In the previous sections of this chapter, we have discussed voltage sags due to short-circuit faults. These voltage sags are the main cause of equipment failure and malfunction, and one of the main reasons for power quality to become an issue during the last decade. Another important cause of voltage sags, one which has actually been of much more concern to designers of industrial power systems in the past, is the starting of large

induction motors. Also the switching on of other loads will cause a voltage sag, just like the switching off of a capacitor bank. But in those latter cases the drop in voltage is rather small, and the voltage only drops but does not recover. Therefore the term "voltage magnitude step" would be more accurate.

During start-up an induction motor takes a larger current than normal, typically five to six times as large. This current remains high until the motor reaches its nominal speed, typically between several seconds and one minute. The drop in voltage depends strongly on the system parameters. Consider the system shown in Fig. 4.140, where Z_S is the source impedance and Z_M the motor impedance during run-up.

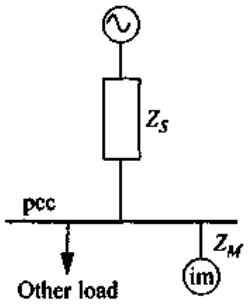

Figure 4.140 Equivalent circuit for voltage sag due to induction motor starting.

The voltage experienced by a load fed from the same bus as the motor is found from the voltage divider equation:

$$V_{sag} = \frac{Z_M}{Z_S + Z_M} \tag{4.144}$$

Like with most previous calculations, a source voltage of 1 pu has been assumed. When a motor of rated power S_{motor} is fed from a source with short-circuit power S_{source}, we can write for the source impedance:

$$Z_S = \frac{V_n^2}{S_{source}} \tag{4.145}$$

and for the motor impedance during starting

$$Z_M = \frac{V_n^2}{\beta S_{motor}} \tag{4.146}$$

with β the ratio between the starting current and the nominal current.

Equation (4.144) can now be written as

$$V_{sag} = \frac{S_{source}}{S_{source} + \beta S_{motor}} \tag{4.147}$$

Of course one needs to realize that this is only an approximation. The value can be used to estimate the sag due to induction motor starting, but for an accurate result one needs a power system analysis package. The latter will also enable the user to incorporate the effect of other motors during starting of the concerned motor. The drop in voltage at the other motor's terminals will slow them down and cause an additional increase in load current and thus an additional drop in voltage.

EXAMPLE Suppose that a 5 MVA motor is started from a 100 MVA, 11 kV supply. The starting current is six times the nominal current. This is a rather large motor for a supply of this strength, as we will see soon. The voltage at the motor terminals during motor starting can be estimated as

$$V_{sag} = \frac{100\,\text{MVA}}{100\,\text{MVA} + 6 \times 5\,\text{MVA}} = 77\% \tag{4.148}$$

In case the voltage during motor starting is too low for equipment connected to the same bus, one can decide to use a dedicated transformer. This leads to the network shown in Fig. 4.141.

Let again Z_S be the source impedance at the pcc, Z_M the motor impedance during run-up, and Z_T the transformer impedance. The magnitude of the voltage sag experienced by the sensitive load is

$$V_{sag} = \frac{Z_T + Z_M}{Z_S + Z_T + Z_M} \tag{4.149}$$

Introducing, like before, the short-circuit power of the source S_{source}, the rated power of the motor S_{motor} and assuming that the transformer has the same rated power of the motor and an impedance ϵ, we get from (4.149):

$$V_{sag} = \frac{(1 + 6\epsilon)S_{Source}}{(1 + 6\epsilon)S_{source} + 6S_{motor}} \tag{4.150}$$

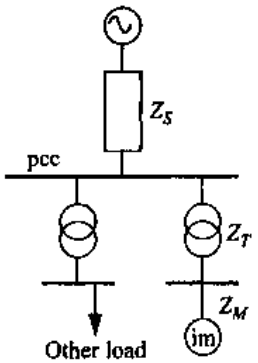

Figure 4.141 Induction motor starting with dedicated transformer for the sensitive load.

EXAMPLE Consider a dedicated supply for the motor in the previous example. The motor is fed through a 5 MVA, 5% 33/11 kV transformer from a 300 MVA, 33 kV supply. Note that the fault current at the 33 kV bus is identical to the fault current at the 11 kV in the previous example. That gives the following parameter values: $S_{source} = 300$ MVA, $S_{motor} = 5$ MVA, and $\epsilon = 0.05$, giving, from (4.150), a sag magnitude of 93%. Most loads will be able to withstand such a voltage reduction. Note that the reduction in sag magnitude is mainly due to the increased fault level at the pcc, not so much due to the transformer impedance. Neglecting the transformer impedance ($\epsilon = 0$ in (4.150)) gives $V_{sag} = 91\%$.

The duration of the voltage sag due to motor starting depends on a number of motor parameters, of which the motor inertia is the main one. When determining the run-up time, it is also important to determine the sag magnitude at the motor terminals.

The torque produced by the motor is proportional to the square of the terminal voltage. That makes that a sag down to 90% causes a drop in torque down to 81%. It is the difference between mechanical load torque and electrical torque which determines the acceleration of the motor, and thus the run-up time. Assume that the mechanical torque is half the electrical torque during most of the run-up if the terminal voltage is nominal. This assumption is based on the general design criterion that the pull-out torque of an induction motor is about twice the torque at nominal operation. When the voltage drops to 90% of nominal the electrical torque drops to 81% of nominal which is 162% of the mechanical torque. The accelerating torque, the difference between electrical and mechanical torque drops from 100% to 62%, a drop of 38%.

EXAMPLE Consider again the 5 MVA induction motor started from a 100 MVA 11 kV supply. The voltage at the motor terminals during run-up drops to 77% as we saw before. The electrical torque drops to 59% of nominal which is 118% of the mechanical torque. The accelerating torque thus drops from 100% to only 18%, and the run-up time will increase by a factor of 6.

A dedicated transformer alone cannot solve this problem, as the voltage at the motor terminals remains low. What is needed here is a stronger supply. To limit the voltage drop at the motor terminals to V_{min}, the source strength, from (4.147), needs to be

$$S_{source} = \frac{6S_{motor}}{1 - V_{min}} \tag{4.151}$$

A 5 MVA motor, with a minimum-permissable voltage of 85% during starting, needs a source strength of at least $\frac{6 \times 5\,\text{MVA}}{0.15} = 200\,\text{MVA}$. To keep the voltage above 90%, the source strength needs to be 300 MVA.

From these examples it will be clear that large voltage drops are not only a problem for sensitive load, but that they also lead to unacceptably long run-up times. The situation becomes even worse if more motors are connected to the same bus, as they will further pull down the voltage. Voltage drops due to induction motor starting are seldom deeper than 85%.